The ATLAS Tracker.

Ingrid-Maria Gregor, DESY
Autumn Block Course 2011
DESY Zeuthen

Thanks to: Christoph Rembser, Adrian Vogel, Ulrich Koetz, Frank Simon, ….

Overview

I. Introduction

II. The ATLAS Inner Detector - Overview

III. Gas Detectors

- The Transition Radiation Tracker

IV. Semiconductor Detectors

- The ATLAS SCT
- The ATLAS Pixel Detectors

V. Conclusion

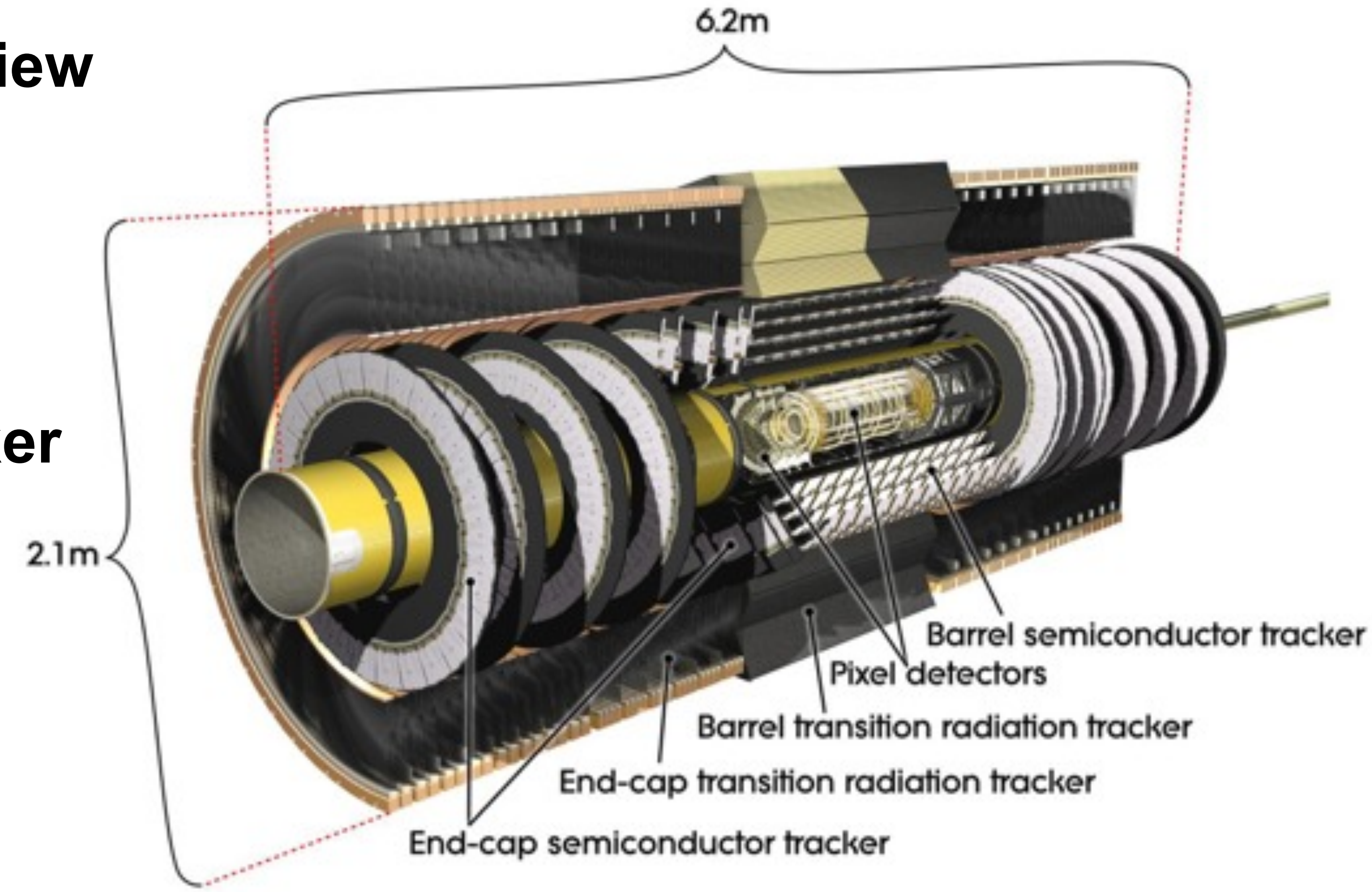

Introduction

The ATLAS Detector

3 Level Trigger system

- L1 – hardware – 100 kHz
  2.5 μs latency
- L2 – software – 3-4 kHz
  10 ms latency
- EF – software – 100 Hz
  1-2 s latency

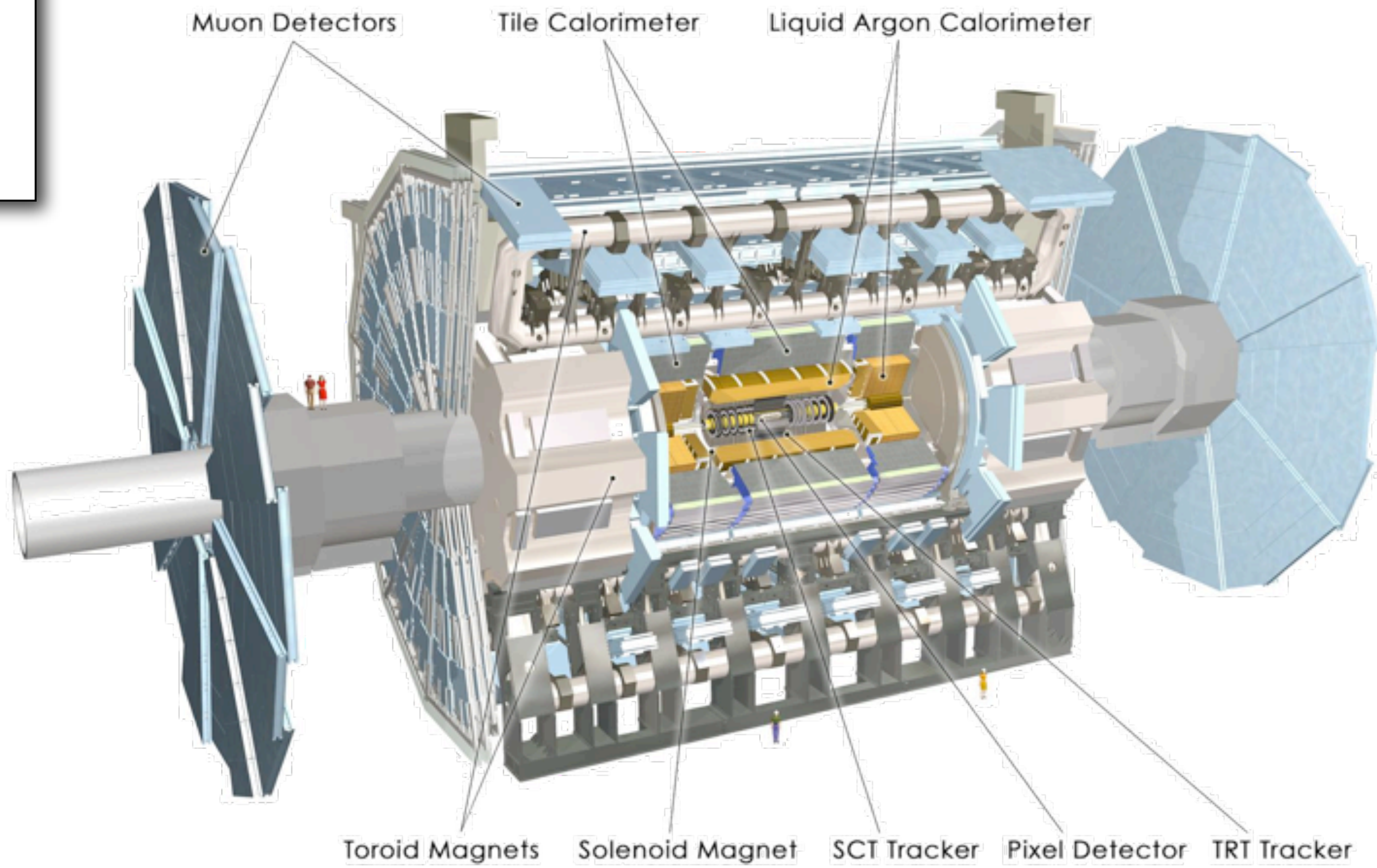

3 Level Trigger system

- L1 – hardware – 100 kHz
  2.5 μs latency
- L2 – software – 3-4 kHz

Muon spectrometer
μ tracking

- MDT (Monitored drift tubes)
- CSC (Cathode Strip Chambers)
- RPC (Resistive Plate Chamber) Trigger
- TGC (Thin Gas Chamber) Trigger
- 4T Toroid Magnet

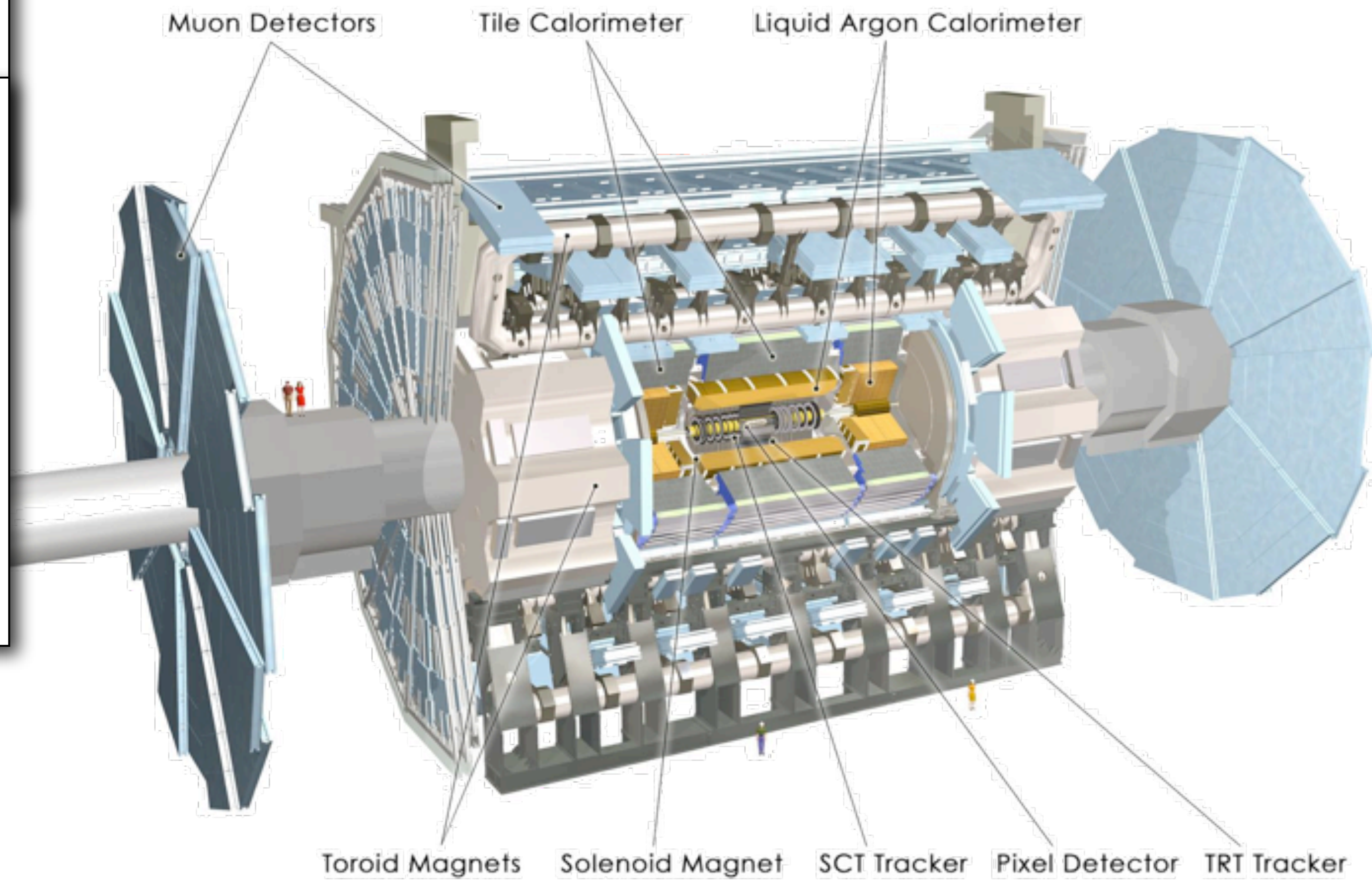

The ATLAS Detector

3 Level Trigger system

- L1 – hardware – 100 kHz
  2.5 μs latency
- L2 – software – 3-4 kHz
  10 ms latency

Muon spectrometer
μ tracking

- MDT (Monitored drift tubes)
- CSC (Cathode Strip Chambers)
- RPC (Resistive Plate Chamber) Trigger
- TGC (Thin Gas Chamber) Trigger

Calorimeter system
EM and Hadronic energy

- Liquid Ar (LAr) EM barrel and end-cap
- LAr Hadronic end-cap
- Tile calorimeter (Fe – scintillator) hadronic barrel

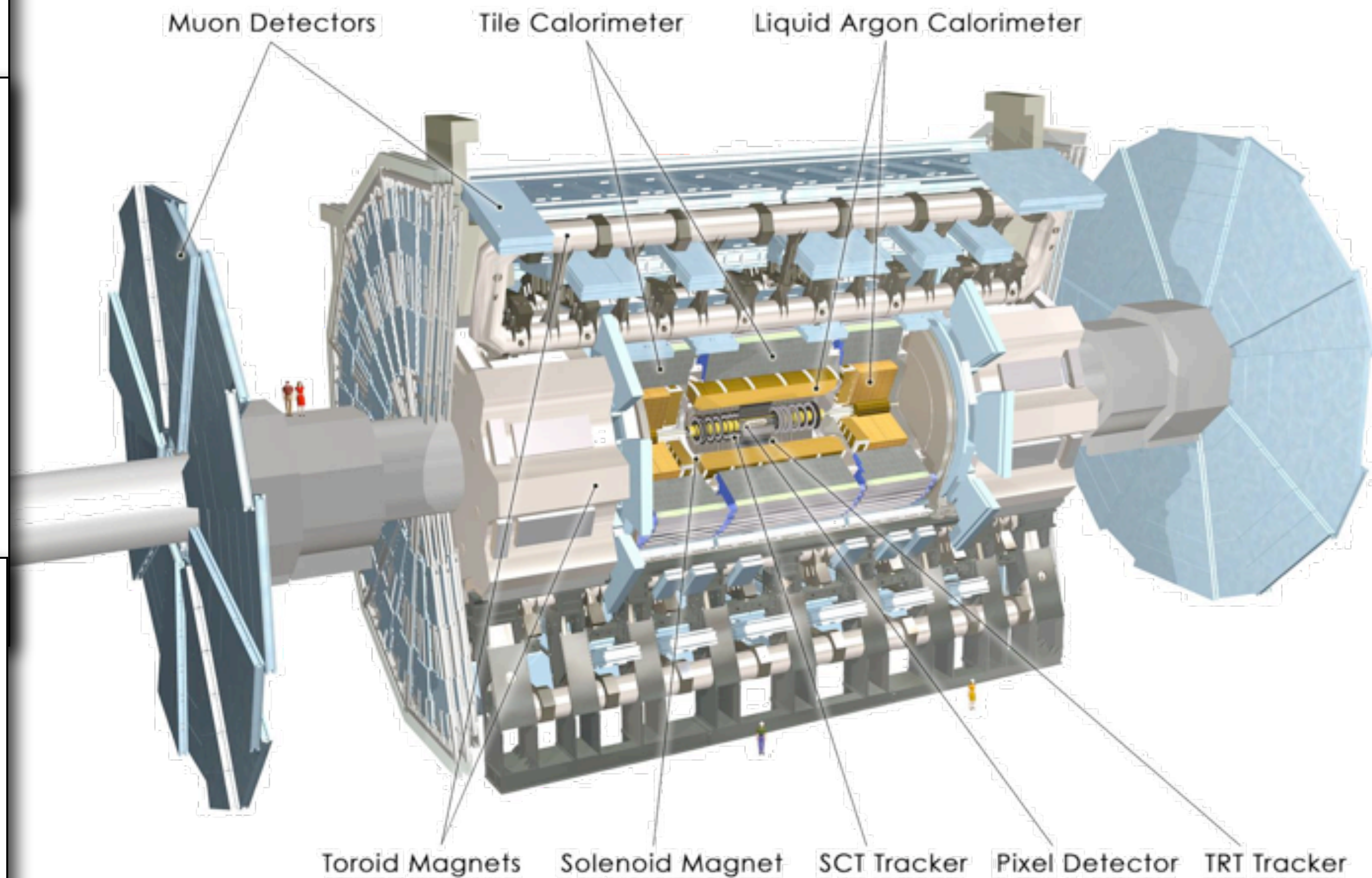

The ATLAS Detector

3 Level Trigger system

- L1 – hardware – 100 kHz
  2.5 μs latency
- L2 – software

Muon spectron
μ tracking

- MDT (Monitore
  tubes)
- CSC (Cathode
  Chambers)
- RPC (Resistive Plate
  Chamber) Trigger
- TGC (Thin Gas Chamber)

Inner Detector (ID)
Tracking

- Silicon Pixels 50 x 400 μm^2
- Silicon Strips (SCT)
  80 μm stereo
- Transition Radiation Tracker
  (TRT) up to 36 points/track
- 2T Solenoid Magnet

Calorimeter system
EM and Hadronic energy

- Liquid Ar (LAr) EM barrel
  and end-cap
- LAr Hadronic end-cap
- Tile calorimeter (Fe –
  scintillator) hadronic barrel

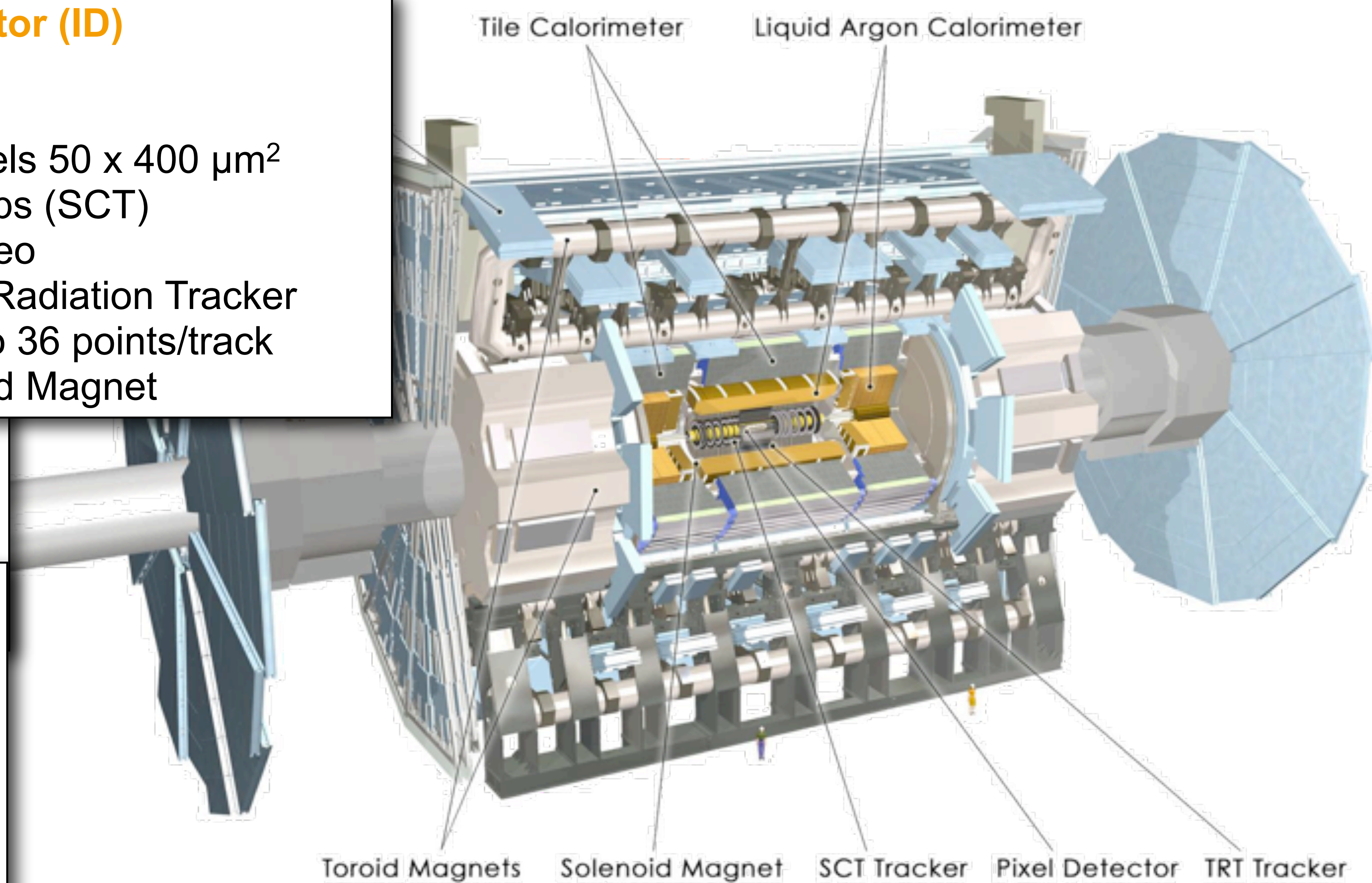

First Interesting Events

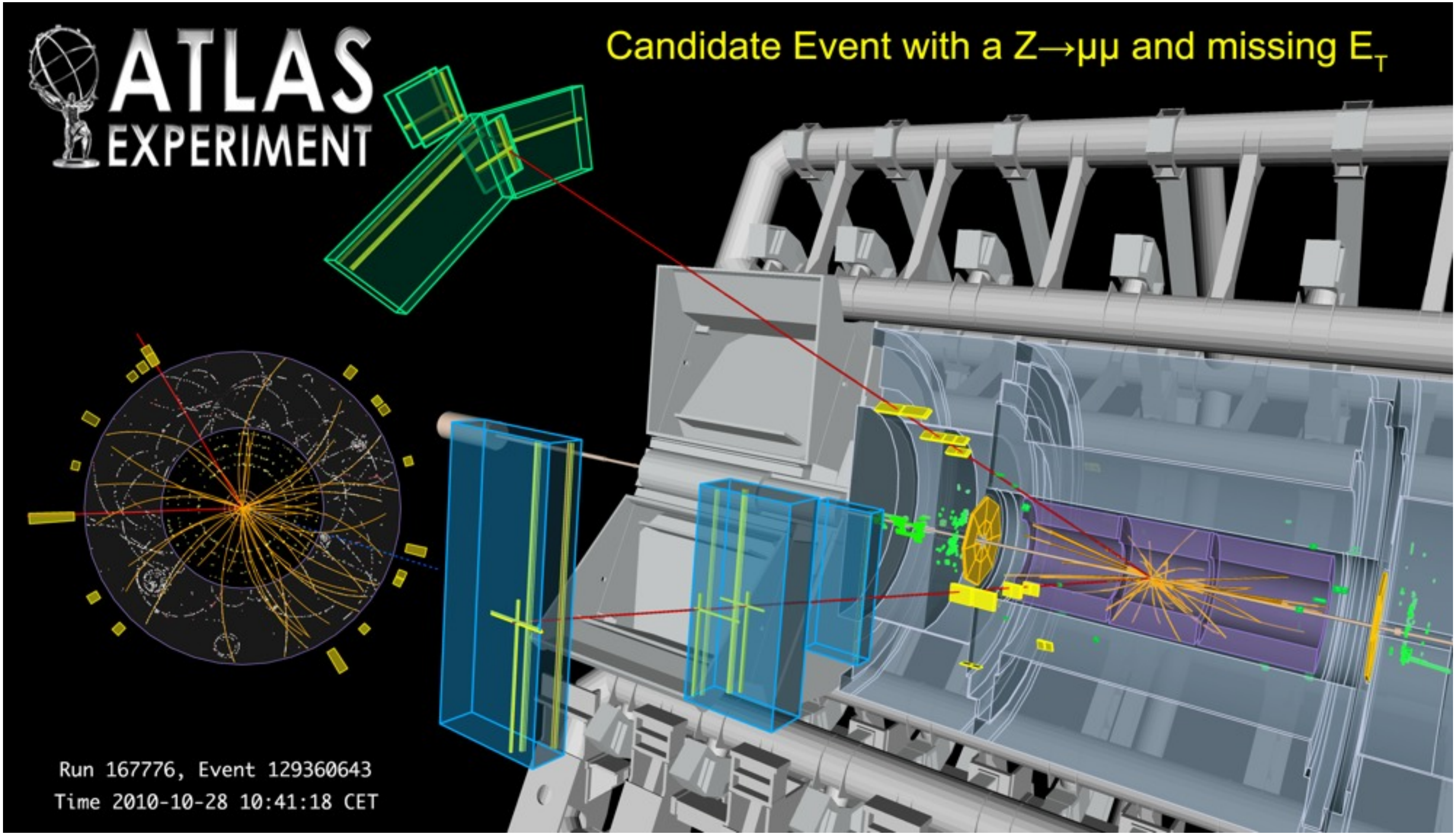

The ATLAS Inner Detector

- Designed to precisely reconstruct charged particles
- 7-points silicon (pixels + strips)
- straw tube quasi-continuous tracker with electron identification capability
- 2 T solenoidal magnetic field
- This talk: Basics and some technical details

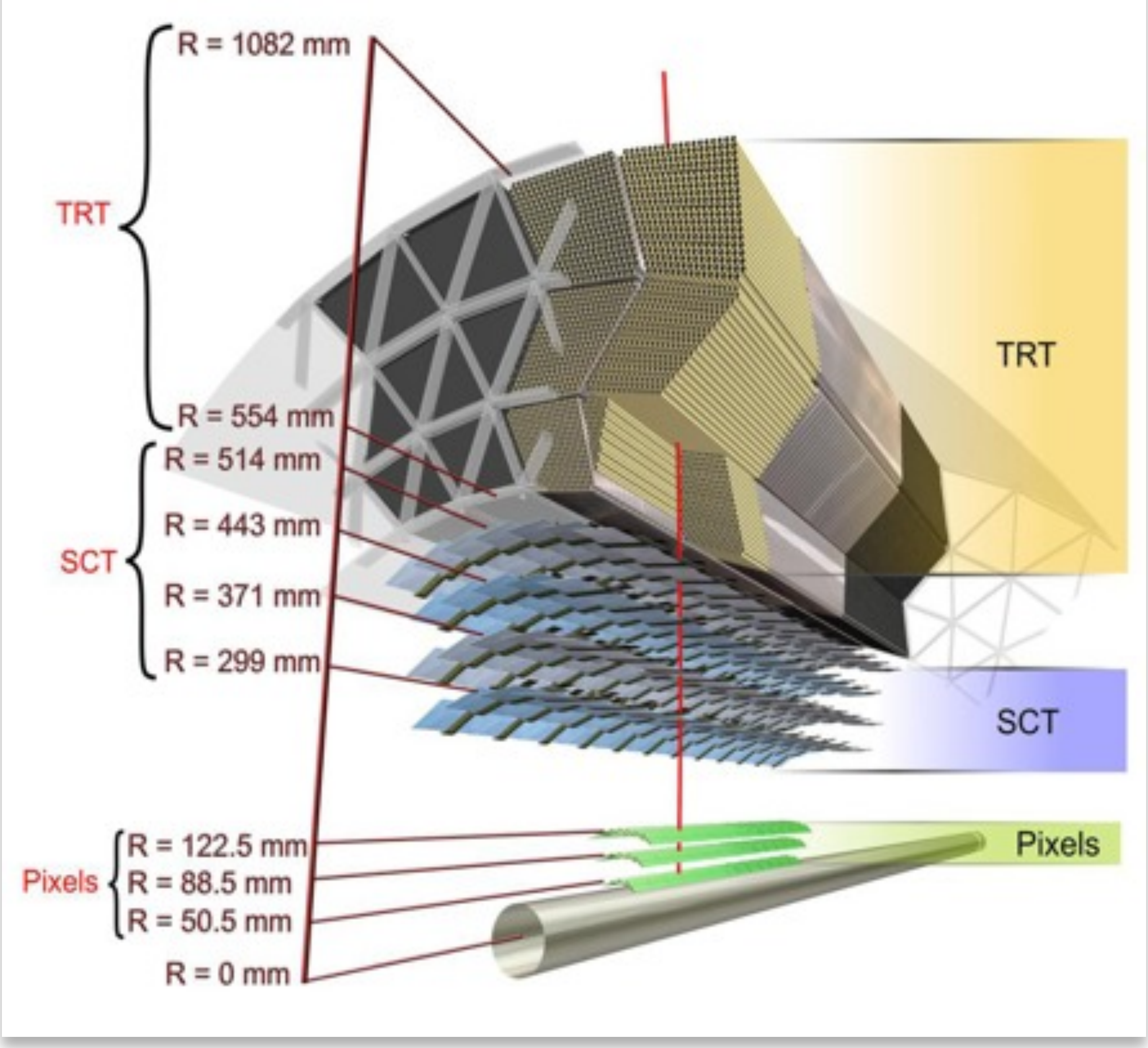

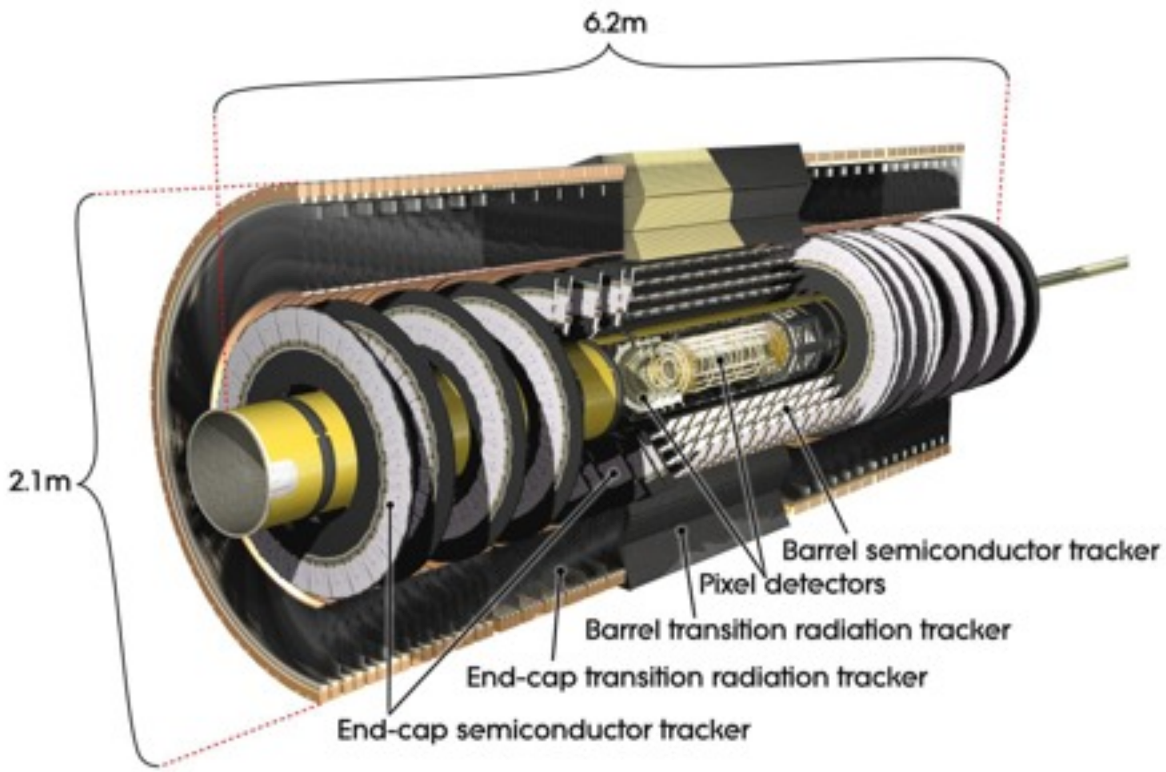

Interactions of “heavy” Particles with Matter

- Mean energy loss is described by the **Bethe-Bloch** formula

$$-\frac{dE}{dx} = 4\pi N_A r_e^2 m_e c^2 z^2 \frac{Z}{A} \cdot \frac{1}{\beta^2} \cdot \left[\frac{1}{2} \ln \frac{2 m_e c^2 \beta^2 \gamma^2 T_{\max}}{I^2} - \beta^2 - \frac{\delta}{2} - \frac{C}{Z}\right]$$

$T_{\max}$ Maximum kinetic energy which can be transferred to the electron in a single collision

I^2 Excitation energy

$\frac{\delta}{2}$ Density term due to polarization: leads to saturation at higher energies

$\frac{C}{Z}$ Shell correction term, only relevant at lower energies

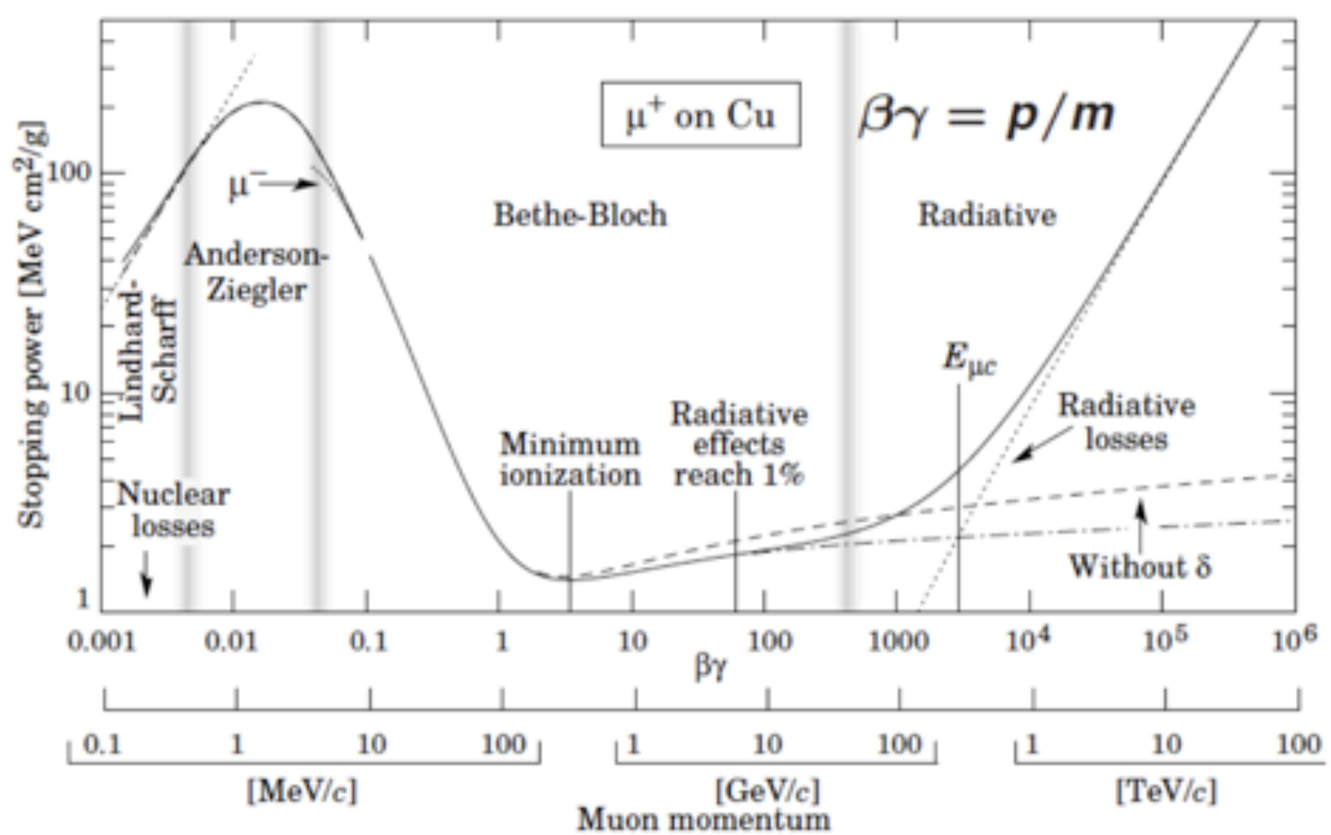

Interactions of “heavy” Particles with Matter

- Mean energy loss is described by the **Bethe-Bloch** formula

$$-\frac{dE}{dx} = 4\pi N_A r_e^2 m_e c^2 z^2 \frac{Z}{A} \cdot \frac{1}{\beta^2} \cdot \left[\frac{1}{2} \ln \frac{2m_e c^2 \beta^2 \gamma^2 T_{\max}}{I^2} - \beta^2 - \frac{\delta}{2} - \frac{C}{Z}\right]$$

$T_{\max}$ Maximum kinetic energy which can be transferred to the electron in a single collision

I^2 Excitation energy

$\frac{\delta}{2}$ Density term due to polarization: leads to saturation at higher energies

$\frac{C}{Z}$ Shell correction term, only relevant at lower energies

$$\left\langle \frac{dE}{dx} \right\rangle \propto \frac{1}{\beta^2}$$

“kinematic term”

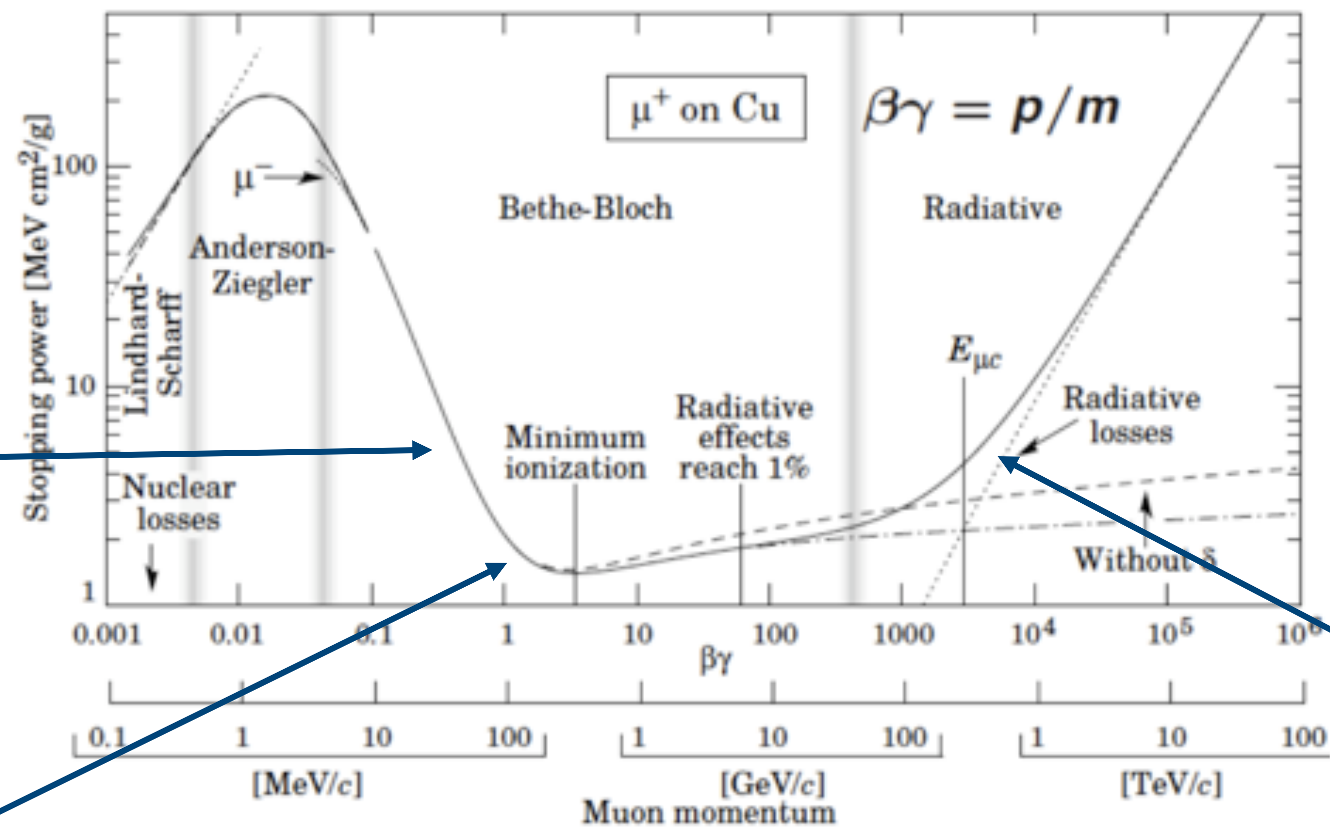

$$\left\langle \frac{dE}{dx} \right\rangle \propto \ln \beta^2 \gamma^2$$

“relativistic rise”

“minimum ionizing particles” $\beta\gamma \approx$ 3-4

Material Dependence of the Energy Loss

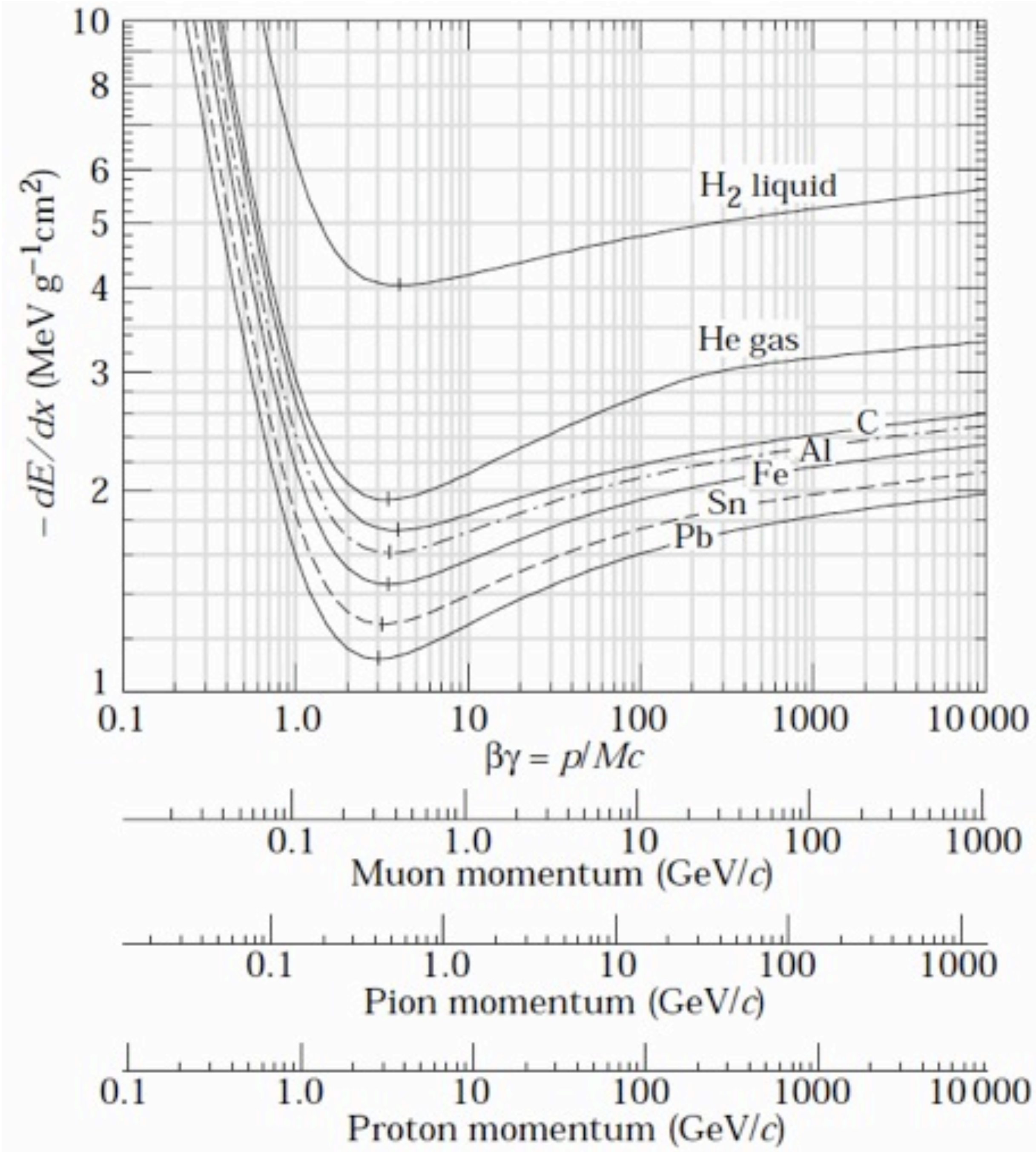

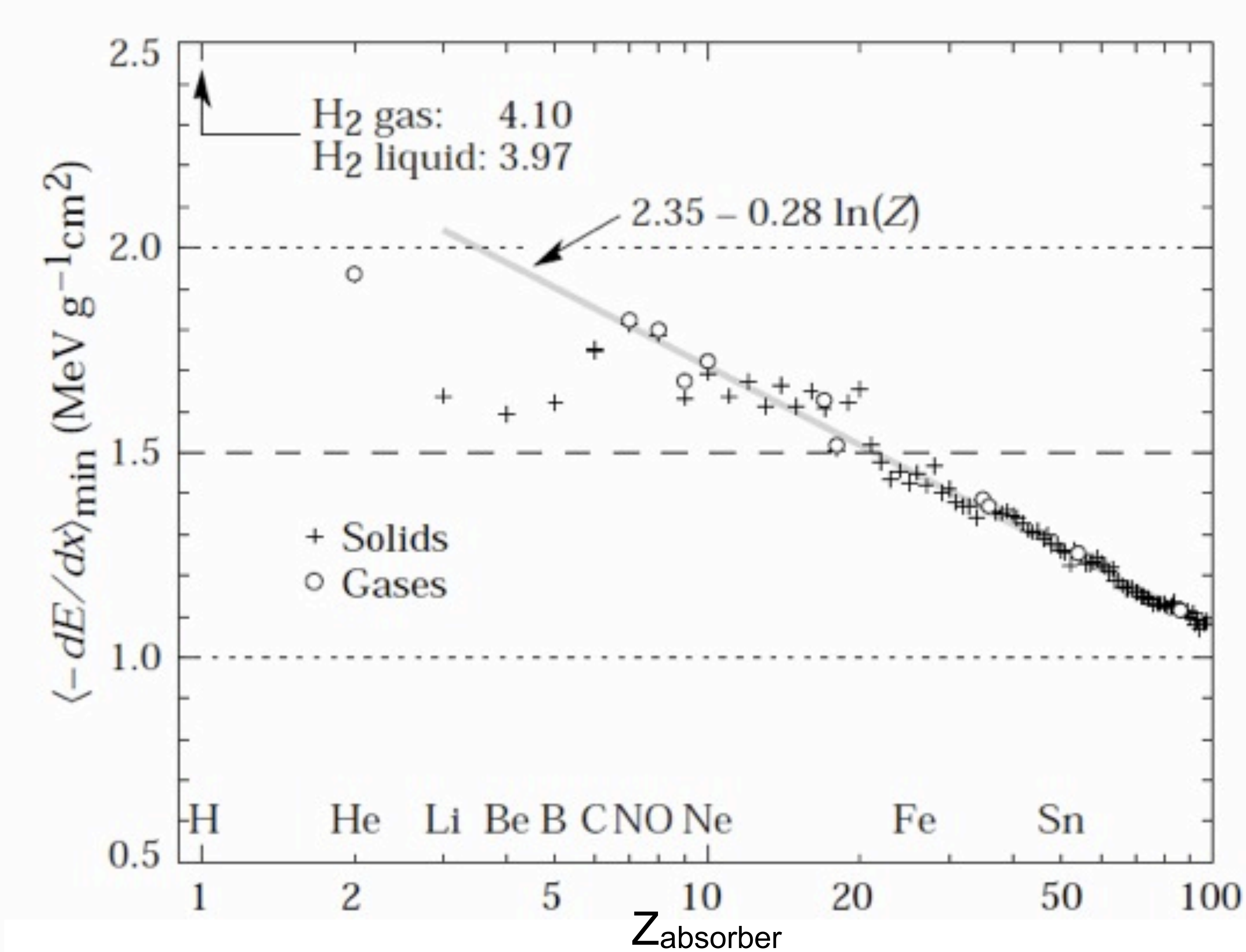

- **Rule of thumb:** energy loss of MIPs ($\beta\gamma \sim 3$): 1-2 MeV g^{-1} cm^2 (except H)

A Closer Account of Energy Loss

- Bethe-Bloch displays only the average
  - energy loss is a statistical process
  - discrete scattering with different results depending on “intensity’ of scattering
  - primary and secondary ionisation

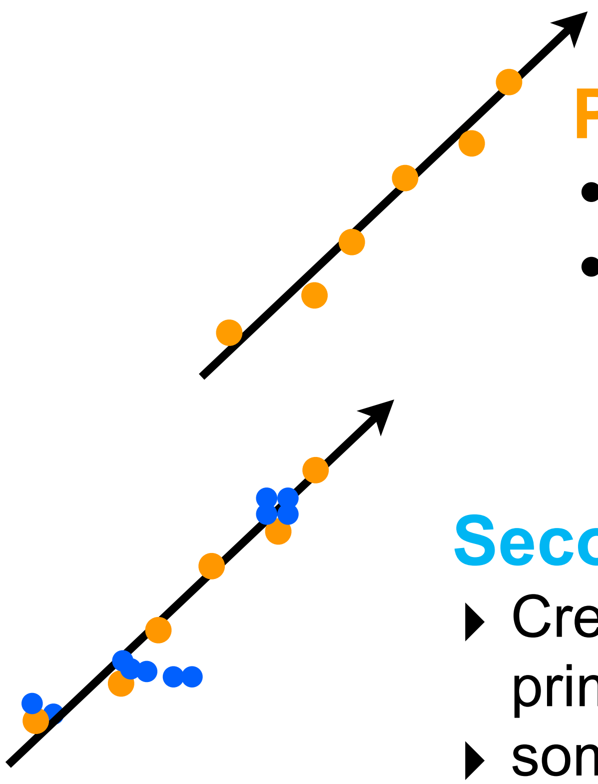

Primary ionisation
- Poisson distributed
- Large fluctuations per reaction

Secondary ionisation
- Created by high energetic primary electrons
- sometime the energy is sufficient for a clear secundary track: δ-Electron

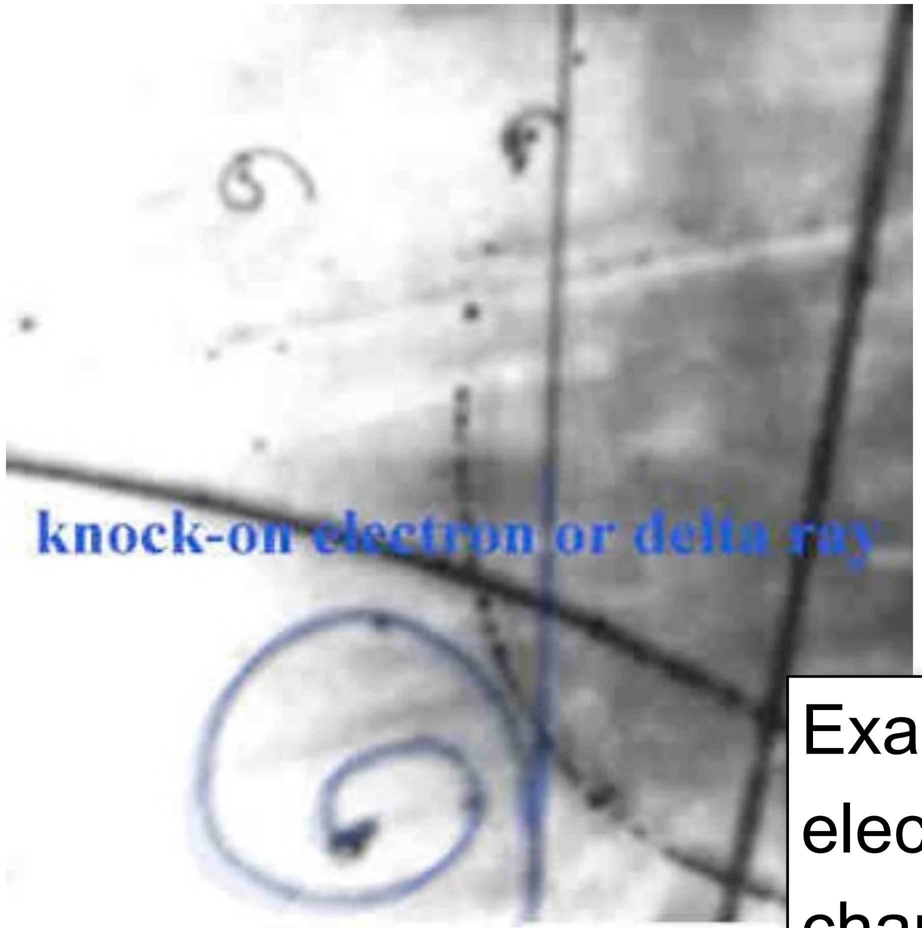

Example of a delta electron in a bubble chamber: visible path

Total ionisation = **primary ionisation**
+ **secondary ionisation**

Energy Loss in Thin Layers

- In case of thin detectors the variation width within the energy transfer of the reactions leads to a large variation of the energy loss:
  - A broad maximum: collisions with little energy loss
  - A long tail towards higher energy loss: few collisions with large energy loss, δ-electrons

The **Landau** distribution is used in physics to describe the fluctuations in the energy loss of a charged particle passing through a thin layer of matter

Thin absorber:
<dE> < ~10Tmax

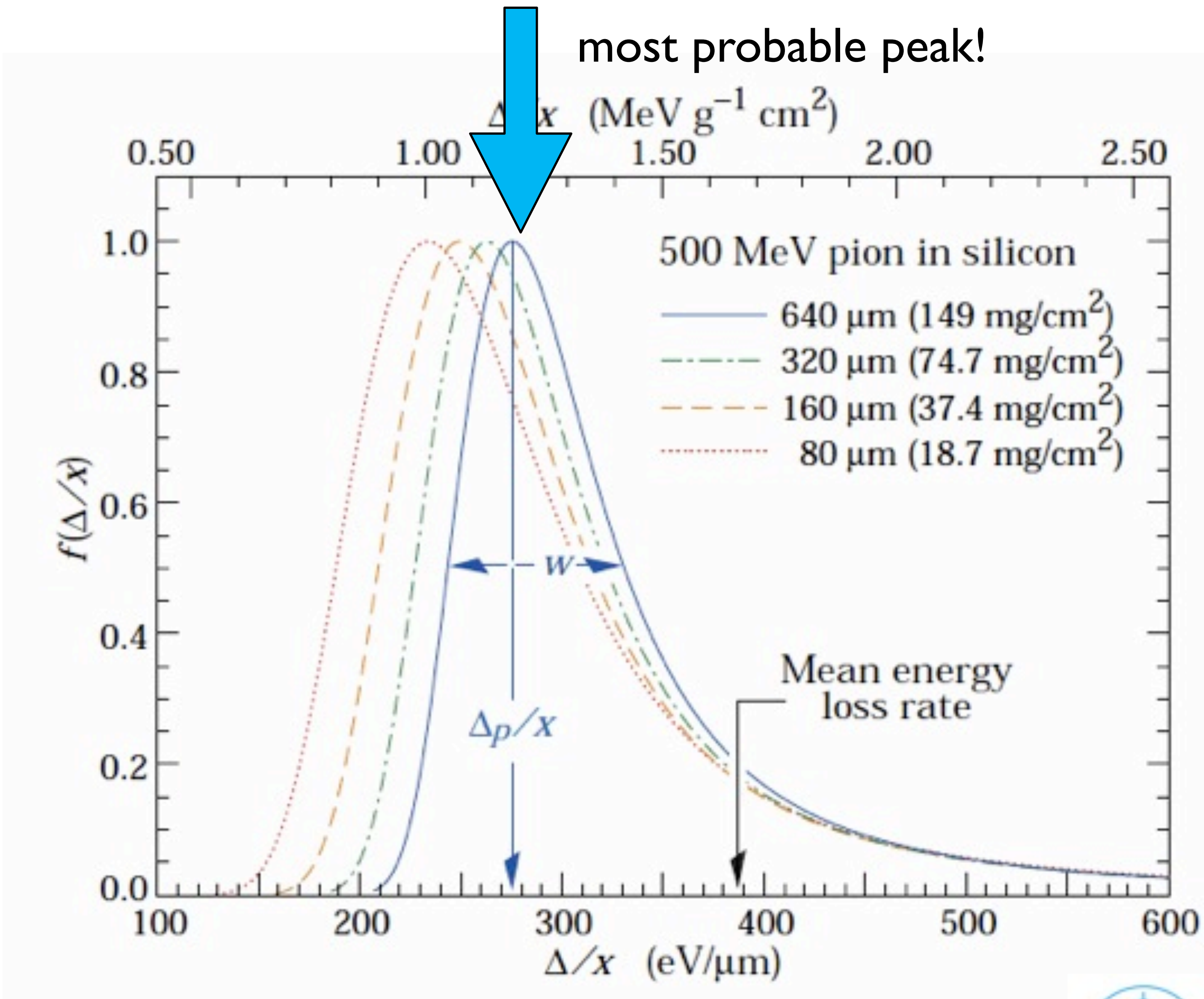

Electrons: Energy Loss

- Ionization loss by electrons (positrons) differs because of the kinematics, spin and the identity of the incident electron with the electrons which it ionizes.

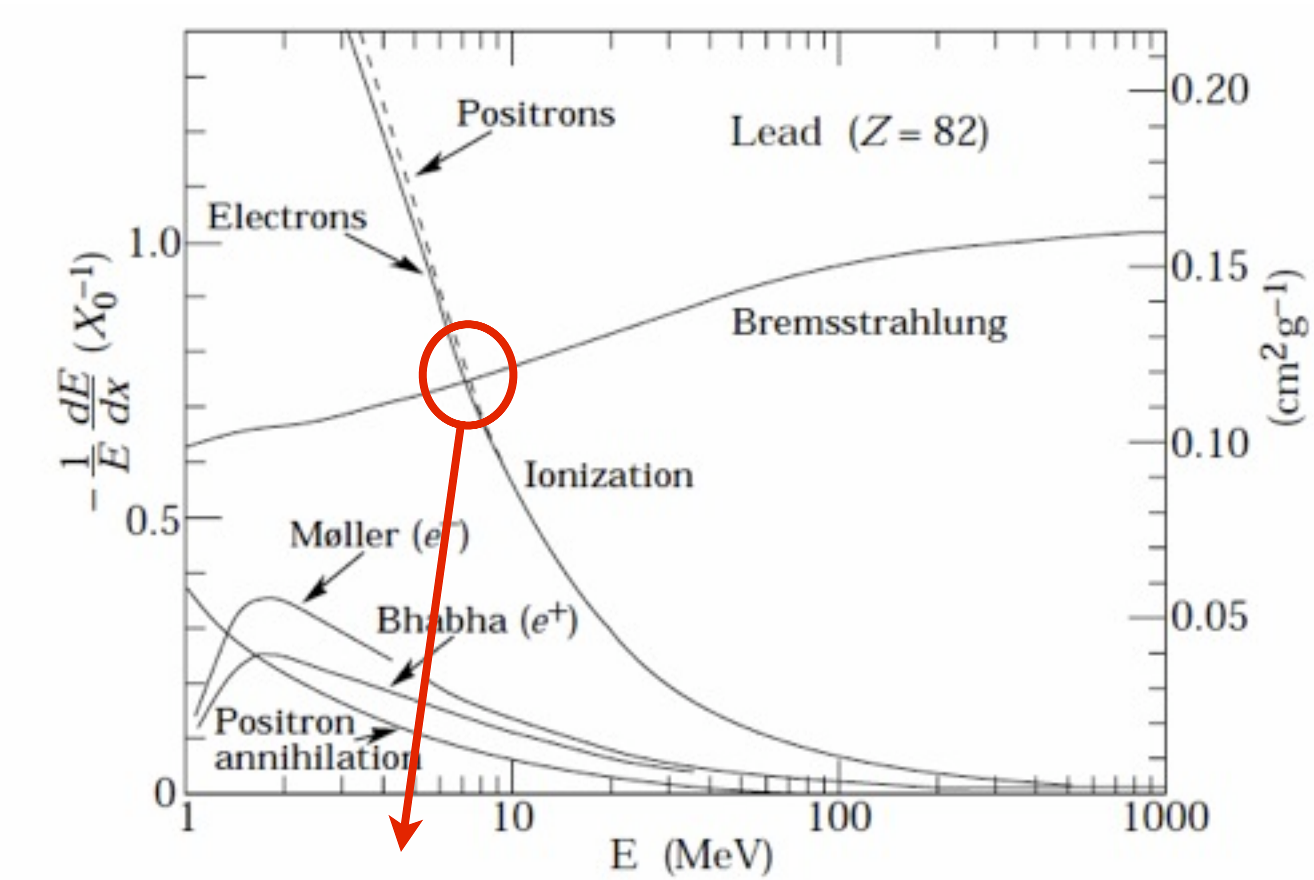

- Bremsstrahlung is dominating at high energies
- At low energies: ionisation, additional scattering

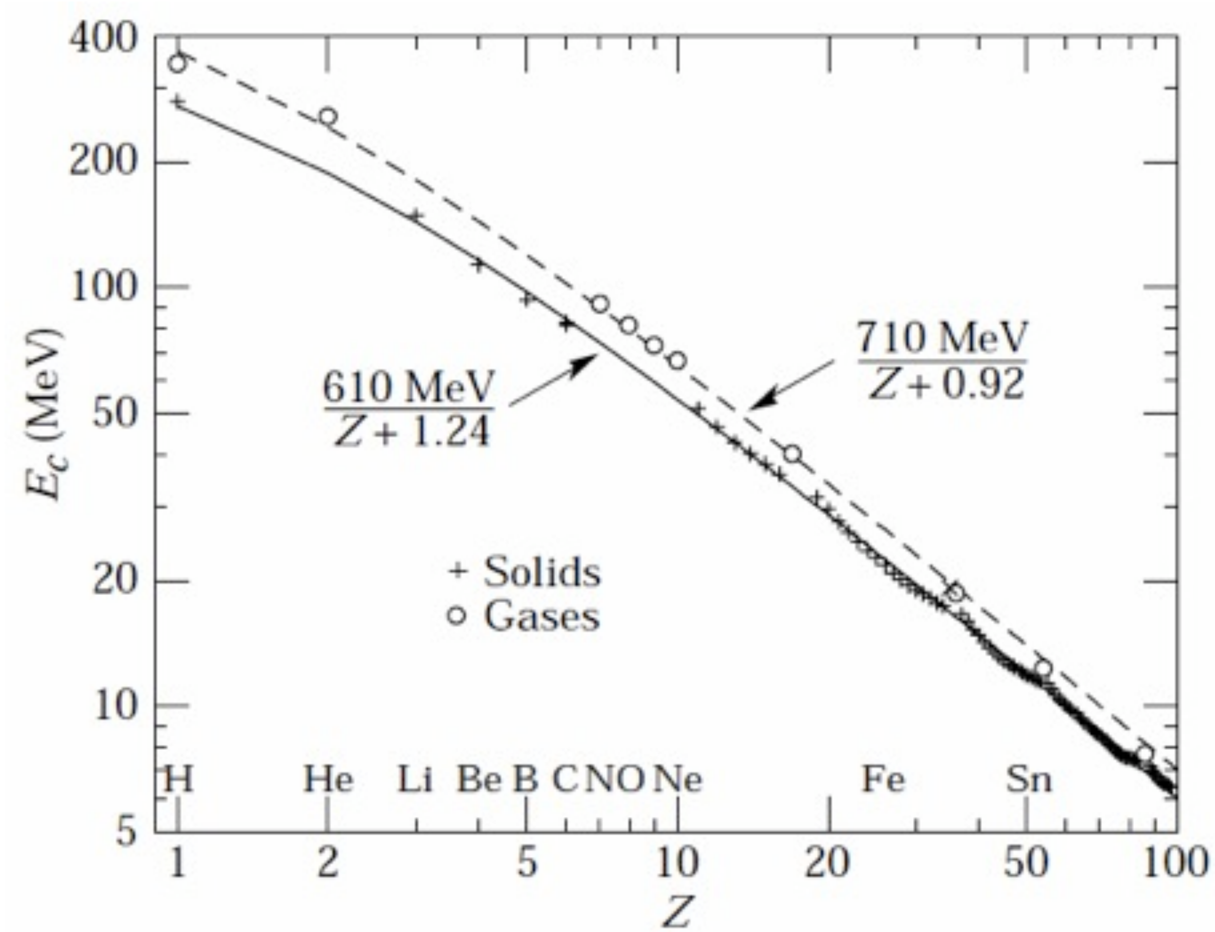

- **Critical energy:** the energy at which the losses due to ionisation and Bremsstrahlung are equal

$$\frac{dE}{dx}(E_c) = \frac{dE}{dx}(E_c)$$

For electrons approximately:

$$E_c^{\text{solid+liq}} = \frac{610MeV}{Z+1.24} \qquad E_c^{\text{gas}} = \frac{710MeV}{Z+1.24}$$

Multiple Scattering!

- Charged particles are forced to deviate from a straight track when moving through a medium: multiple scattering due to Coulomb field

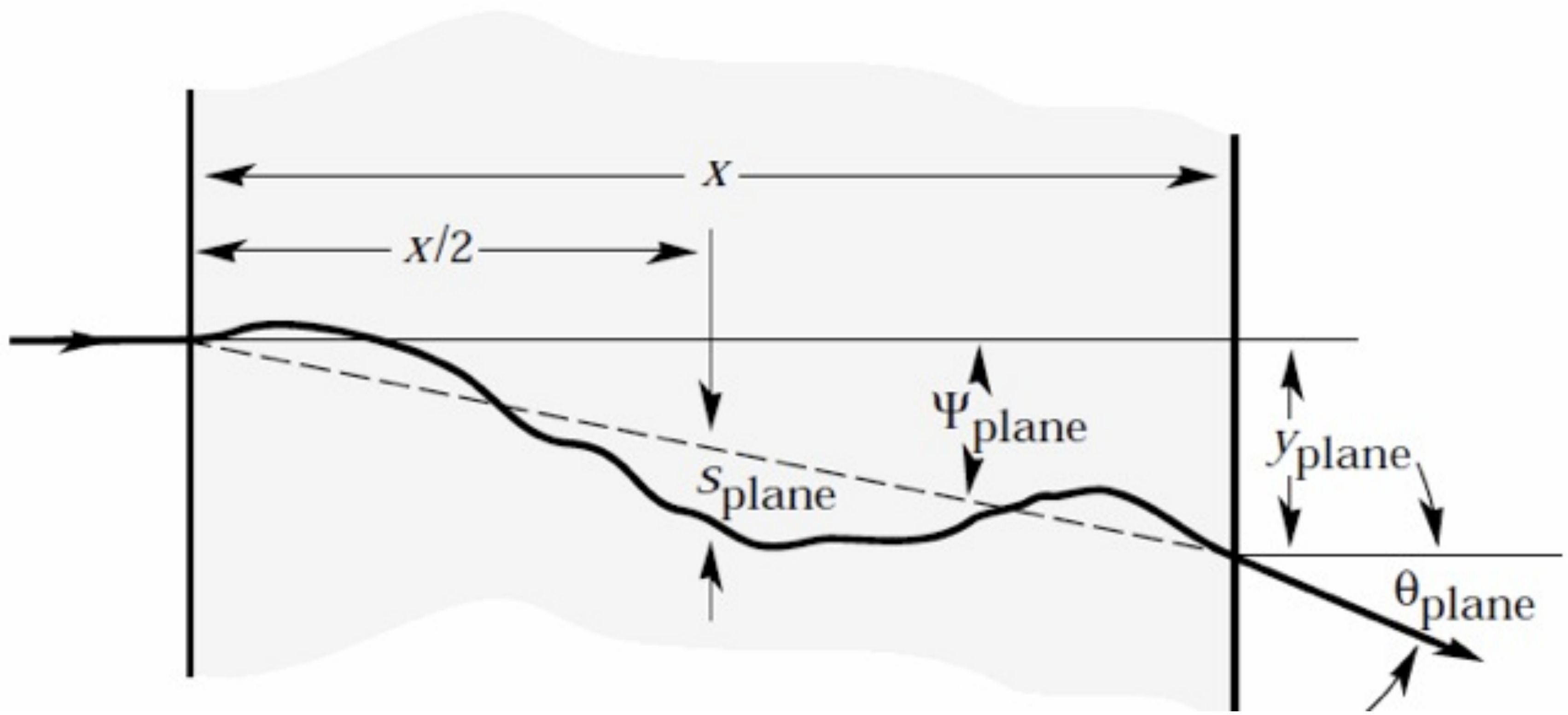

$$\theta_0 = \theta_{\text{plane}}^{\text{rms}} = \frac{1}{\sqrt{2}}\theta_{\text{space}}^{\text{rms}} \qquad \theta_0 = \frac{13.6\,\text{MeV}}{\beta c p} z \sqrt{x/X_0}\left[1 + 0.038\ln(x/X_0)\right]$$

- relevant for relativistic particles, for material thickness from $10^{-3}\,X_0$ bis $100\,X_0$

Requirements for Tracking Detectors

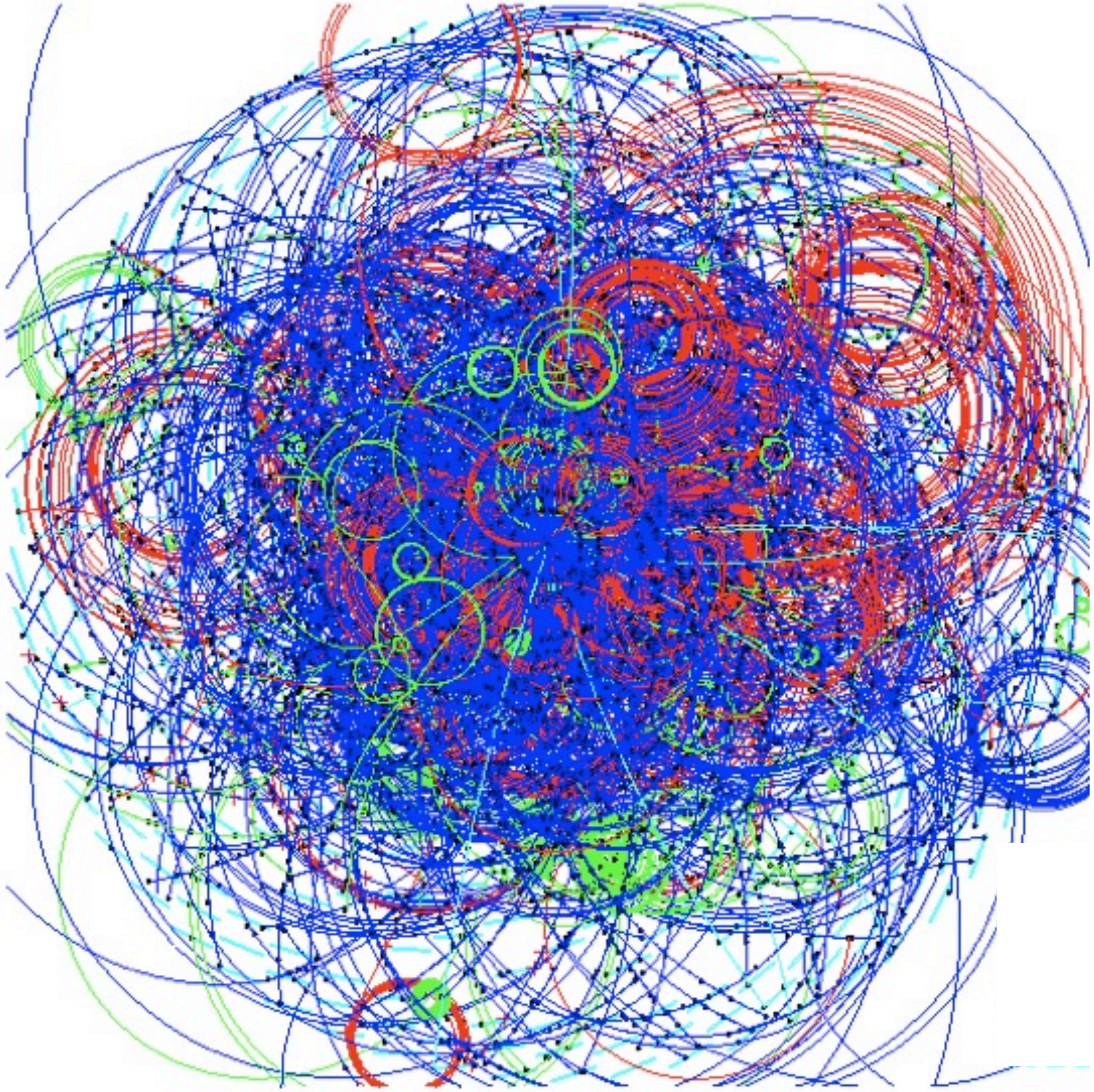

E.g. search for
$H \rightarrow Z^0 Z^0 \rightarrow \mu^+ \mu^- \mu^+ \mu^-$

with $\Delta m_Z < 2$GeV
up to $p_z \sim 500$GeV

=> reconstruction of high p_t tracks with
+ high efficiency
  • single track $\varepsilon > 95\%$
  • in jet $\varepsilon > 90\%$
+ momentum resolution
  • $\Delta p_t / p_t = 0.01$ pt [GeV]

Resolution of Tracking Detectors

- An important figure of merit is the resolution of a tracking detector
- Depending on detector geometry and charge collection
  - Pitch (distance between channels)
  - Charge sharing between channels

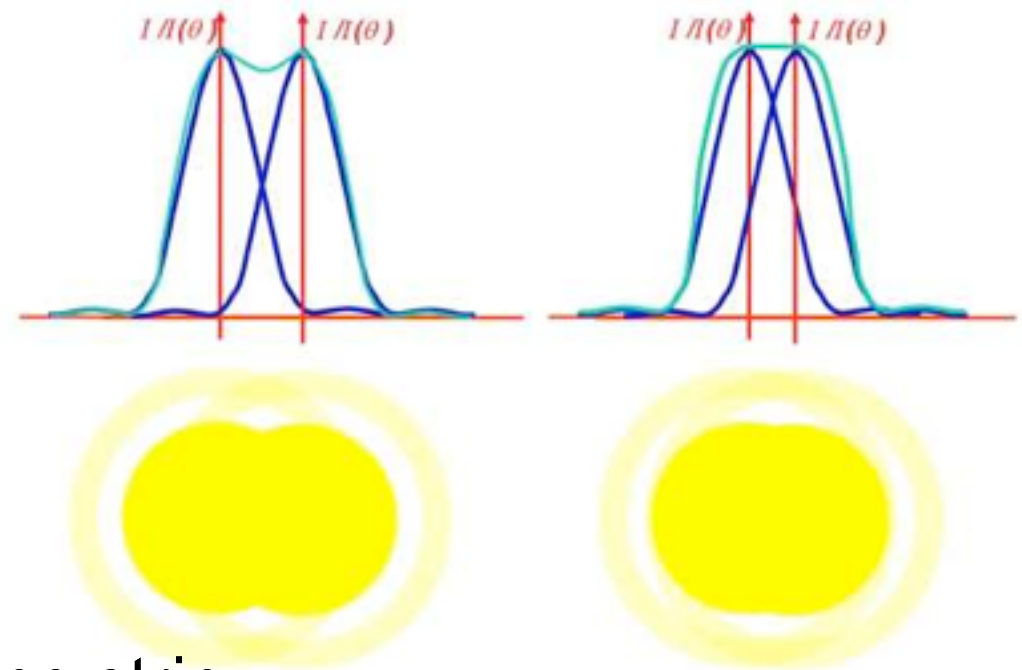

- Simple case: all charge is collected by one strip
- Traversing particle creates signal in hit strip
- Flat distribution along strip pitch; no area is pronounced

➔ Probability distribution for particle passage:

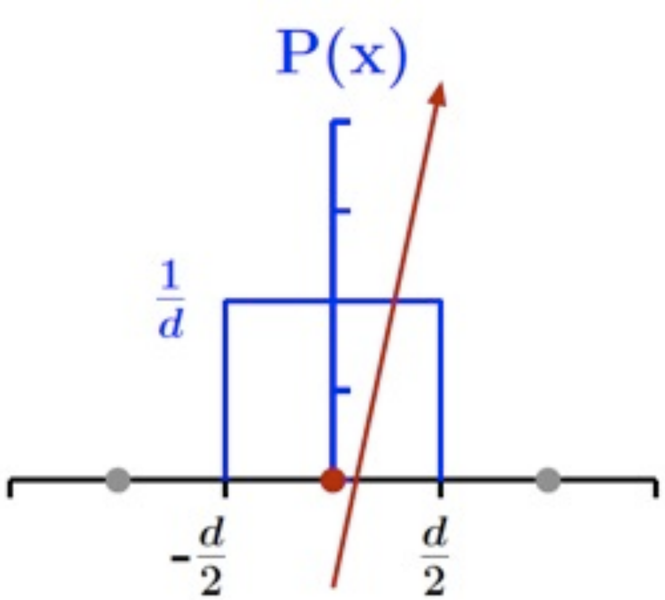

$$P(x) = \frac{1}{d} \qquad \Rightarrow \int_{-d/2}^{d/2} P(x)\,dx = 1$$

The reconstructed point is always the middle of the strip:

$$\langle x \rangle = \int_{-d/2}^{d/2} x\,P(x)\,dx = 0$$

Resolution of Tracking Detectors II

- Calculating the resolution orthogonal to the strip:

$$\sigma_x^2 = \langle (x - \langle x \rangle)^2 \rangle = \int_{-d/2}^{d/2} x^2 \, P(x) \, dx = \frac{d^2}{12}$$

- Resulting in a general term (also valid for wire chambers):

$$\sigma = \frac{d}{\sqrt{12}}$$

very important !

- For a silicon strip detector with a strip pitch of 80 µm this results in a minimal resolution of ~23µm
- In case of charge sharing between the strip (signal size decreasing with distance to hit position)
  - Resolution improved by center of gravity calculation

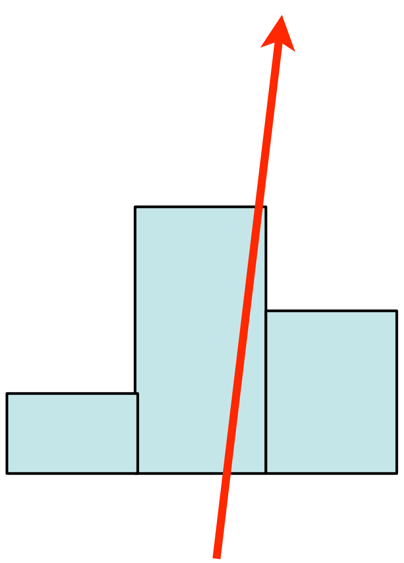

Impact Parameter Resolution

- Resolution error of the impact parameter

polar angle

$$\sigma^2_{r\phi} = \sigma^2_{rz} = a^2 + b^2 \cdot \frac{1}{(p \cdot sin^{\frac{3}{2}}\theta)^2}$$

intrinsic resolution of the tracking system (no multiple scattering)

influence of multiple scattering (geometry)

Accelerator	a (µm)	b (µm)
LEP	25	70
SLD	8	33
LHC	12	70
RHIC-II	13	19
ILC/CLIC	<5	<15

Gas Detectors

A Classic: Ionisation Chamber

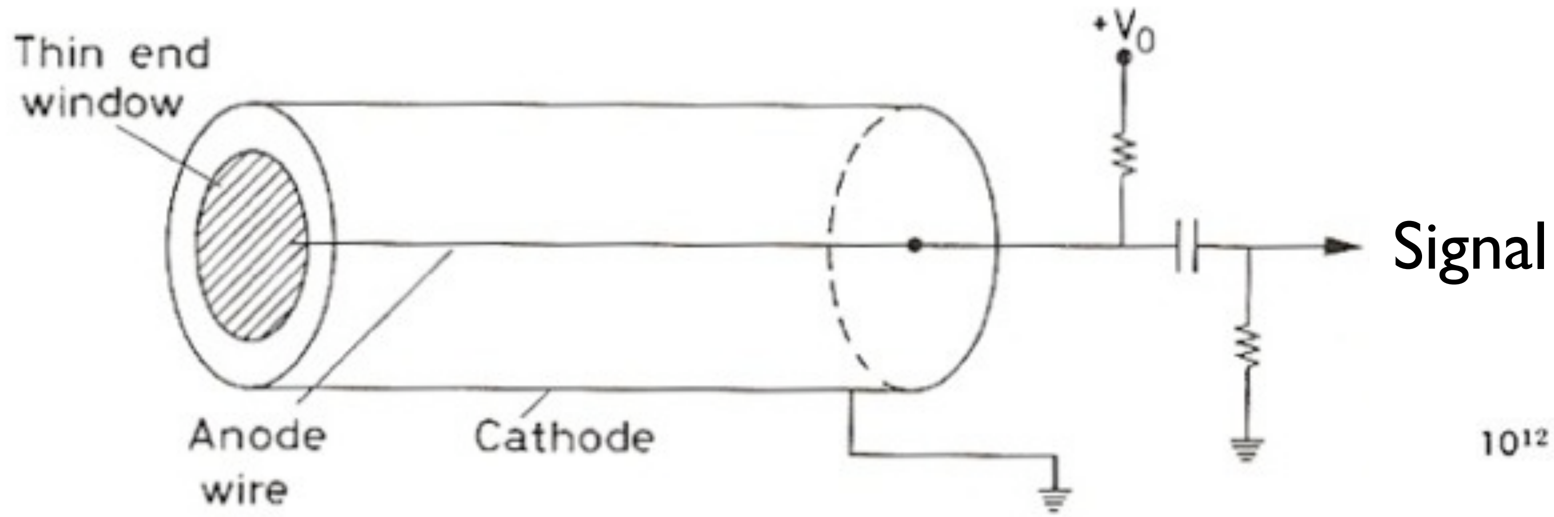

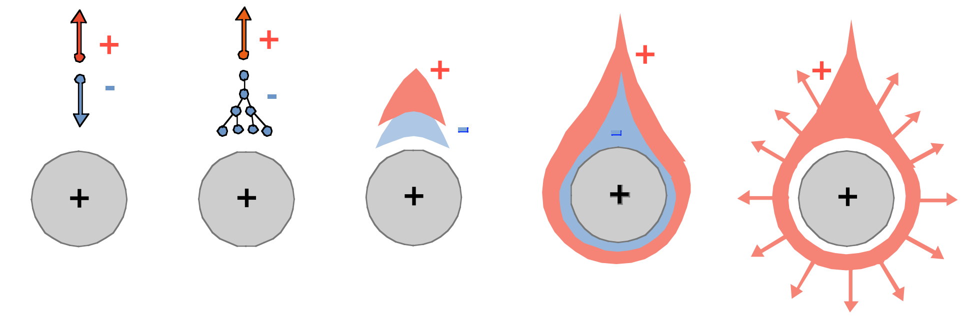

- Passage of particles creates within the gas volume electron-ion pair
- Electrons are accelerated in a strong electrics field -> amplification
- The signal is proportional to the original deposited charge or is saturated (depending on the voltage)

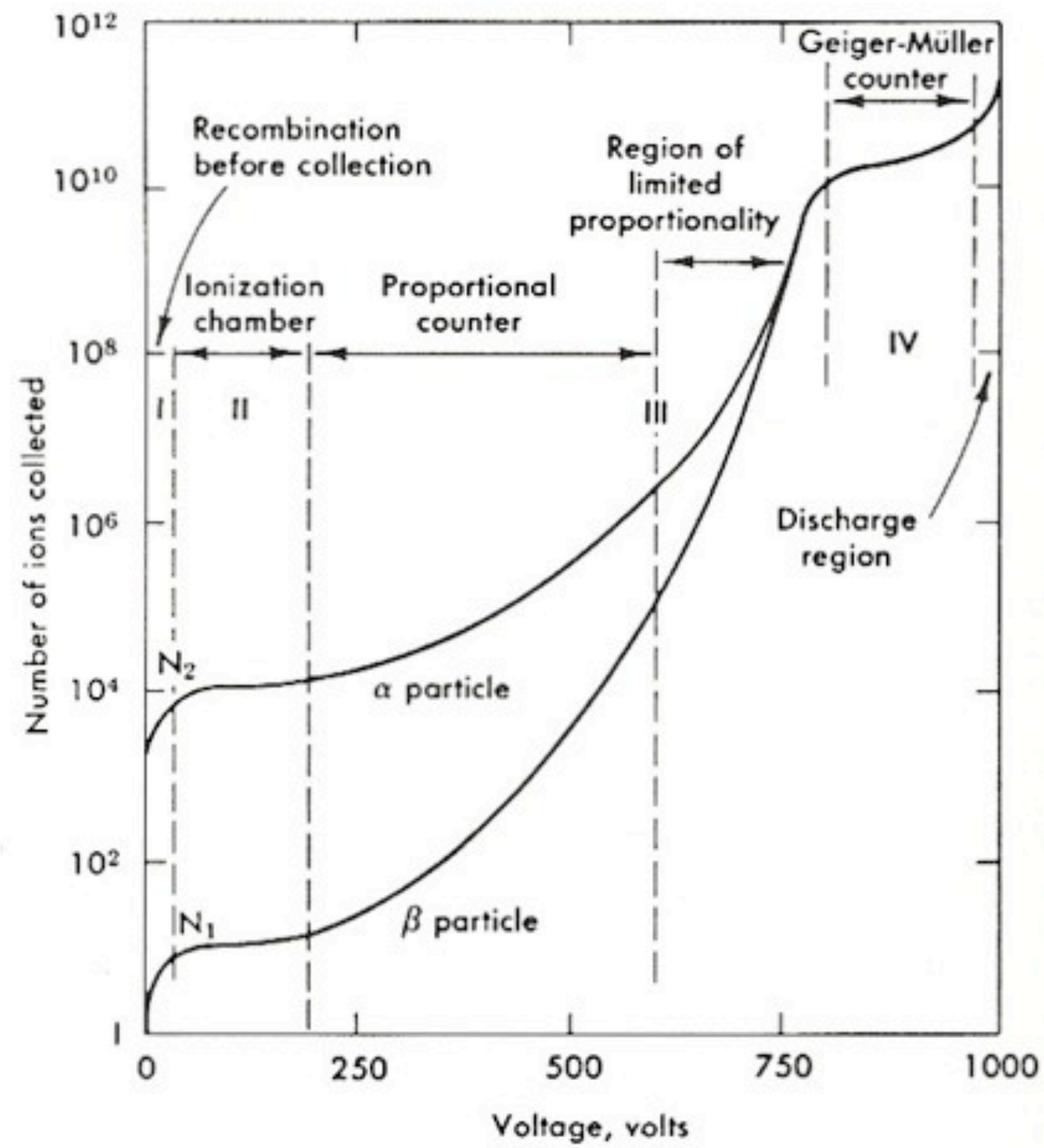

Transition Radiation

- produced by relativistic charged particles when they cross the interface of two media of different dielectric constants
- significant radiation only at large γ (O ~ 1000) in the keV range. Very useful for electron/pion separation

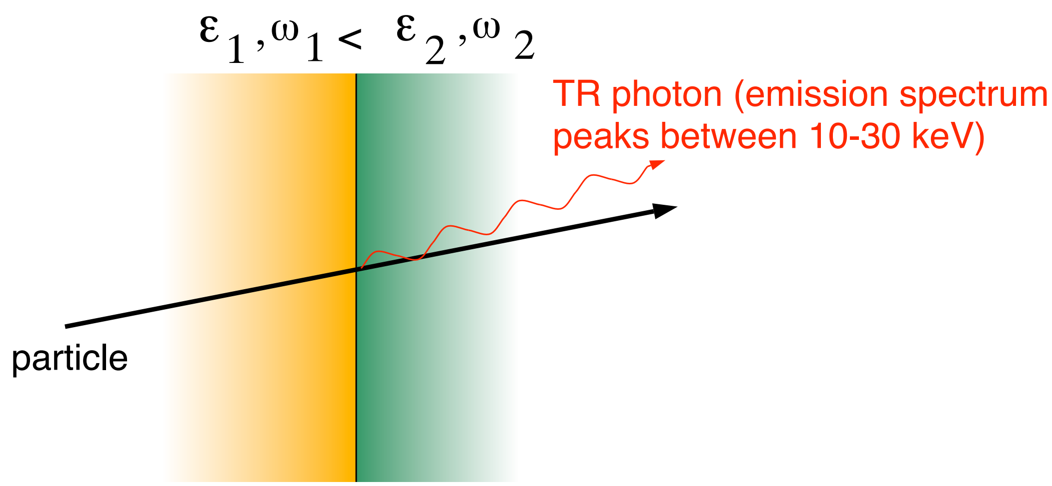

Intensity

$$I \propto m\gamma = \frac{1}{\sqrt{(1-\beta^2)}}$$

=> particle identification

- sharp maximum at $\theta = 1/\gamma$

  => detector has to be sensitive to photons (10-30**k**eV) along a particle track.
- Advantages:
  - not destructive for particles
  - particle identification
  - not expensive
  - robust (assembly & transport)

ATLAS TRT

- many thin radiator fibres/foils increase emission probability
- xenon gas acts as X-ray absorber
- ternary readout electronics register high-threshold hits (6 keV) sampled in 25-ns time bins

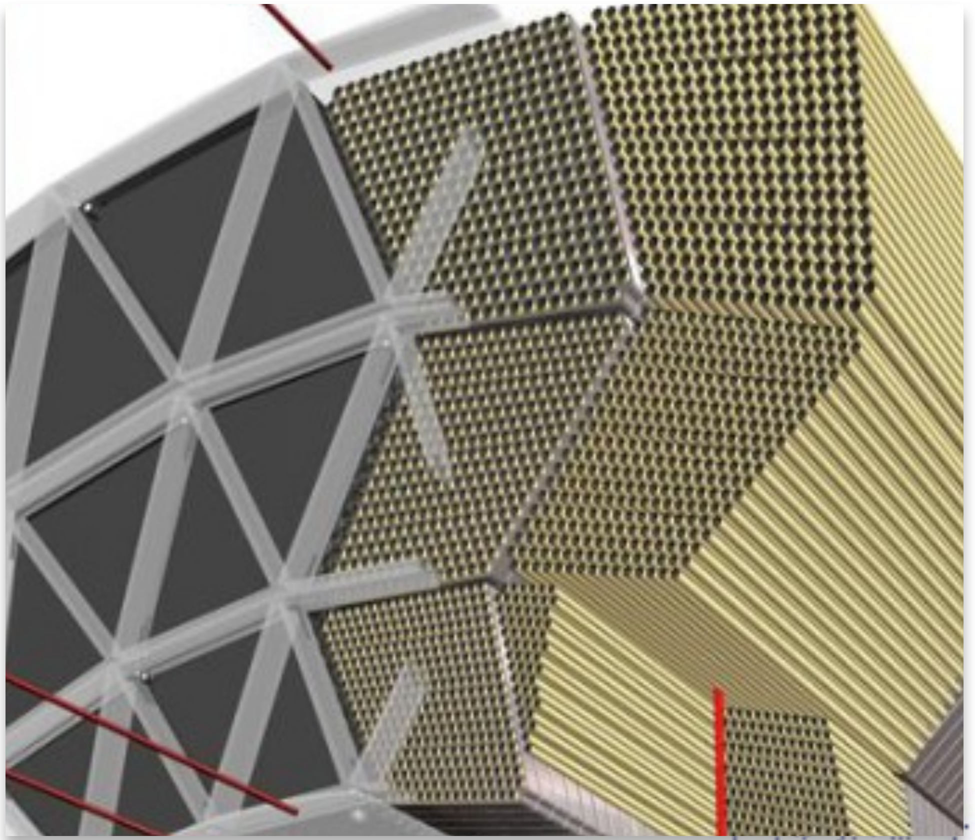

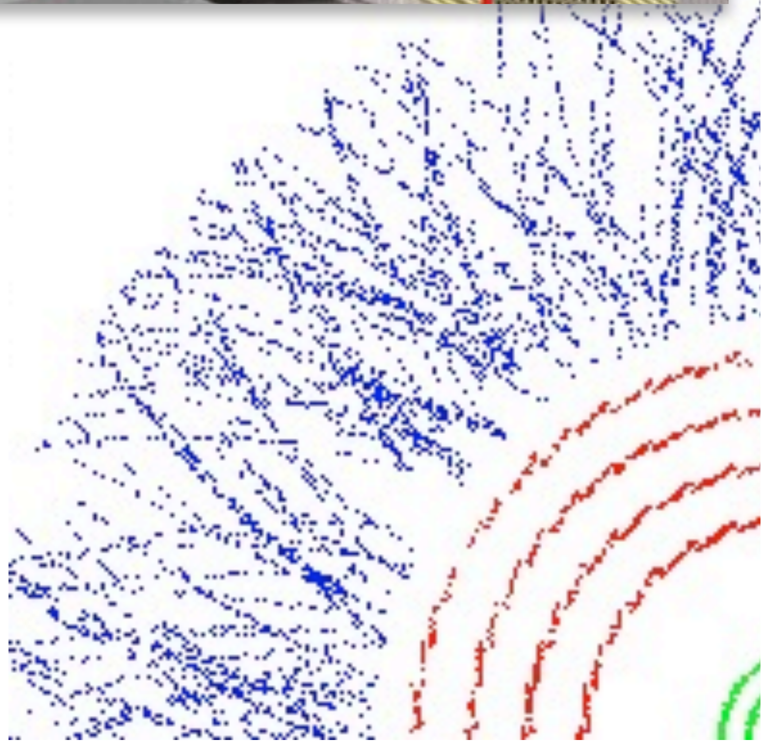

TRT Barrel

- longitudinal straws of 1.5 m length
- three layers of 32 modules each, 52 544 straws
- wires electrically split, read out on both sides
- ranging from r = 0.5 m to r = 1.1 m, covering $|\eta| < 1$

TRT Endcap A and C

- radial straws of 0.4 m length
- 8 inner wheels, 12 outer wheels per side, 122 880 straws
- wires read out at their outer end
- ranging from $|z| = 0.8$ m to $|z| = 2.7$ m, covering $1 < |\eta| < 2$

Transition radiation tracker

Signal formation

- charged particles ionize the gas
- electrons drift towards the wire
- gas amplification avalanche
- first arrival determines drift time

Signal readout

- signal gets amplified
- sampled in 24 time bins of 3.12 ns
- each time bin compared against threshold (≈ 300 eV): 24-bit pattern
- buffered in 6-μs readout pipeline
- passed on to central ATLAS DAQ

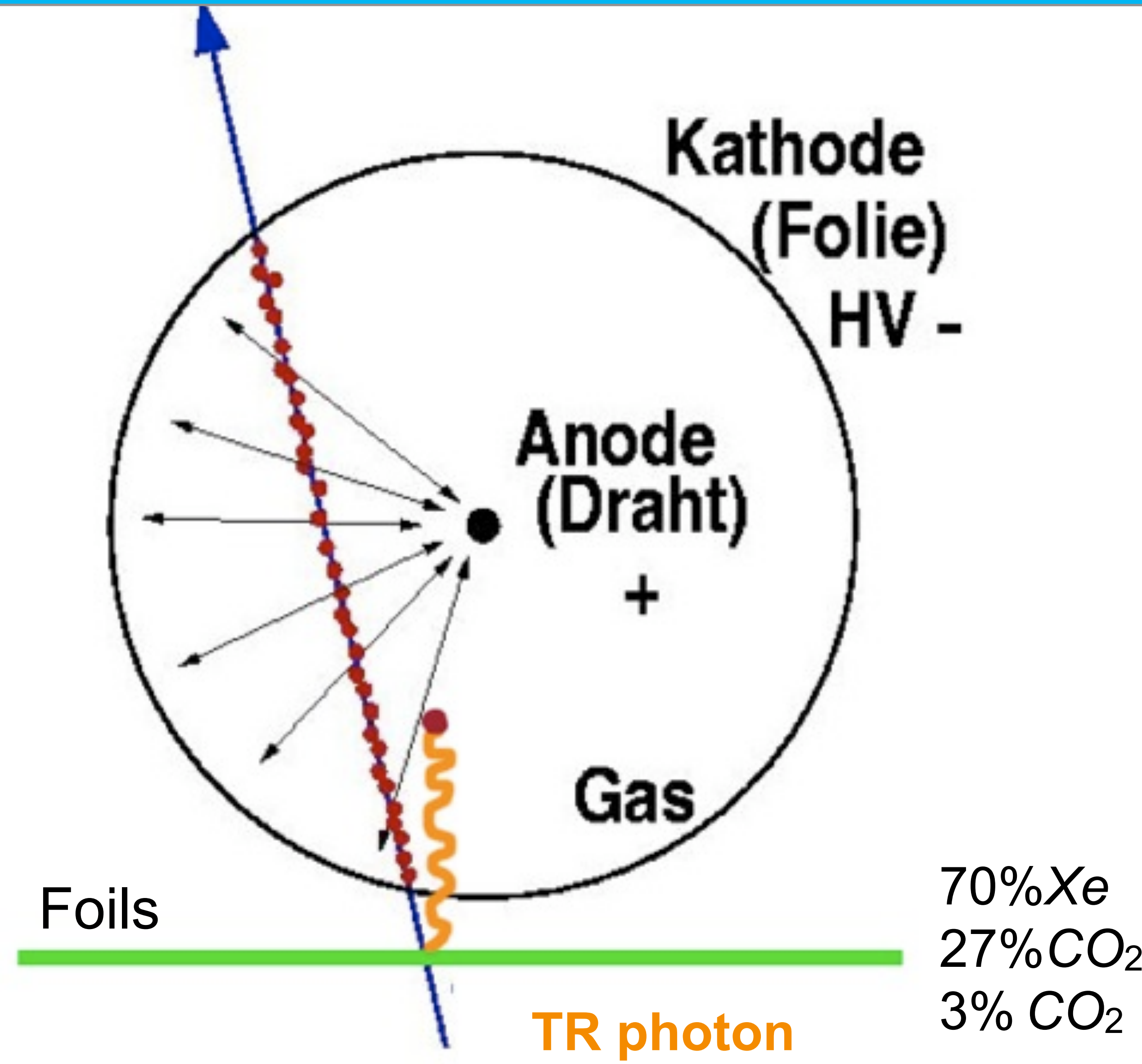

allows self suporting structures

A Stack of Straws

Endcap (~32000 straws)
radial from beam axis

ATLAS Inner Detector

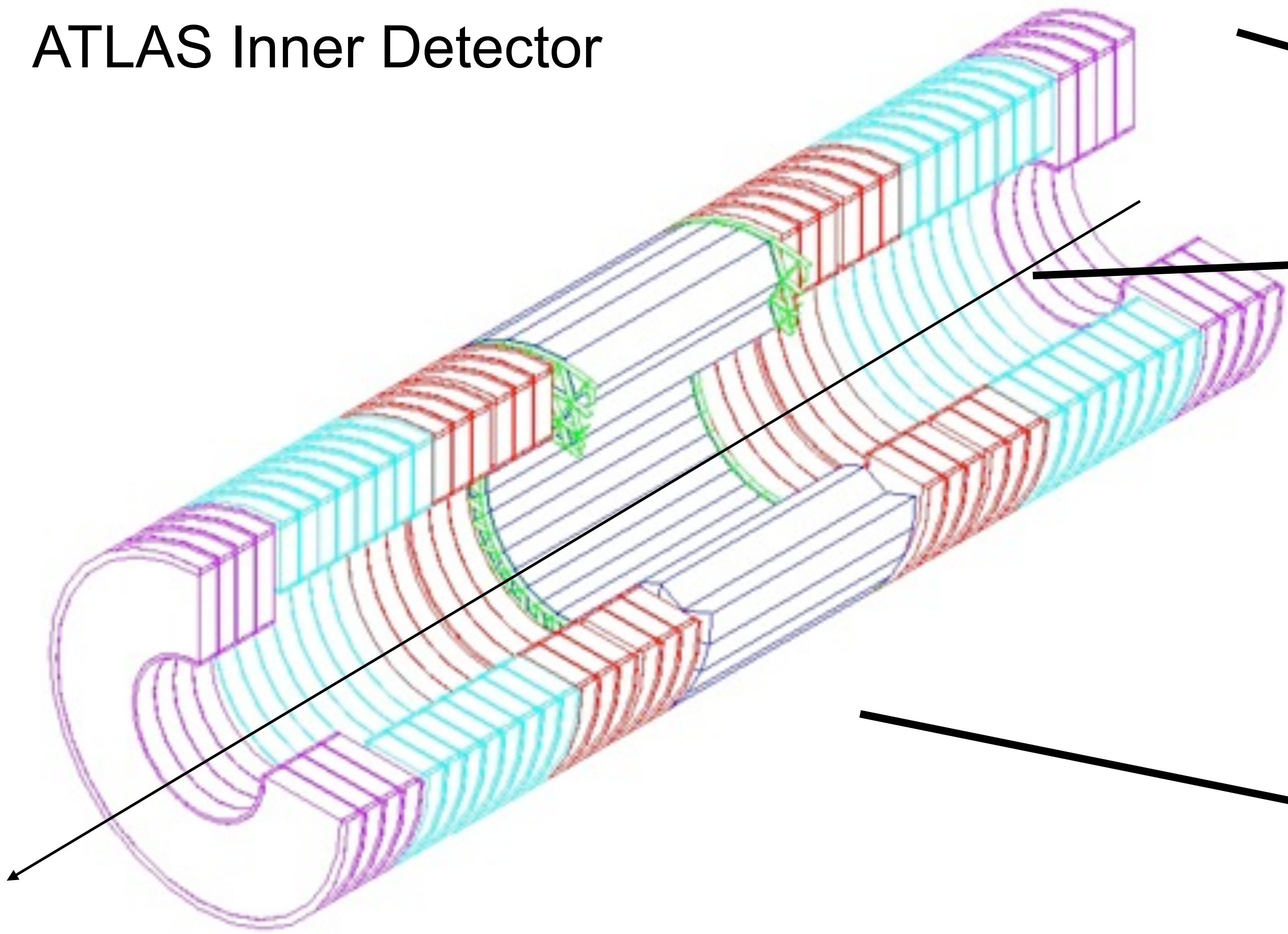

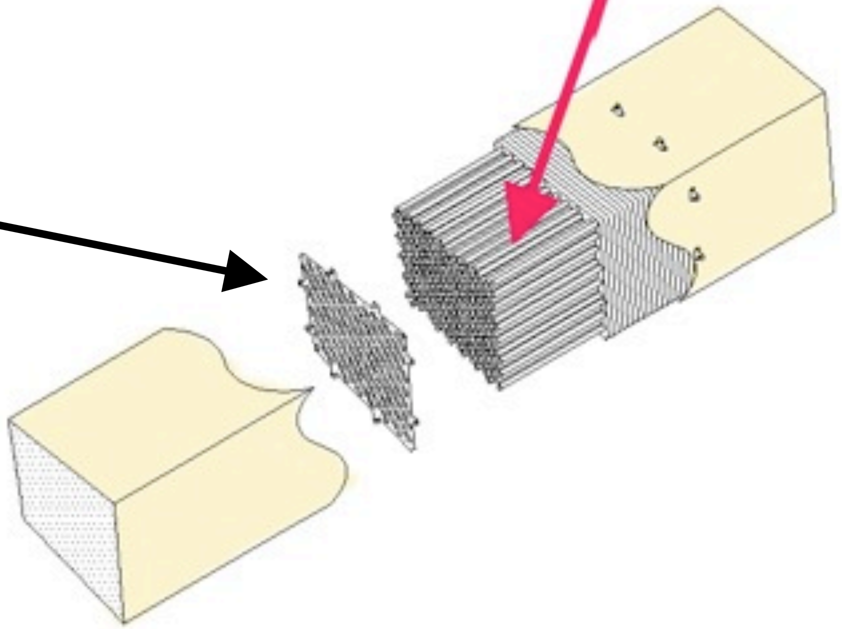

Barrel (~10000 straws)
parallel to beam axis

The First ATLAS TRT End-Cap (3 Aug 2005)

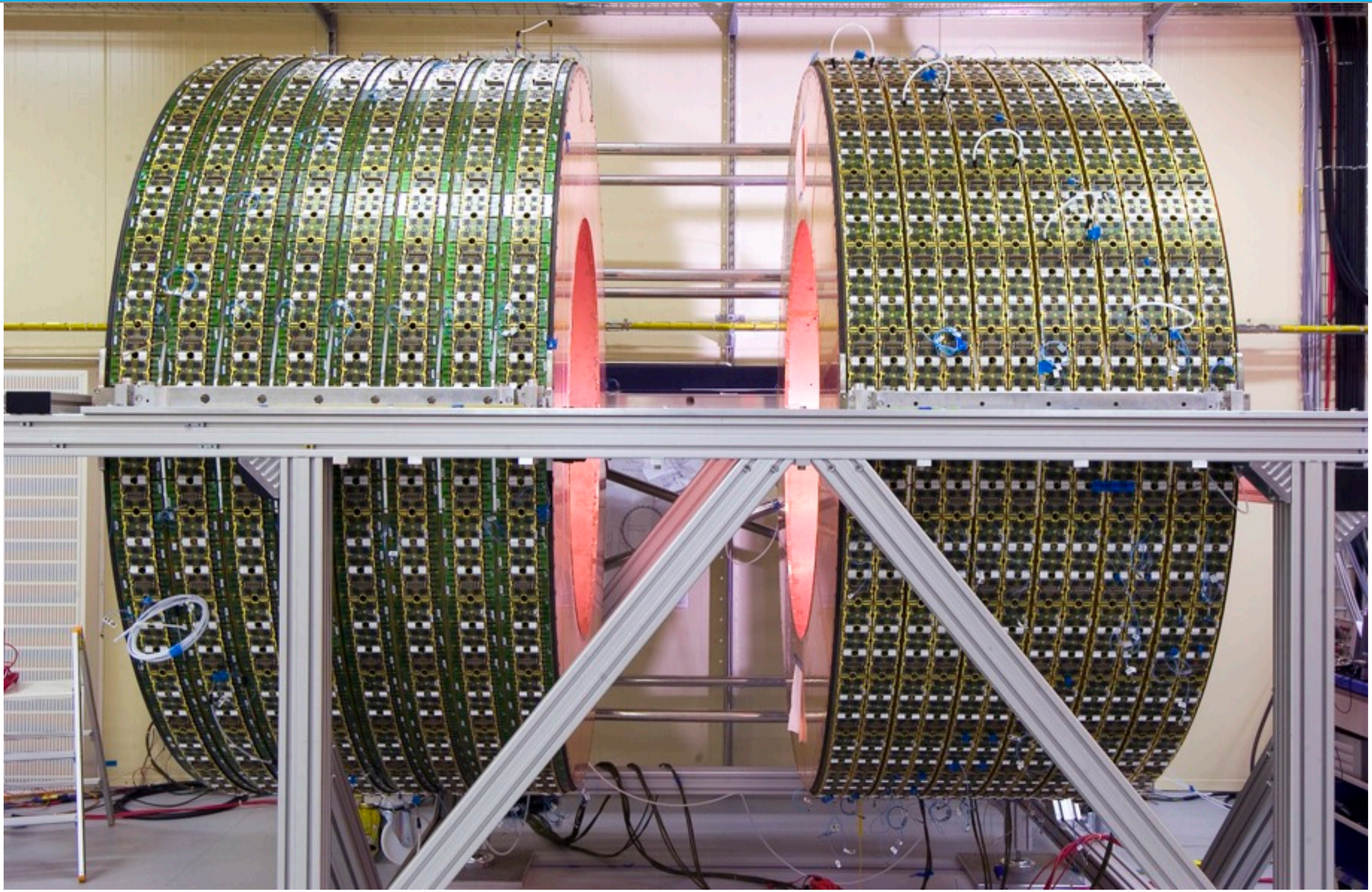

Semiconductor Detectors

Large Silicon Systems

- ~1950: Discovery that pn-Junctions can be used to detect particles.
  - Semiconductor detectors used for energy measurements (Germanium)
- Since ~ 30 years: Semiconductor detectors for precise position measurements.
  - precise position measurements possible through fine segmentation (10-100µm)
  - multiplicities can be kept small (goal:<1%)

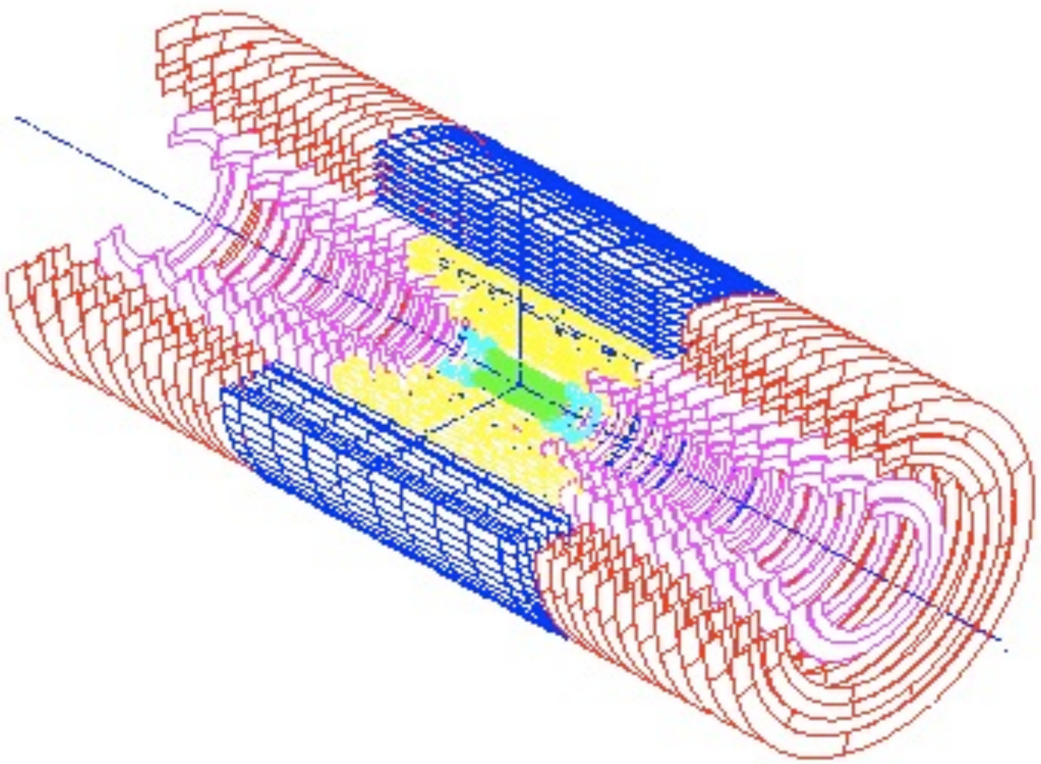

CMS Silicon Tracker (~2007)

~12,000 modules

~ 223 m^2 silicon area

~25,000 silicon wafers

~ 10M readout channels

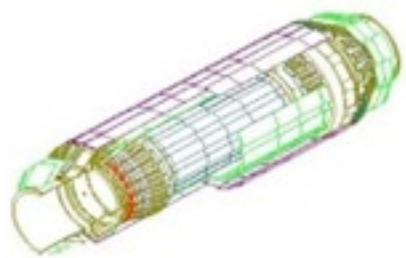

DELPHI (1996-2000)

~ 1.8m^2 silicon area

~ 175 000 readout channels

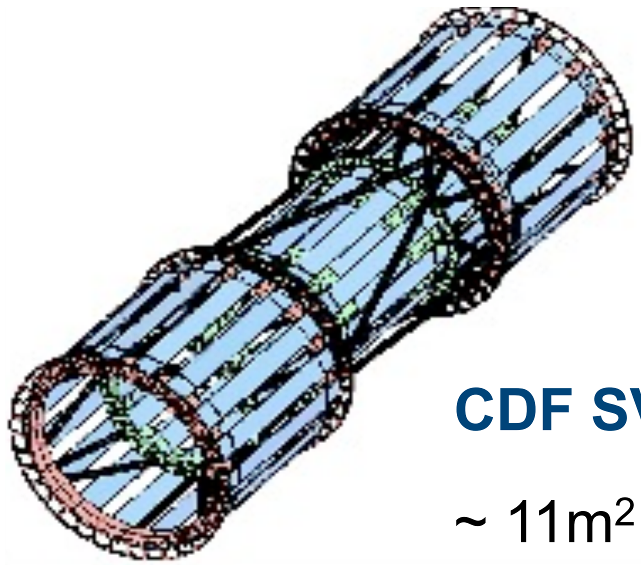

CDF SVX IIa (2001-2011)

~ 11m^2 silicon area

~ 750 000 readout channels

Semiconductor Basics I

- In free atoms the electron energy levels are discrete.
- In a solid, energy levels split and form a nearly-continuous band.

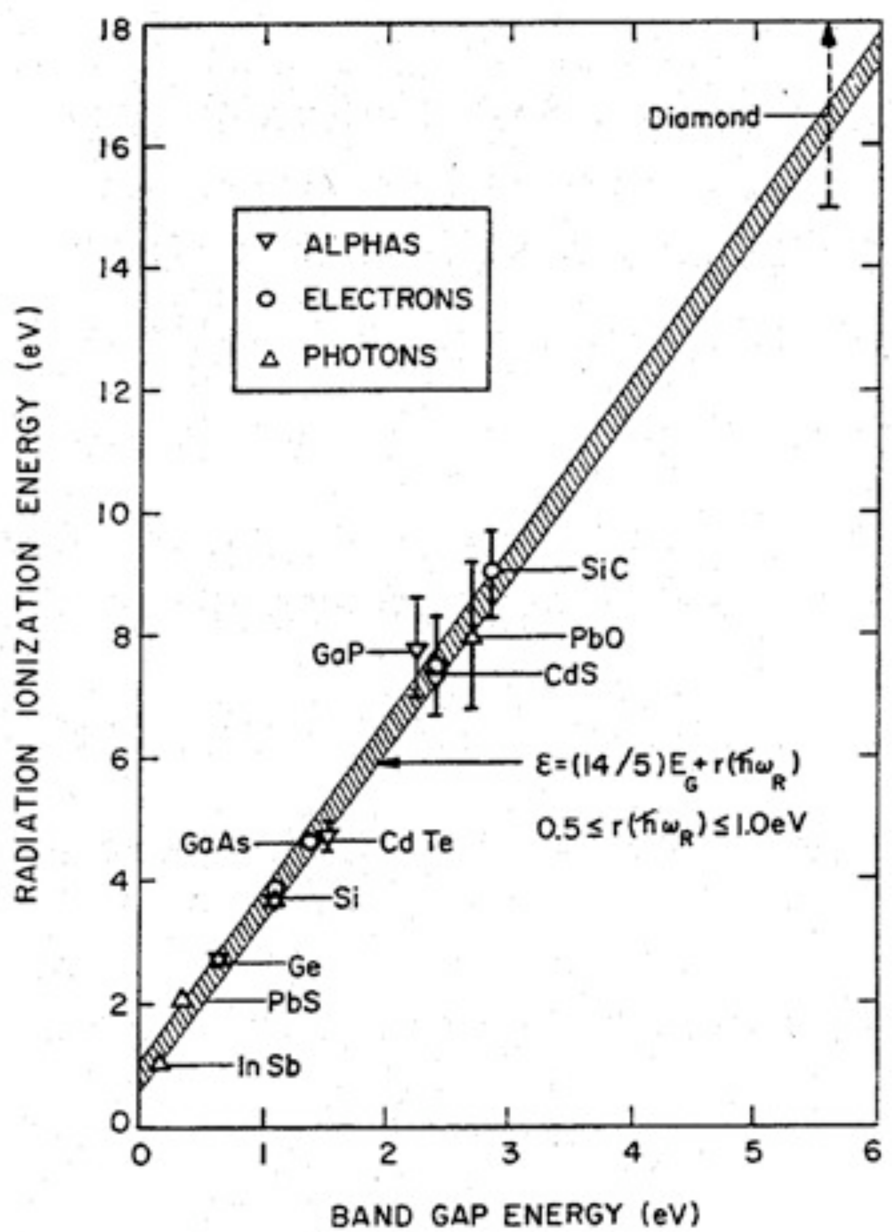

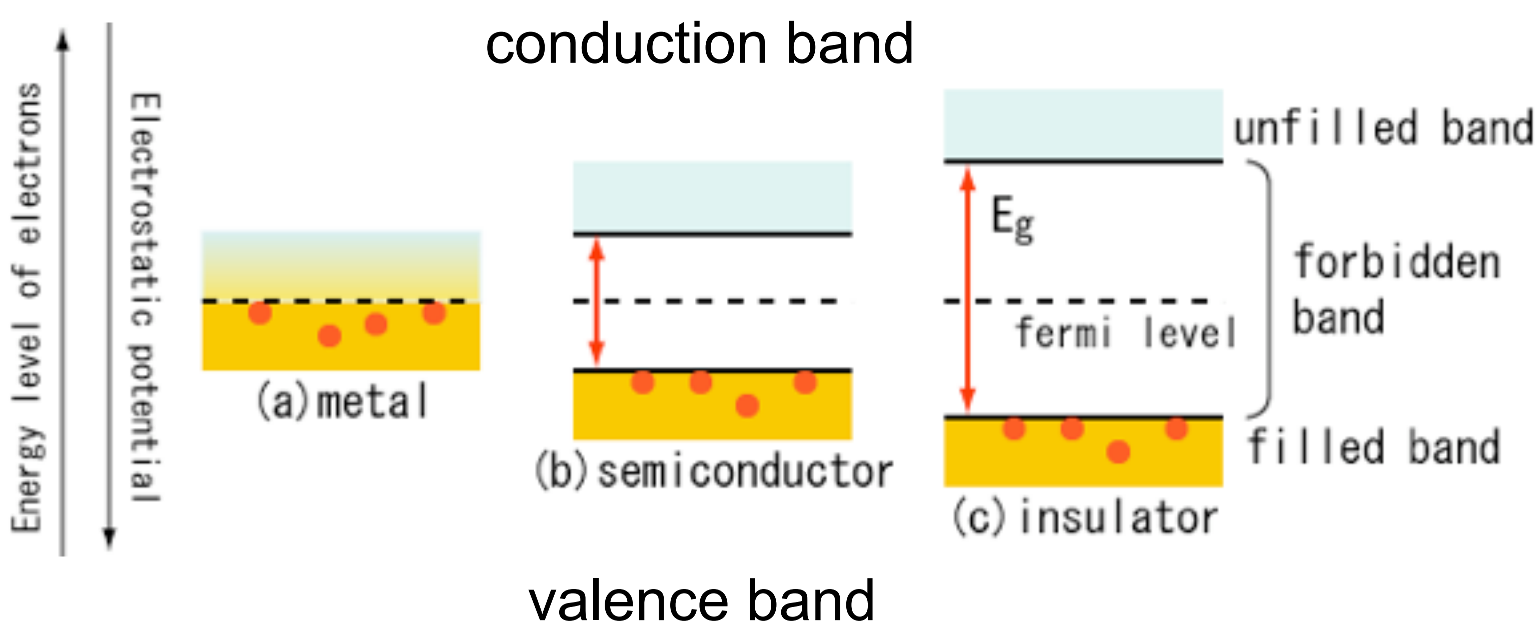

- Large gap: the solid is an insulator.
- No gap: it is a conductor.
- Small band gap: semiconductor

- For silicon, the band gap is 1.1 eV, but it takes 3.6 eV to ionize an atom. The rest of the energy goes to phonon exitations (heat).

Doping Silicon

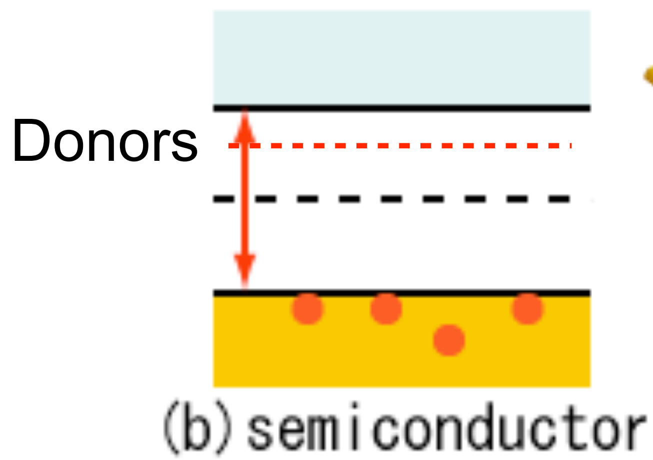

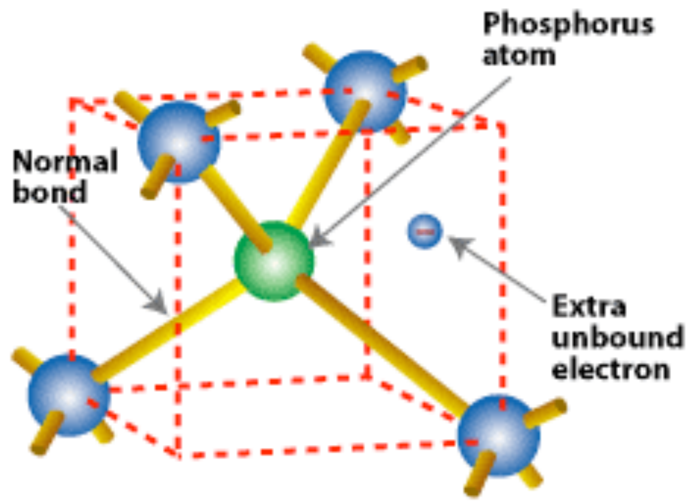

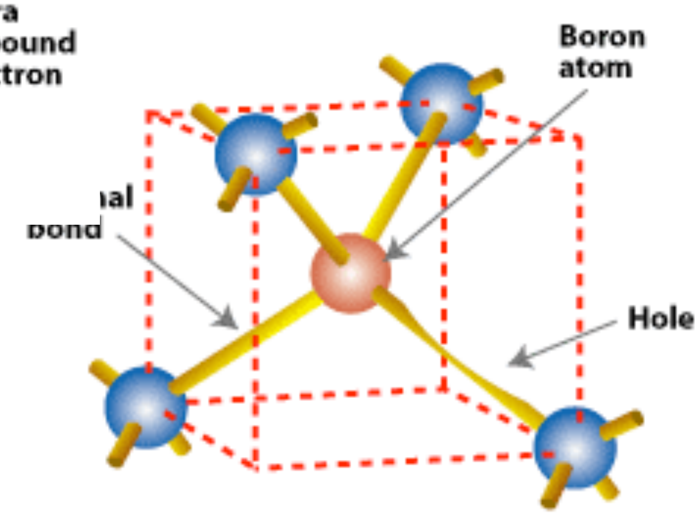

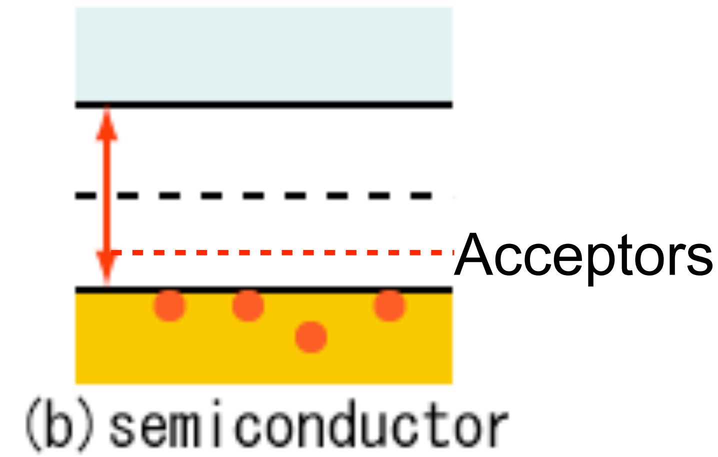

n-type:

- In an n-type semiconductor, negative charge carriers (electrons) are obtained by adding impurities of donor ions (eg. Phosphorus (type V))

- Donors introduce energy levels close to conduction band thus almost fully ionized

Electrons are the majority carriers.

p-type:

- In a p-type semiconductor, positive charge carriers (holes) are obtained by adding impurities of acceptor ions (eg. Boron (type III))

- Acceptors introduce energy levels close to valence band thus 'absorb' electrons from VB, creating holes

Holes are the majority carriers.

PN-Junction

- p- and n-doted semiconductor combined
- Gradient of electron and hole densities results in a diffuse migration of majority carriers across the junction.
- Migration leaves a region of net charge of opposite sign on each side, called the depletion region (depleted of charge carriers).

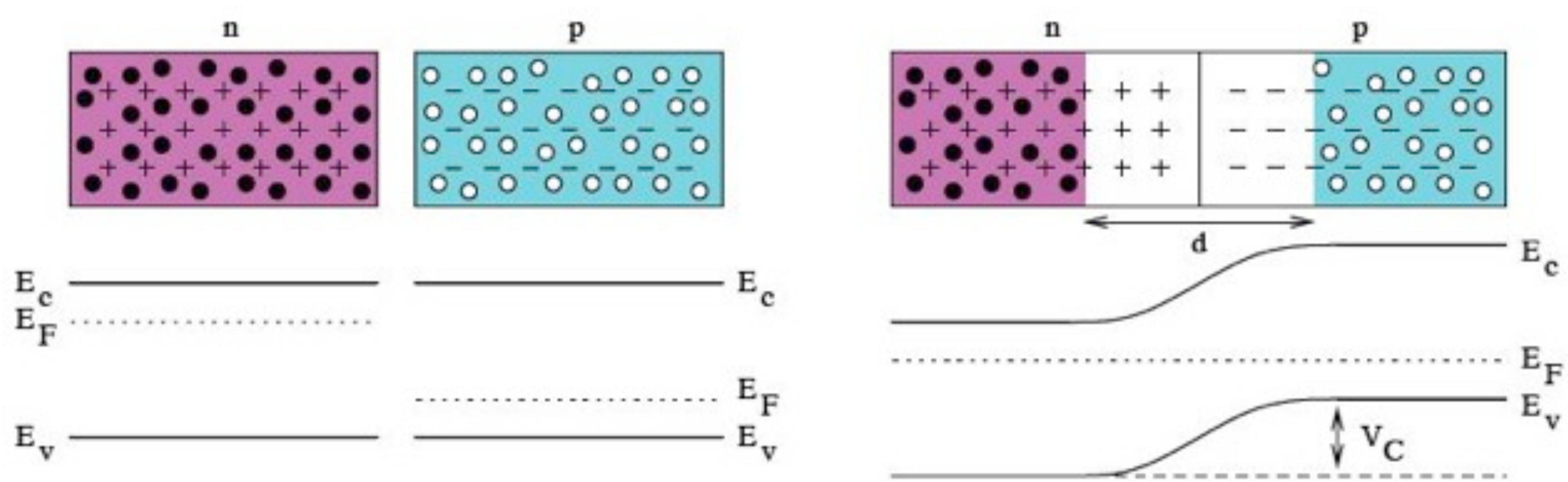

- Artificially increasing this depleted region by applying a **reversed bias voltage** allow charge collection from a larger volume

$$d = \sqrt{\frac{2\epsilon\epsilon_0 V}{e}\left(\frac{1}{n_D} + \frac{1}{n_A}\right)} \qquad \text{with} \qquad n_A >> n_D \qquad d = \sqrt{\frac{2\epsilon\epsilon_0 V}{e n_D}}$$

Principle of semiconductor Detectors

1. Creation of electric field:
   voltage to deplete thickness d

$$V_{\text{dep}} = d^2 N_{\text{eff}} \frac{q}{2\epsilon\epsilon_0}$$

N_{eff} : doping concentration

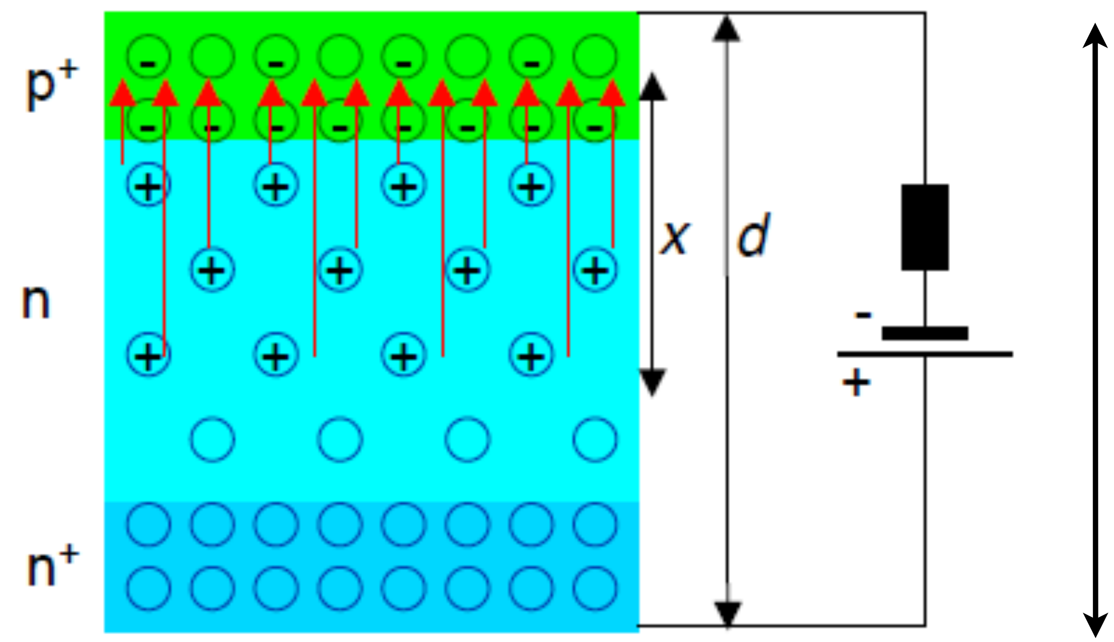

in "classical" HEP detectors 100-300 um

2. Keep dark current low

$$I \propto \frac{1}{\tau_g} \cdot T^2 \exp - \frac{E_g}{2kT} \times \text{volume}$$

τ_g : charge carrier life time

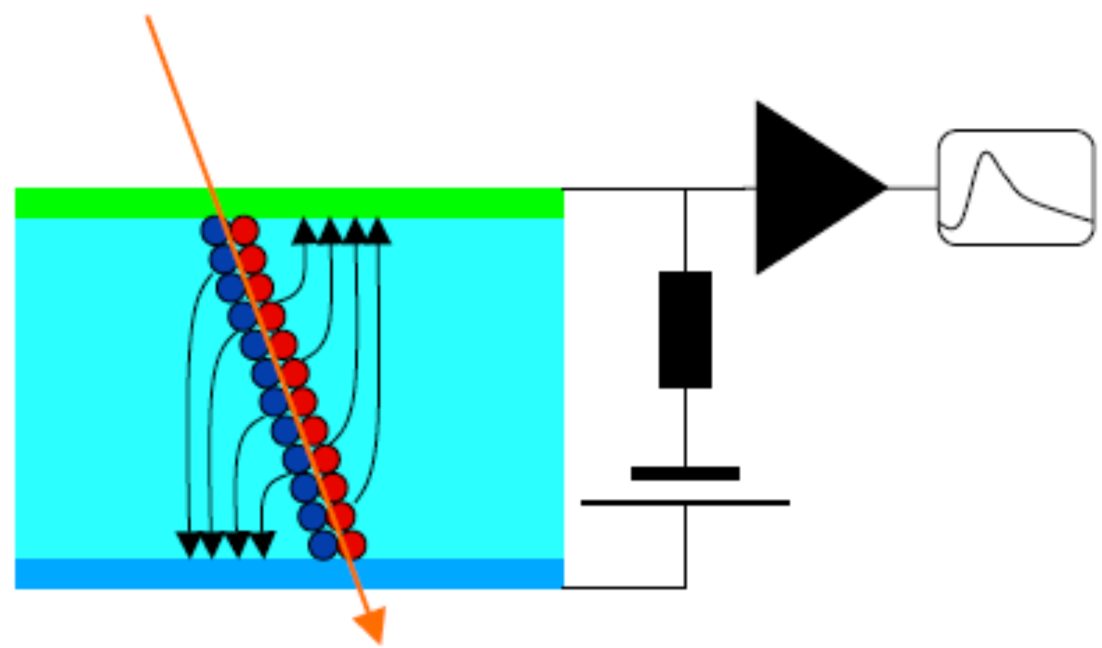

3. Ionising particles create free charge carrier

4. Charge carrier drift to electrodes and induce signal

Material Properties

	Si	Ge	GaAs	CdTe	Diamant	SiC
band gap	1.12	0.67	1.42	1.56	5.48	2.99
energy for e-p pair [eV]	3.6	2.9	4.2	4.7	13.1	6.9
e- for MIP (300µm)	24000	50000	35000	35000	9300	19000
Z	14	32	31+33	48+52	6	14+6

Why is silicon used more often ?

- Silicon is the only material which can be produced in larger wafers in high quality
- compare to kT = 0.026 eV at room temperature -> dark current under control
- high density compared to gases: ρ=2.33g/cm^3
- good mechanical stability -> possible to produce mechanically stable layers
- large charge carrier mobility
- fast charge collection δt~10ns

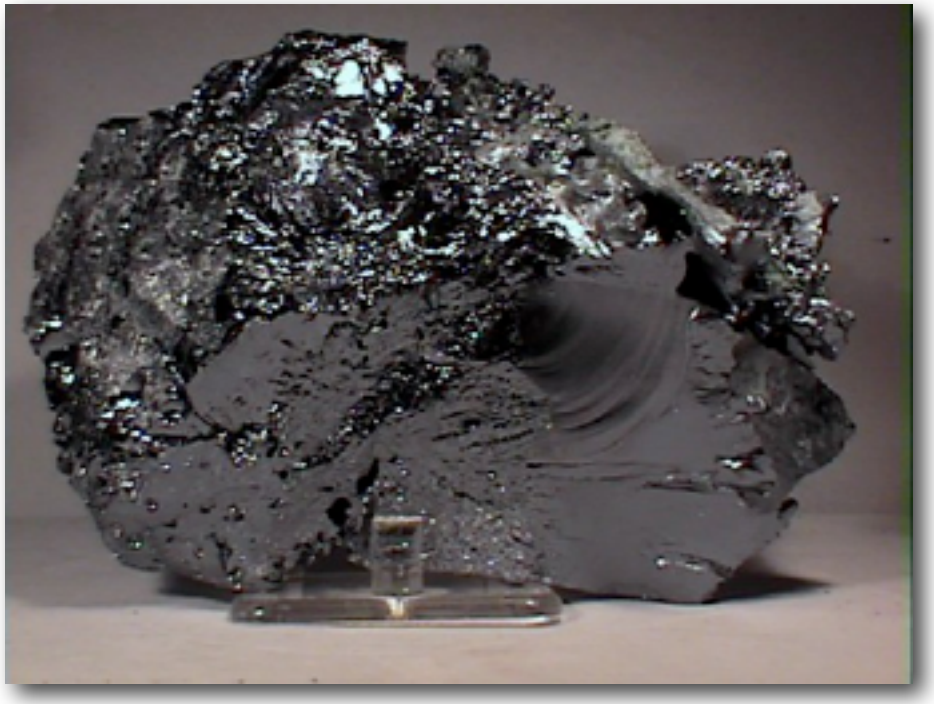

Protons in Silicon

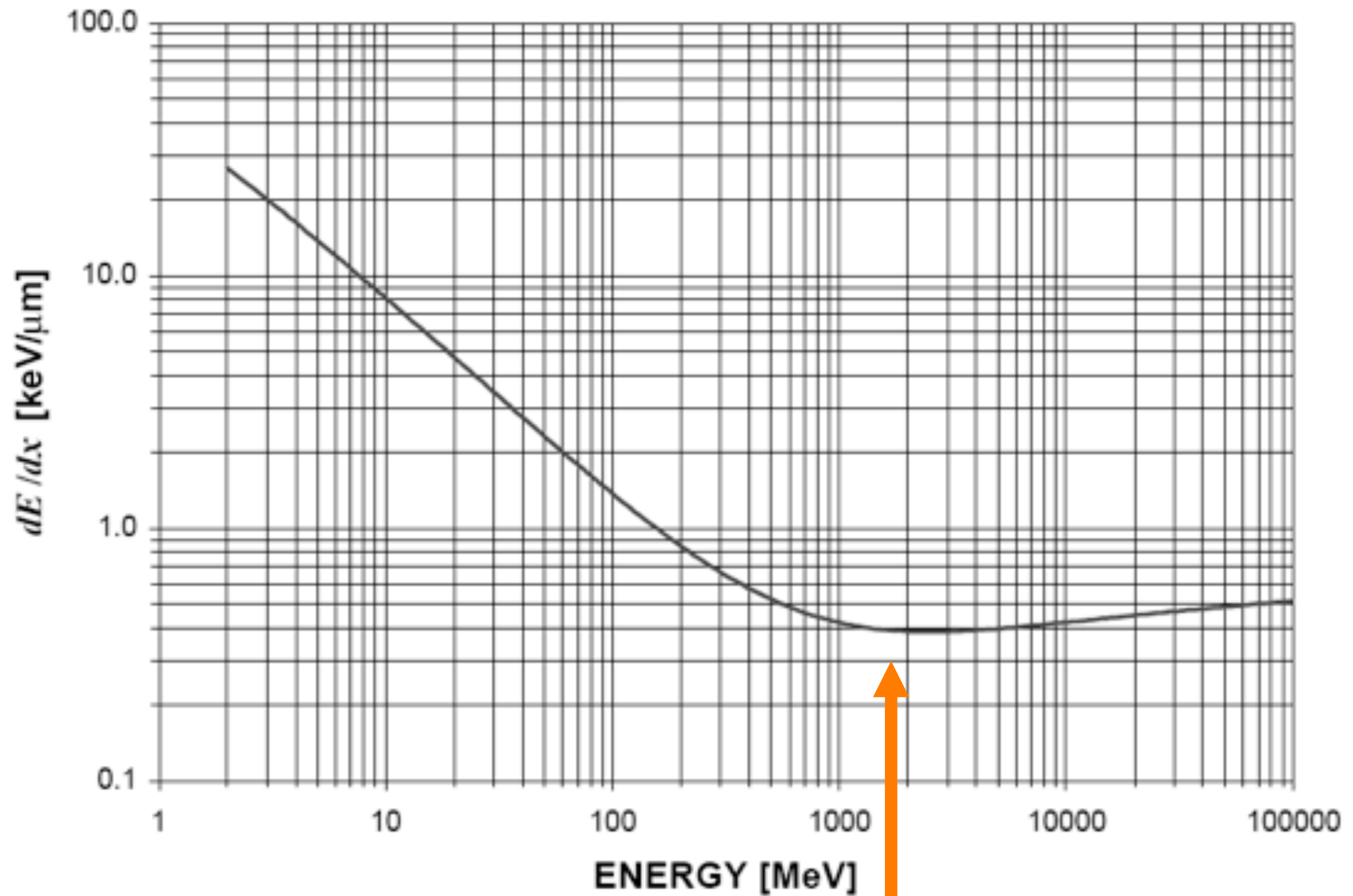

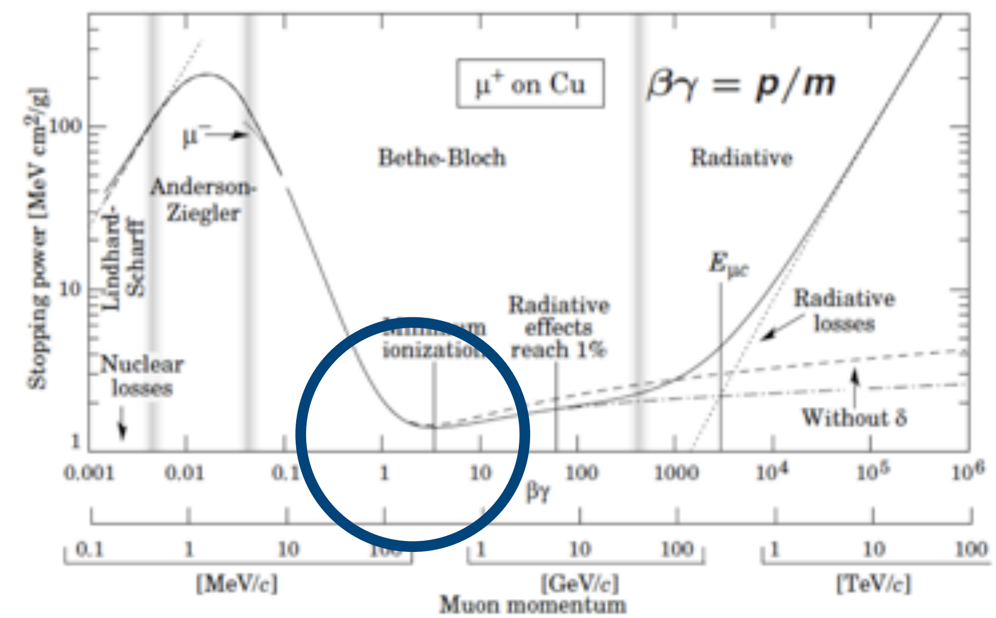

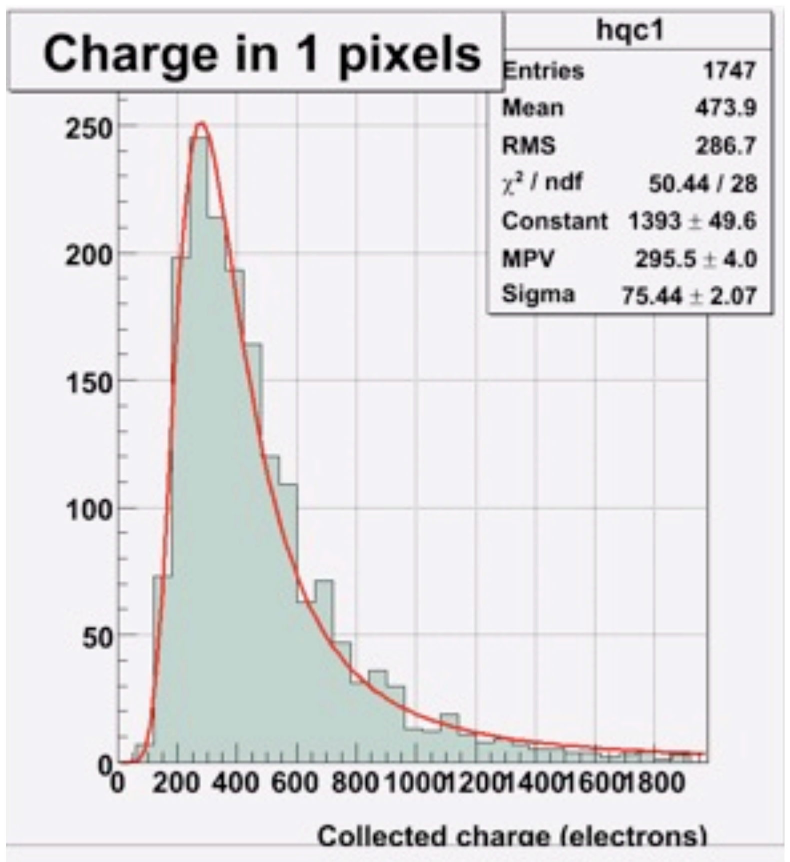

- 0.4 keV/µm
- -> 3.6 eV creates electron hole pair
- => ~110 electron-hole pairs per µm (mean value)
- most probably number: 80 electrons

Problem: Radiation Damage

- Impact of Radiation on Silicon:
- Silicon Atoms can be displaced from their lattice position
- Point defects (EM Radiation)
- Damage clusters (Nuclear Reactions)
- Important in this context:
  - Bulk Effects: Lattice damage: Generation of vacancies and interstitial atoms (NIEL: Non Ionizing Energy Loss) **(main problem for sensors)**
  - Surface effects: Generation of charge traps (Oxides) (by ionizing energy loss) **(main problem for electronics)**

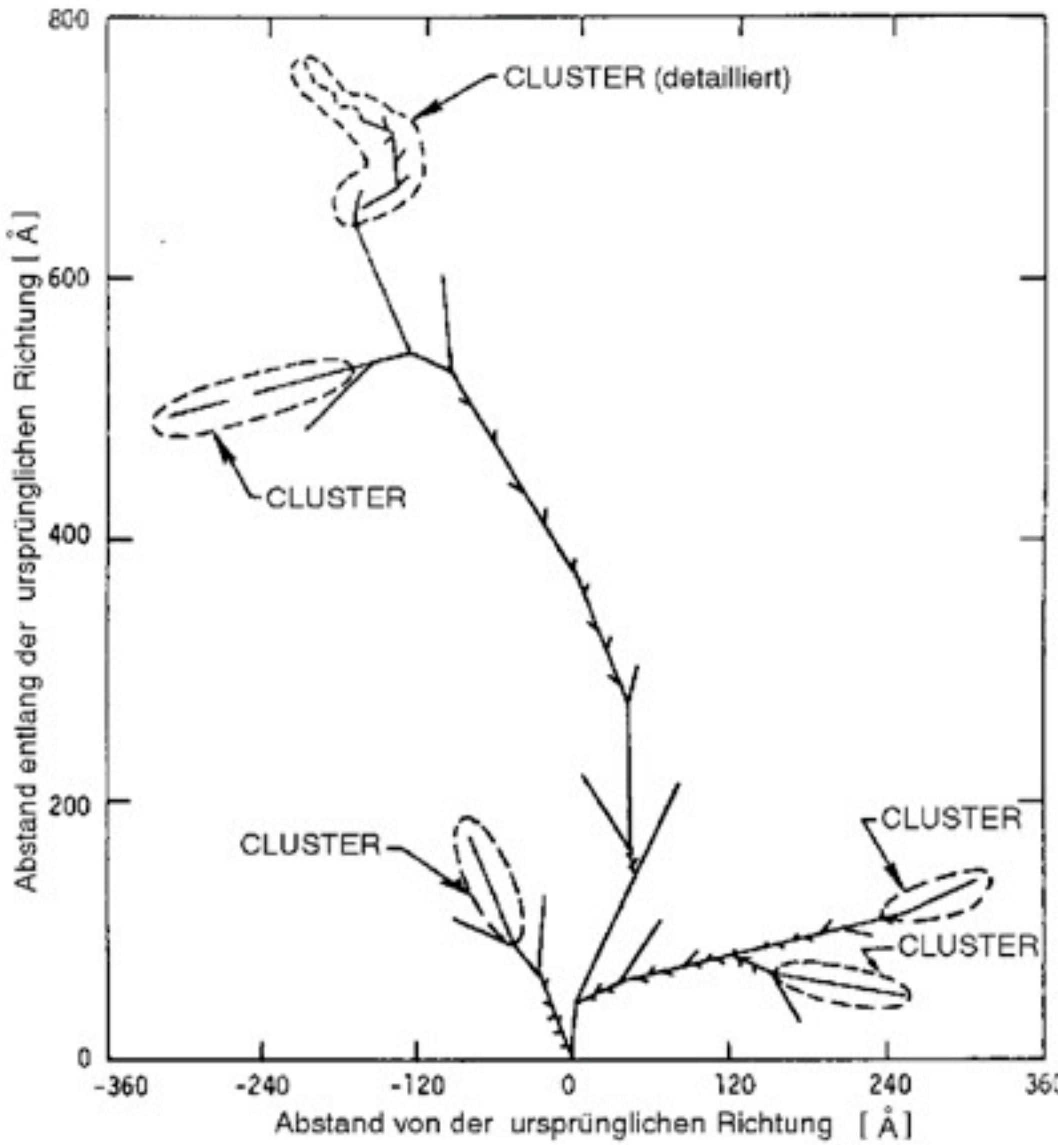

Filling of energy levels in the band gap

➪ direct excitation now possible

➪ higher leakage current

➪ more noise

➪ “Charge trapping”, causing lower charge collection efficiency

Can also contribute to space charge: Higher bias voltage necessary.

Consequences of Radiation Damage

Macroscopic constant: leakage current and depletion voltage

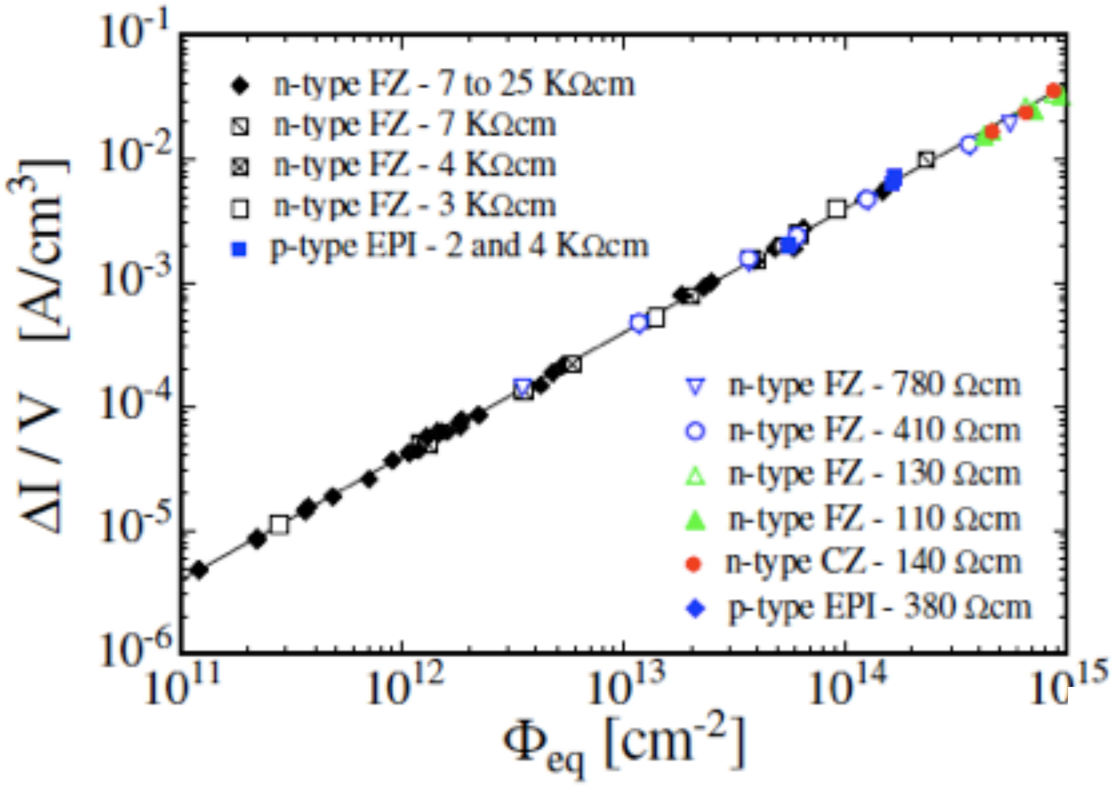

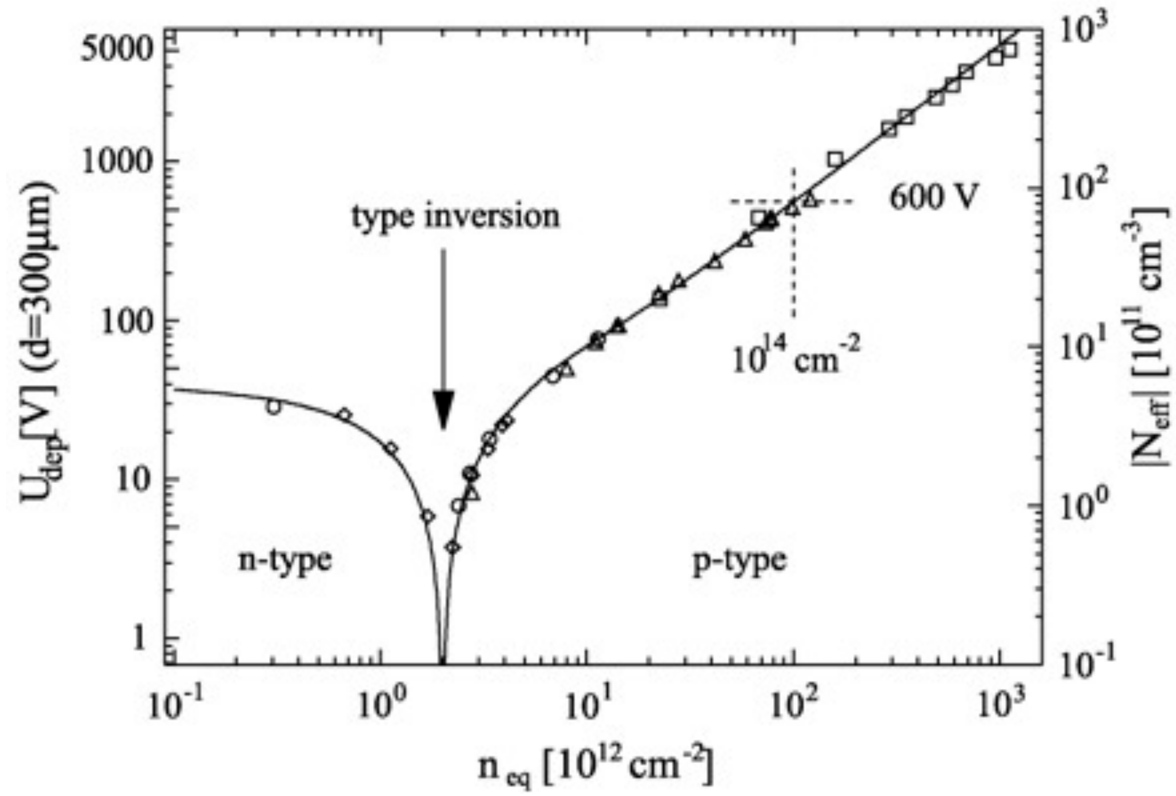

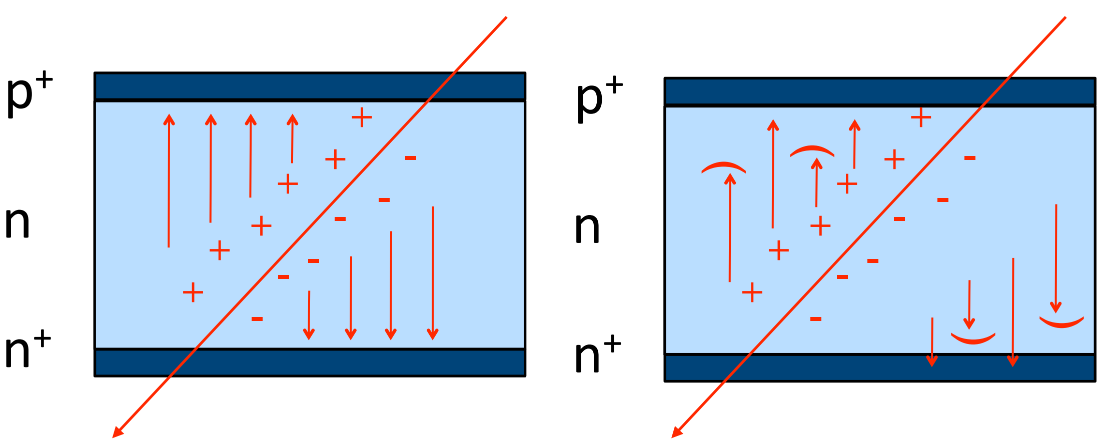

Charge trapping in defects

Counter measures

- Geometrical: develop sensors that can withstand higher depletion voltages
- Thinner sensors (but FE electronics with higher sensitivity needed)
- Environment: sensor cooling (~-10 C)
- Slowing down of “reverse annealing”
- Lower leakage currents

ATLAS Silicon Tracker (SCT)

Strip Detectors

- First detector devices using the lithographic capabilities of microelectronics
- First Silicon detectors -> strip detectors
- Can be found in all high energy physics experiments of the last 25 years

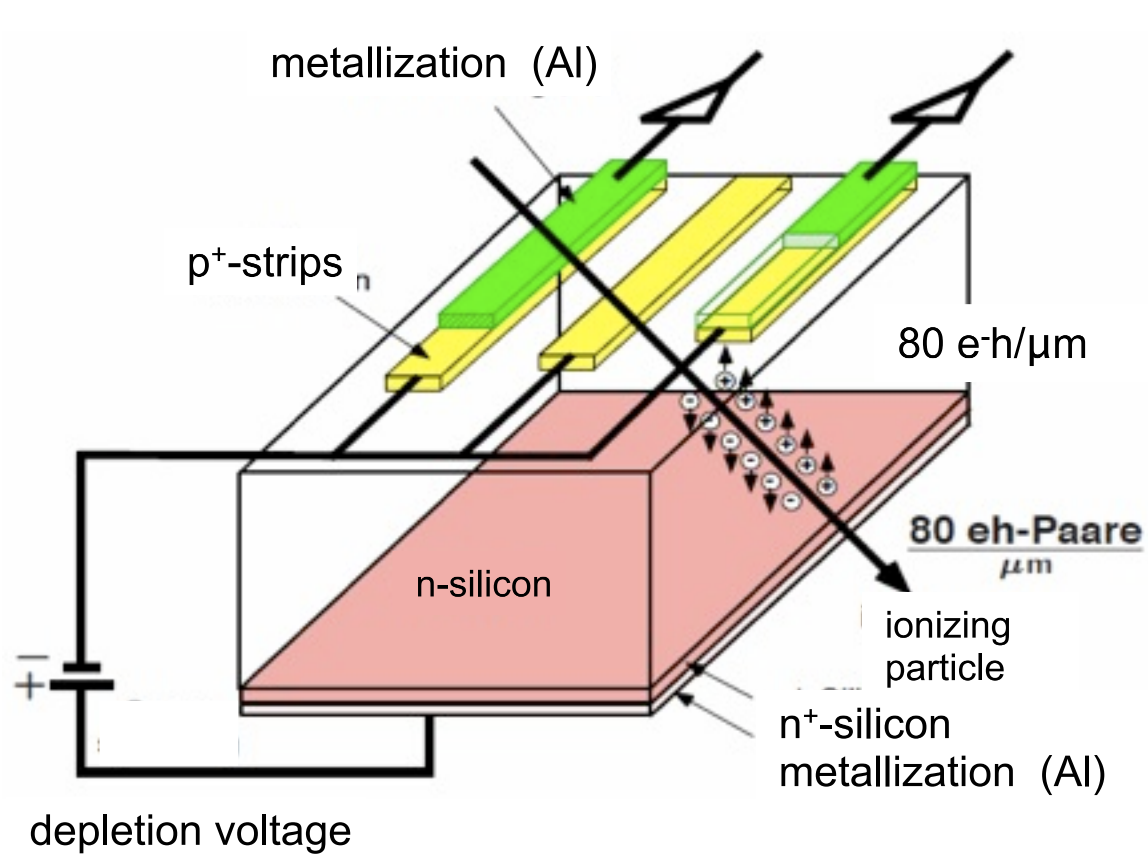

Principal: Silicon strip detector

- Arrangement of strip implants acting as charge collecting electrodes.
- Placed on a low doped fully depleted silicon wafer these implants form a one-dimensional array of diodes
- By connecting each of the metalized strips to a charge sensitive amplifier a position sensitive detector is built.
- Two dimensional position measurements can be achieved by applying an additional strip like doping on the wafer backside (double sided technology)

First HEP Application: NA11

- After discovery of charm (1974), τ-lepton (1975) and beauty (1977) with lifetimes cτ ~100 μm: need fast (ns), and precise (μm) electronic tracking detectors

- strip detector for NA11 in 1981
  - 1200 strip-diodes
  - 20 μm pitch
  - 60 μm readout pitch
  - 24 x 36 mm^2 active area ~0.01m^2
  - position resolution ~5.4 μm
  - 8 layer at the start
    - ➔ precise track reconstruction

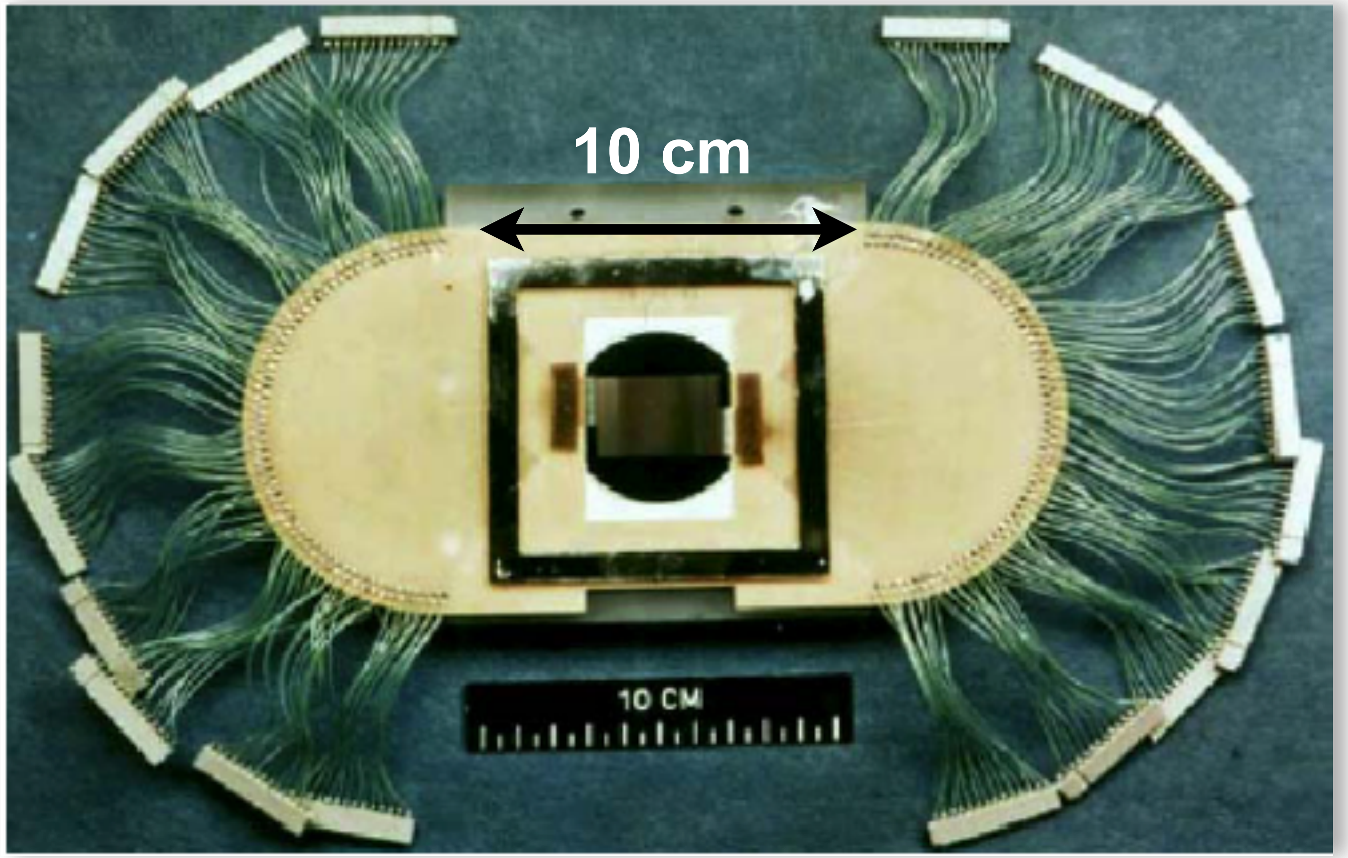

- readout electronic: ~1m^2!

Silicon Microstrip Detectors for LHC

Early 1990's: At the time of the Conceptual Design of the pp Experiments

- Radiation damage poorly understood
- Cost/unit area was prohibitively large
- Large no. of channels required

What was known :

- leakage current increased linearly with fluence
- type inversion – higher and higher bias voltage required
- reverse annealing

What was done (~10 years R&D)

- HV behaviour improved by careful processing and use of multiple guard rings
- Si detectors had to be kept permanently cold
- Fast pre-amplifiers developed to cope with 25ns colliding bunches
- Cost/unit area significantly reduced by growing larger diameter ingots (6" instead of 4"), single-sided processing (p-on-n)
- Implementation of front-end read-out chip in industry standard deep sub-micron technology

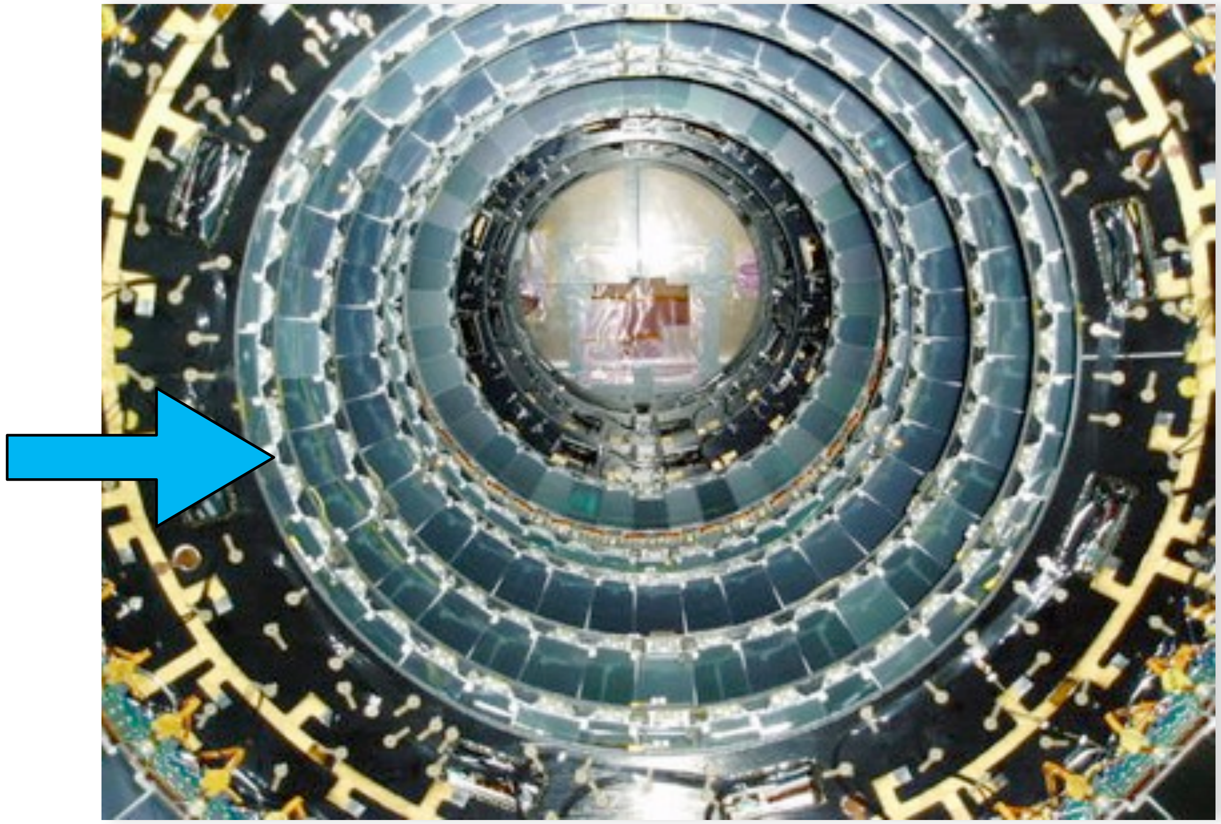

ATLAS SCT Barrel

SCT Construction and Collision First Data …

$61 m^2$ of silicon micro-strip detectors
~20,000 separate sensors ordered

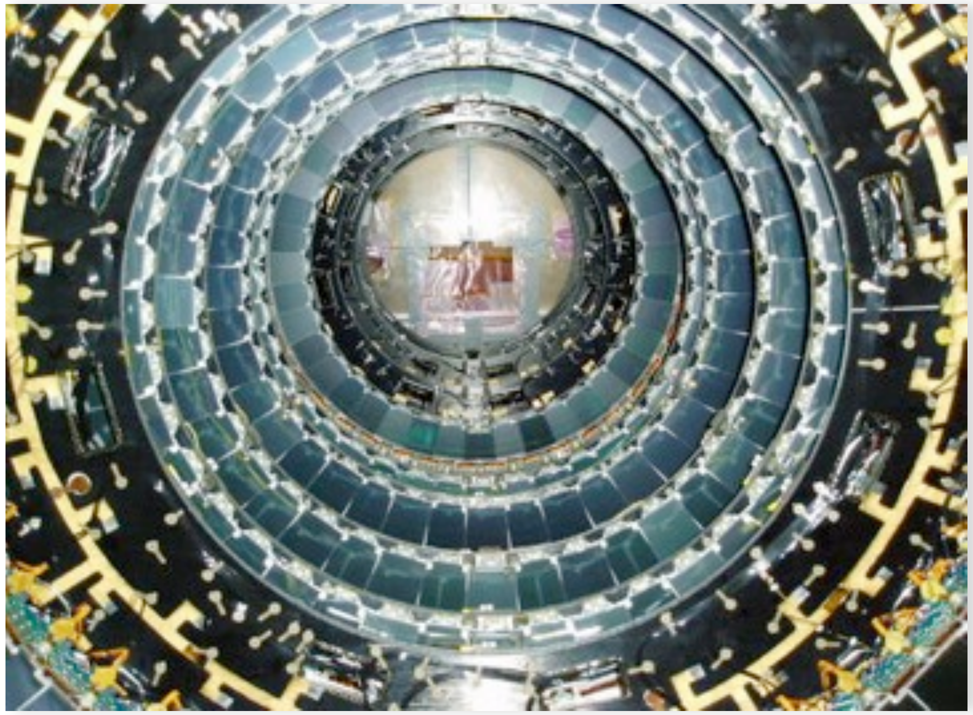

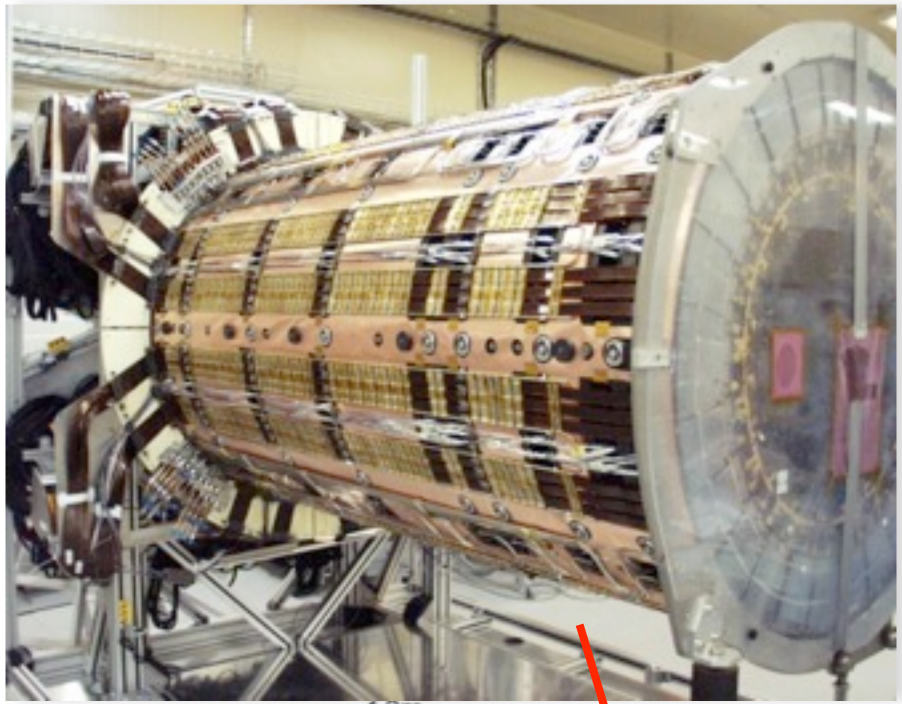

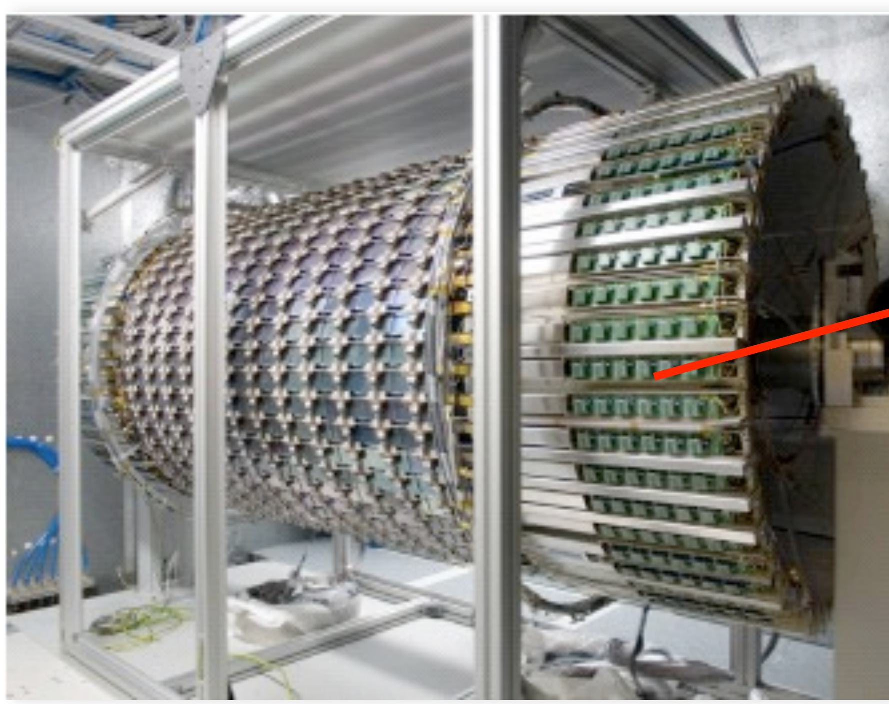

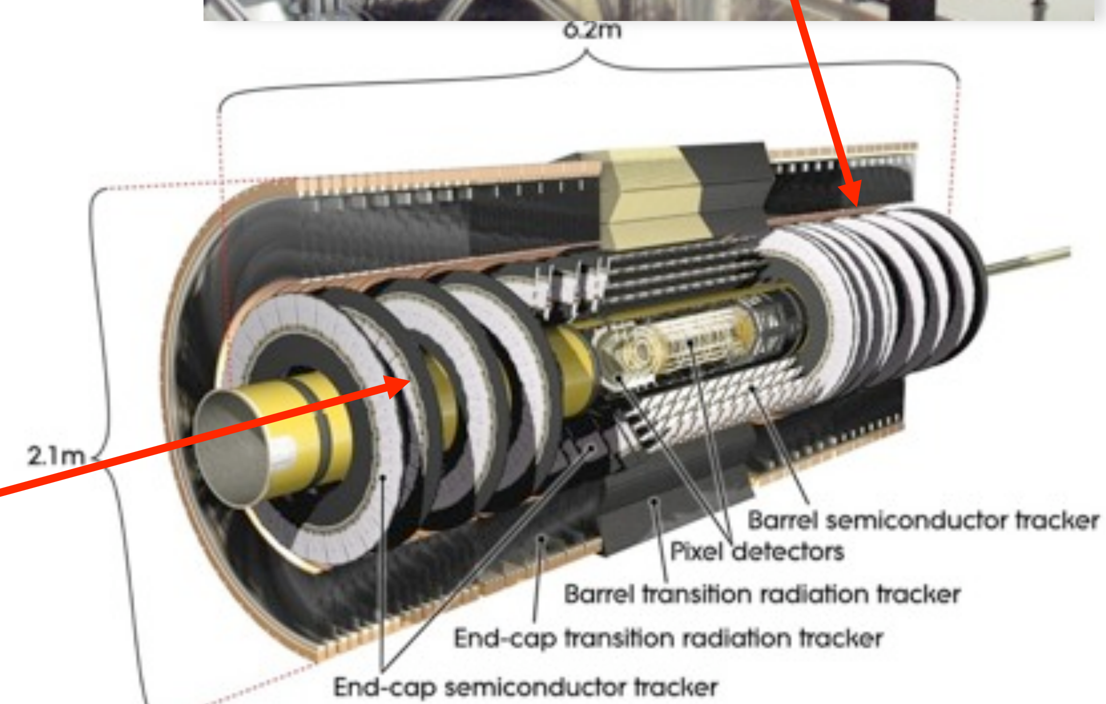

Designed to record events in collisions at 40 million bunch crossings per second.
Measure particles trajectories with 10μm precision (7 Mio channels).
withstand radiation levels of up to100kGy

The Semiconductor Tracker

- The SemiConductor Tracker (SCT) is organized in 4 layers barrel, built with 2112 modules and two 9 disks end-caps, made of 1976 modules.
- The total number of strips is 6.3 10^6.

The barrel module consists of four single sided p-on-n strip detectors:

- Pitch 80 μm
- Strip length 120 mm
- Stereo angle 40 mrad

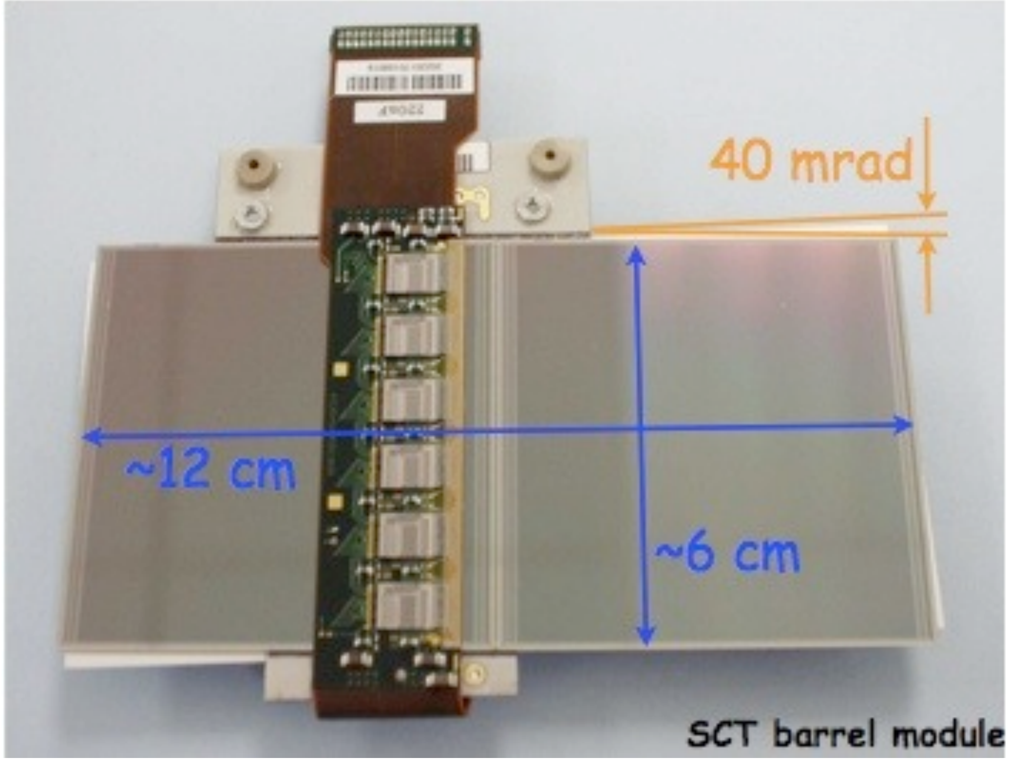

The end-caps are built with three different modules:

- Pitch 57-95 μm
- Strip length 55-120 mm

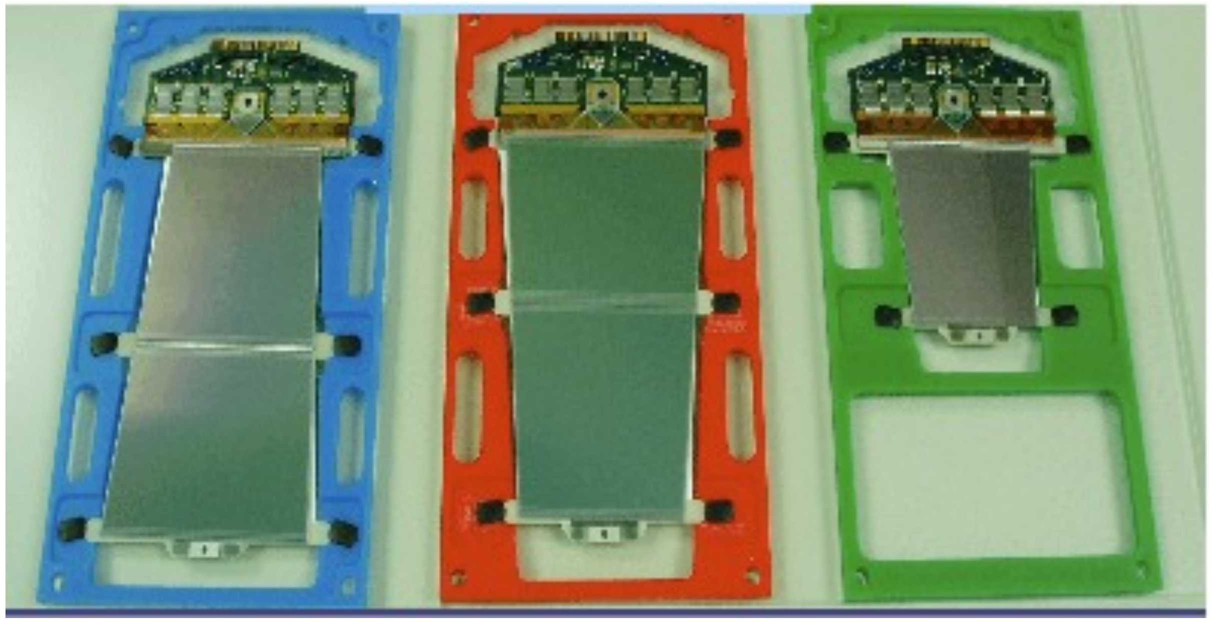

ATLAS Pixel Detector

Limits of Strip Detectors

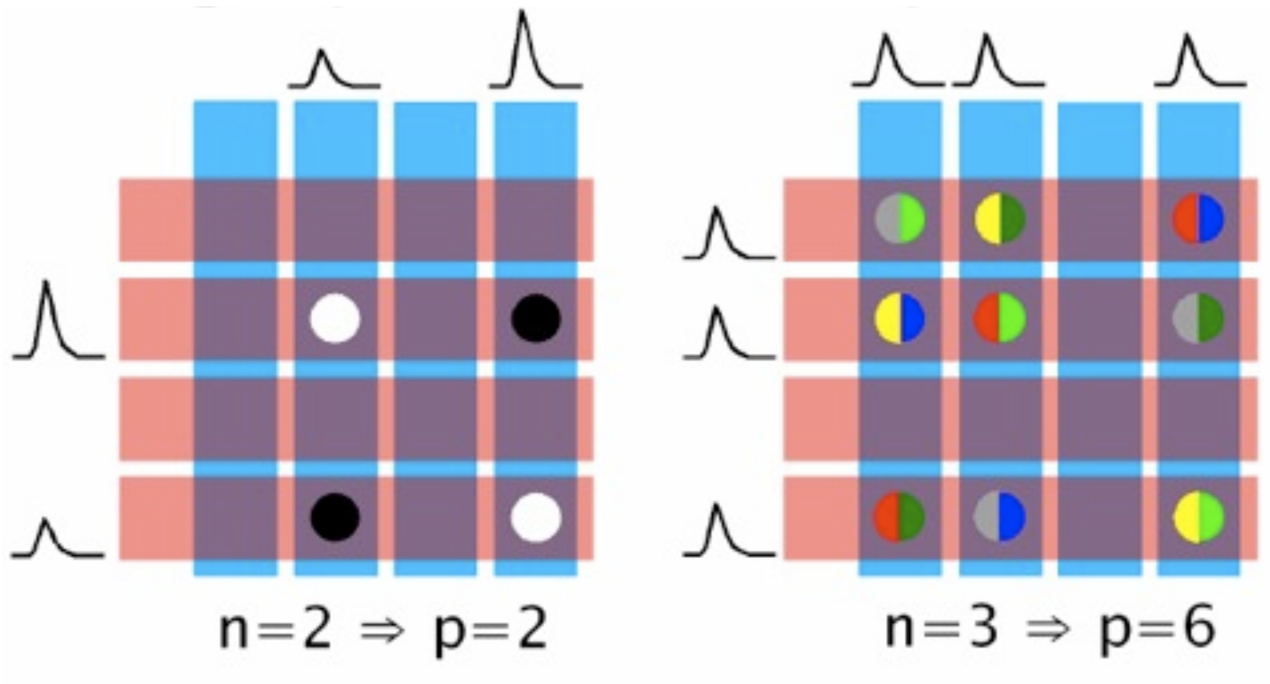

- In case of high particle fluences ambiguities give difficulties for the track reconstruction

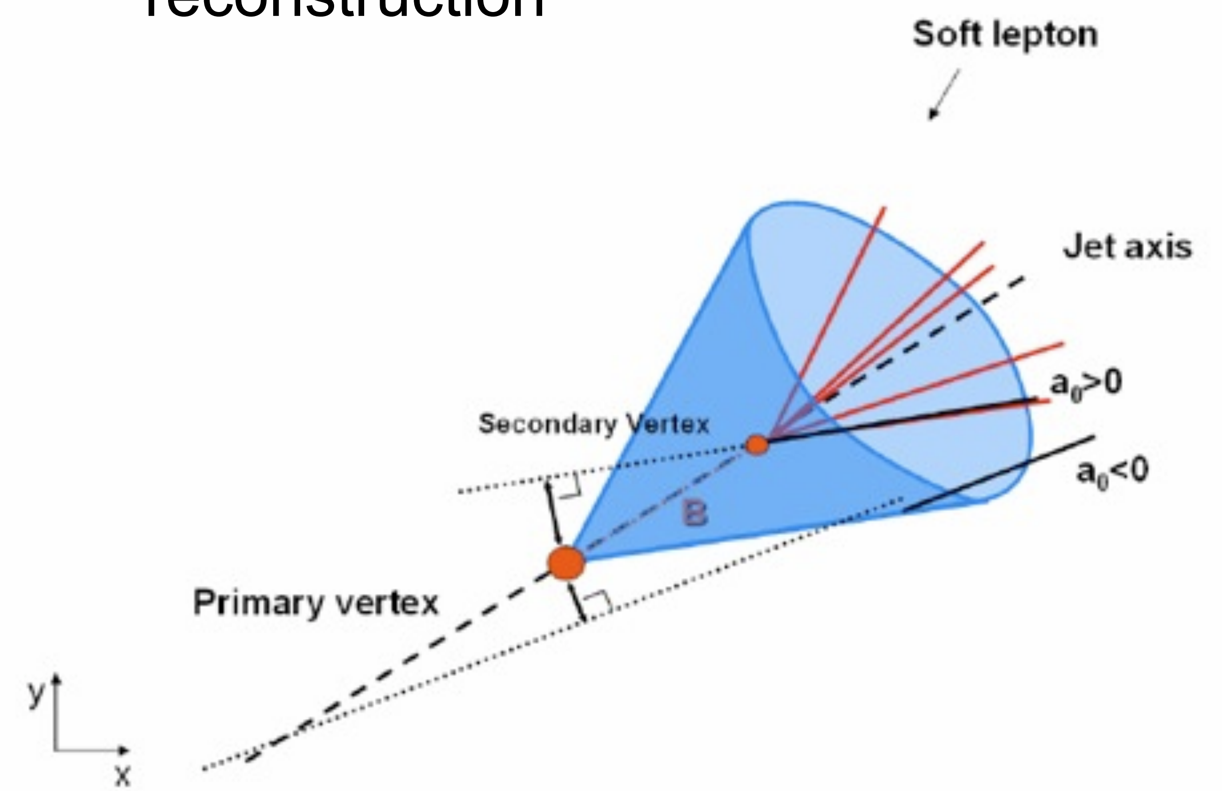

- Deriving the point resolution from just one coordinate is not enough information to reconstruct a secondary vertex

- Pixel detectors allow track reconstruction at high particle rate without ambiguities
- Good resolution with two coordinates (depending on pixel size and charge sharing between pixels)
- Very high channel number: complex read-out
- Readout in active area a detector

First pixels (CCDs) in NA11/NA32: ~1983

Hybrid Pixels – "classical" Choice HEP

- The read-out chip is mounted directly on top of the pixels (bump-bonding)
- Each pixel has its own read-out amplifier
- Can choose proper process for sensor and read-out separately
- Fast read-out and radiation-tolerant

… but:

- Pixel area defined by the size of the read-out chip
- High material budget and high power dissipation

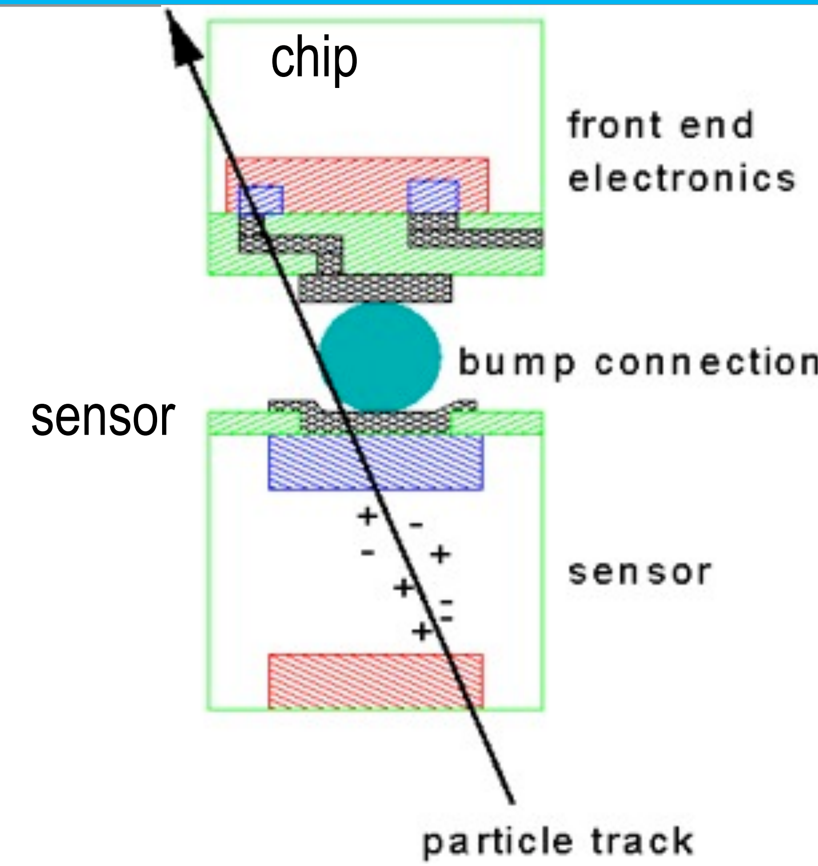

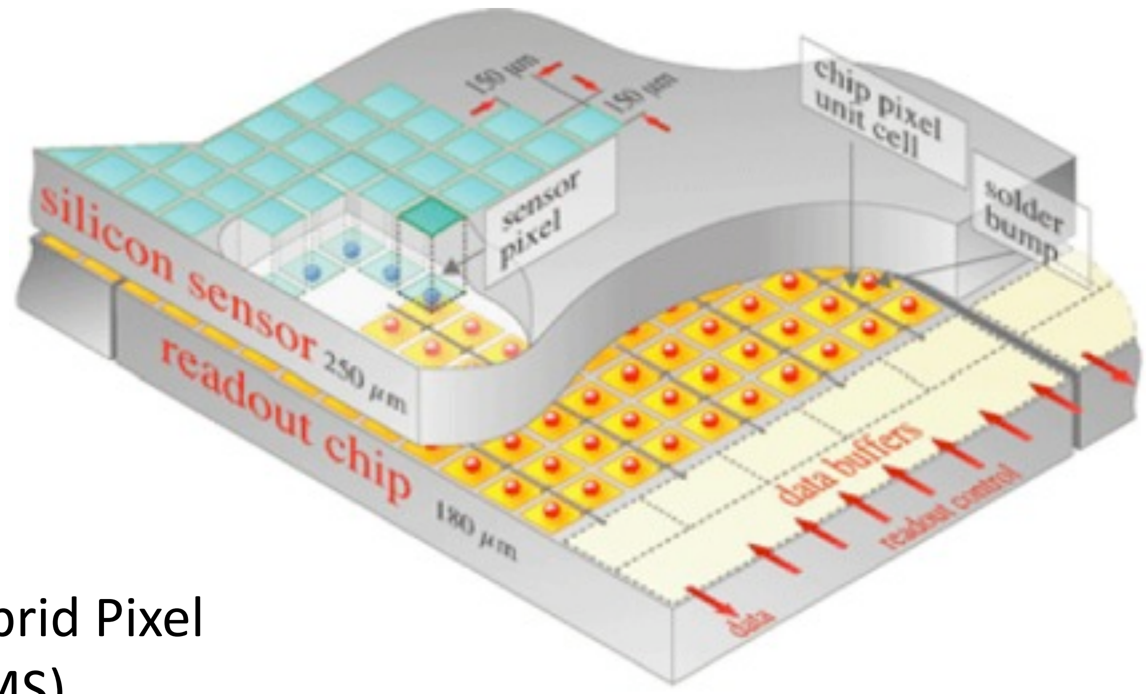

Hybrid Pixel (CMS)

- CMS Pixels: ~65 M channels 150 µm x 150 µm
- ATLAS Pixels: ~80 M channels 50 µm x 400 µm (long in z or r)
- Alice: 50 µm x 425 µm
- LHCb
- Phenix
- ….

The ATLAS Pixel Detector

- The Pixel Detector is made of 1744 modules (~80 10^6 channels).
- A module is a 6x2 cm^2 detector with 46080 read-out channels;
- Pixel size is 50x400 μm^2, but larger pixels are used to cover the space between the FE chips.
- Connection to external world via a single (low mass) cable providing all the required services:
  - Bias voltage
  - Analog and digital LV
  - Clock
  - Serial command line
  - Serial data outputs
  - Temperature measurements

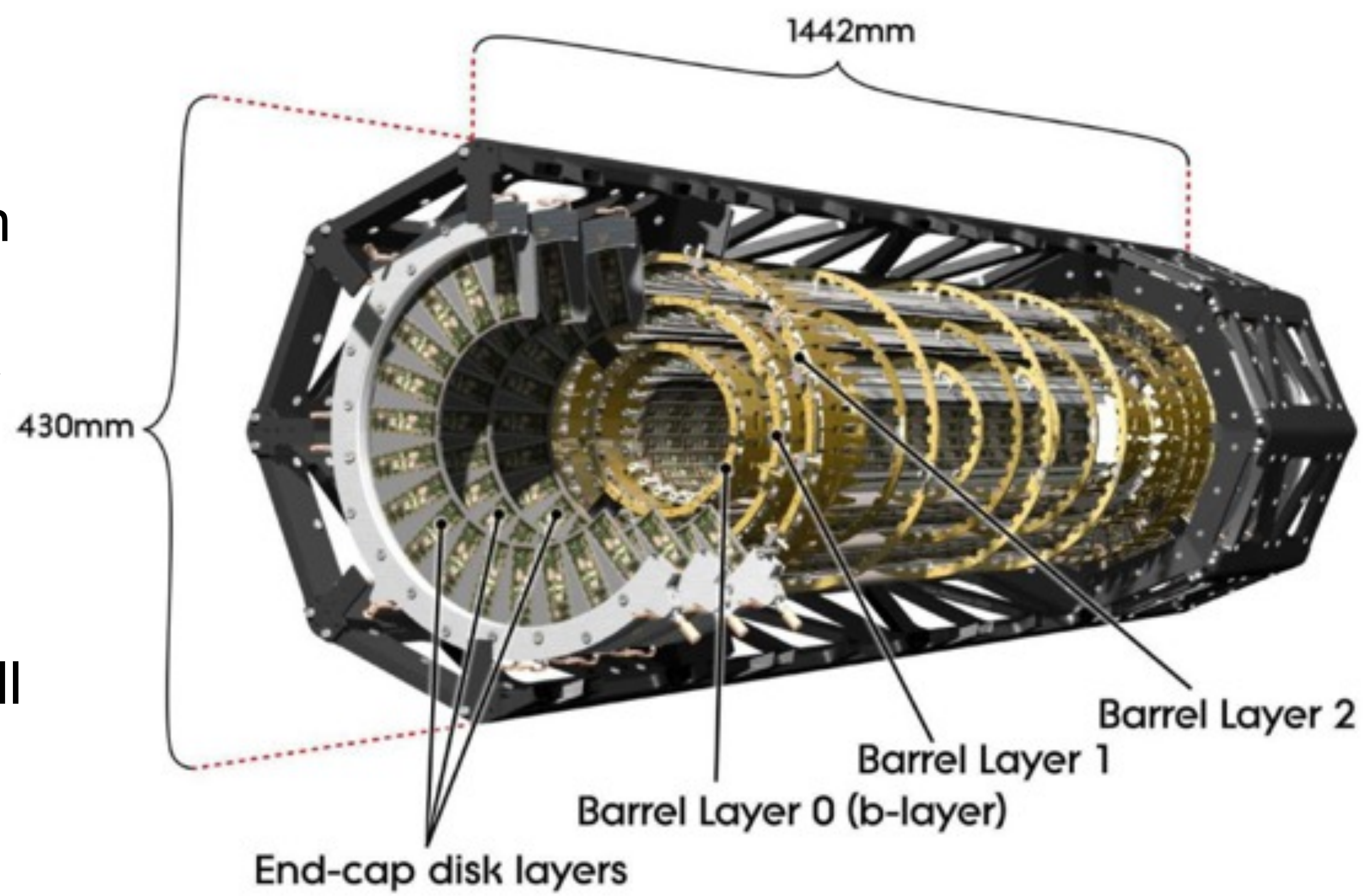

The same module is used in the barrel and in the disks:

- staves (13 modules along the beam axis) for the barrel.
- sectors (6 modules on a two-sided octant) for the disks.

Pixel Detector Module Breakdown

A pixel module contains:

- 1 sensor (2x6cm)
- ~40000 pixels
- 16 front end (FE) chips (2x8 array)
- bump bonded to sensor
- Flex-hybrid
- 1 module control chip (MCC)

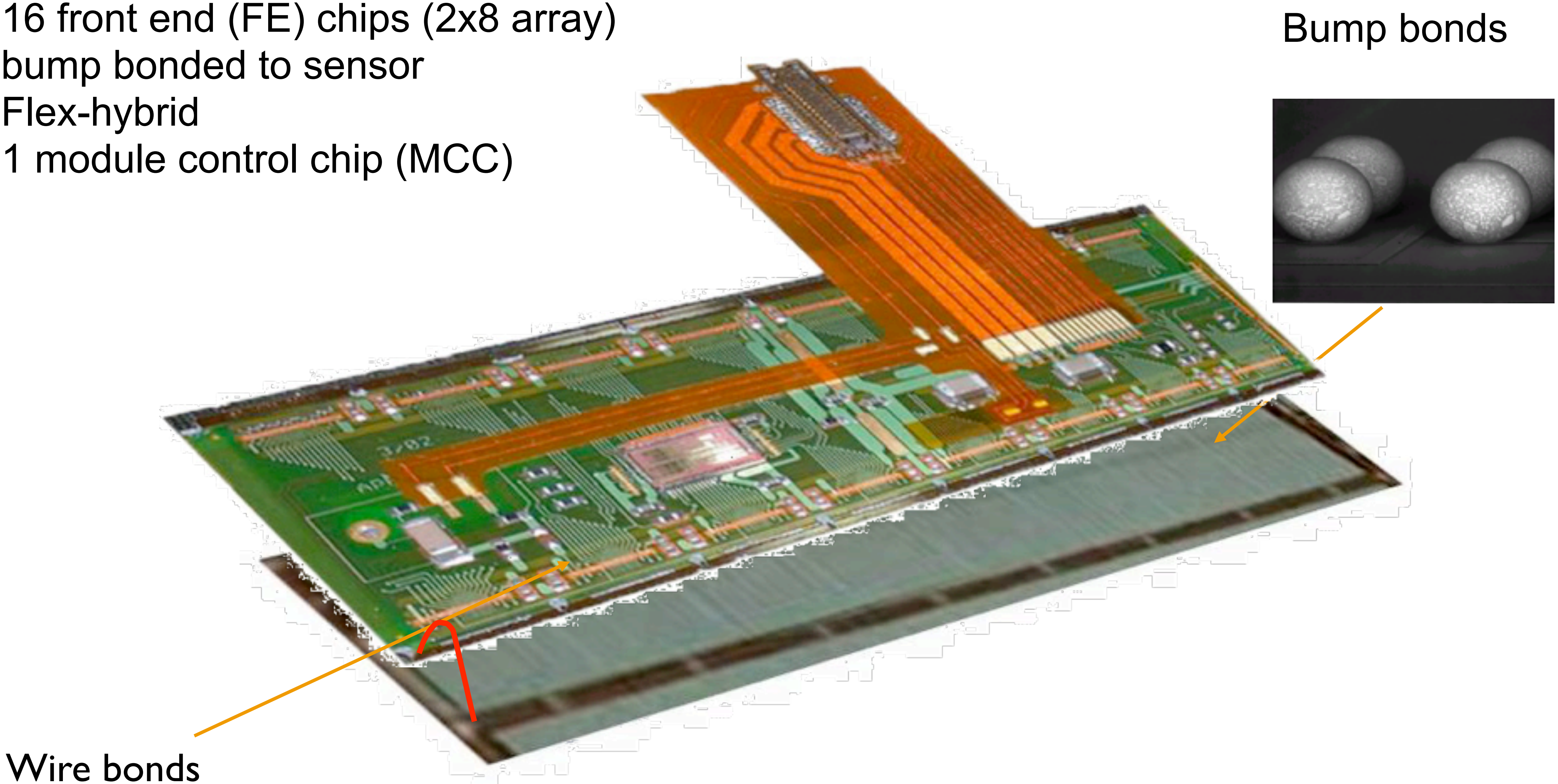

Pixel Detector Mo akdown

A pixel module contains:
- 1 sensor (2x6cm)
- ~40000 pixels
- 16 front end (FE) chips (2x8 array)
- bump bonded to sensor
- Flex-hybrid
- 1 module control chip (MCC)

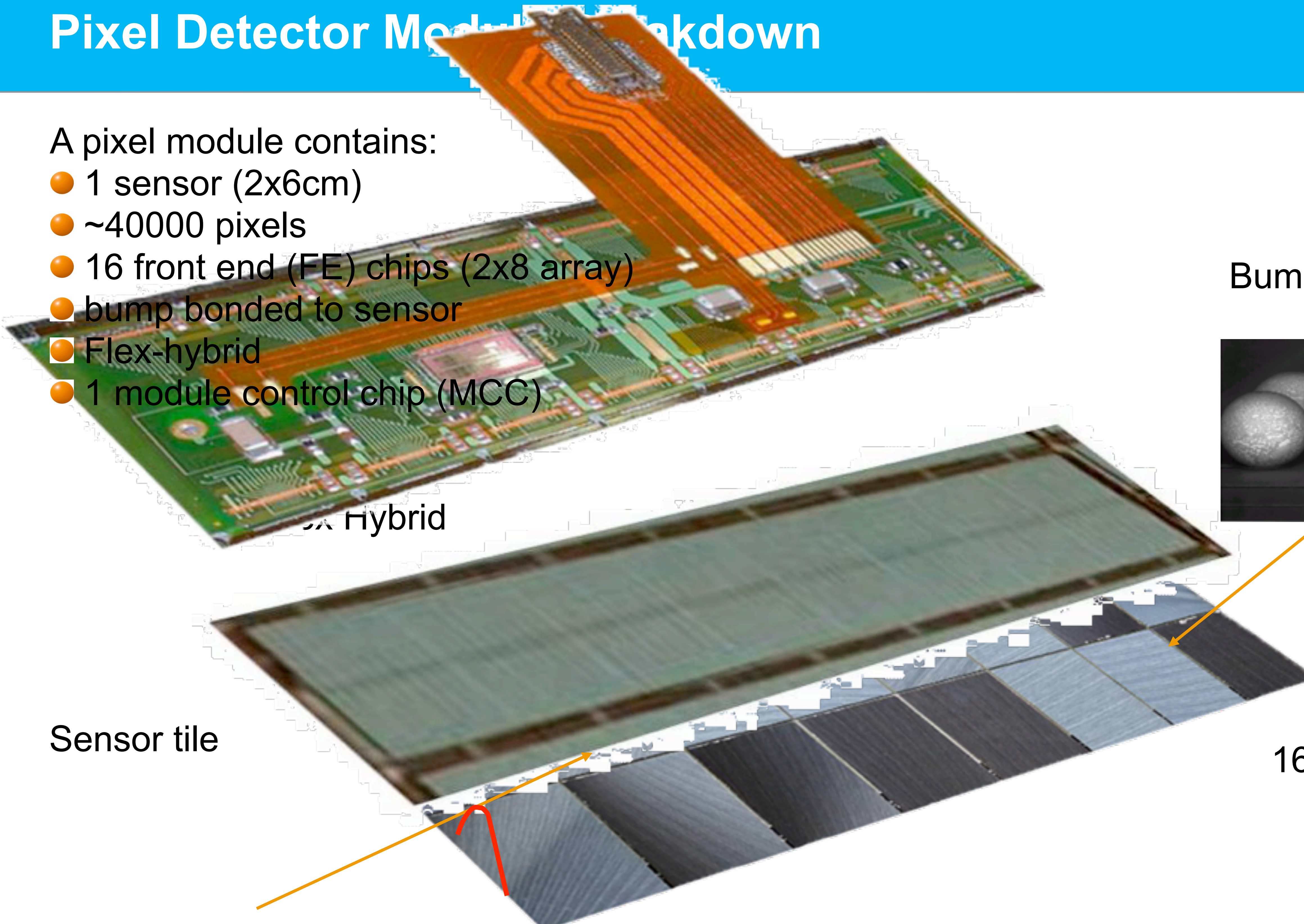

Bump bonds

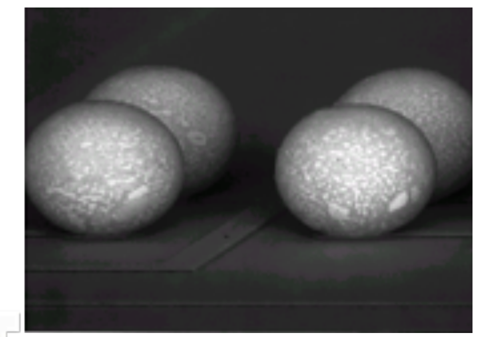

Pixel Detector M… akdown

A pixel module contains:

- 1 sensor (2x6cm)
- ~40000 pixels
- 16 front end (FE) chips (2x8 array)
- bump bonded to sensor
- Flex-hybrid
- 1 module control chip (MCC)

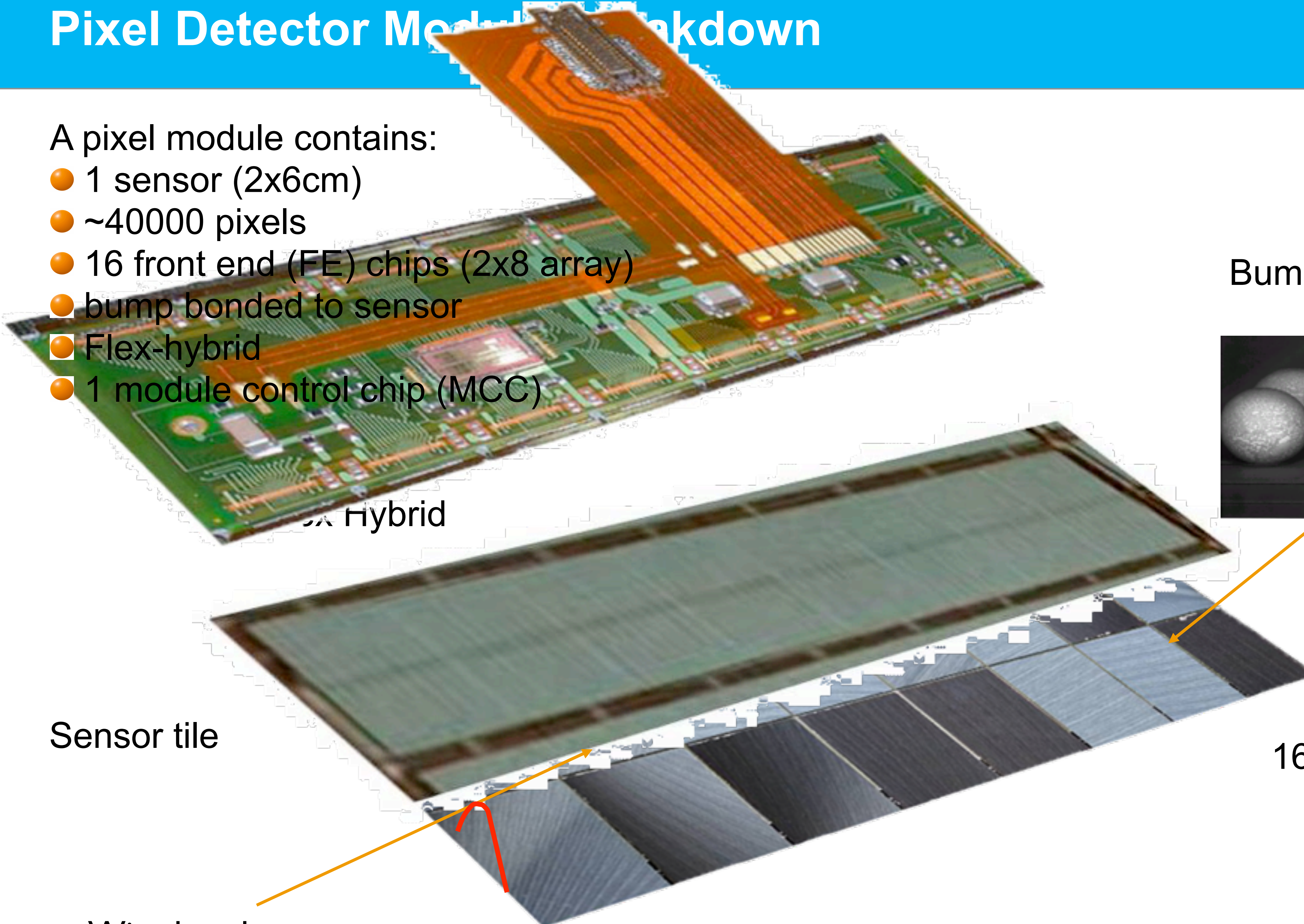

Bump bonds

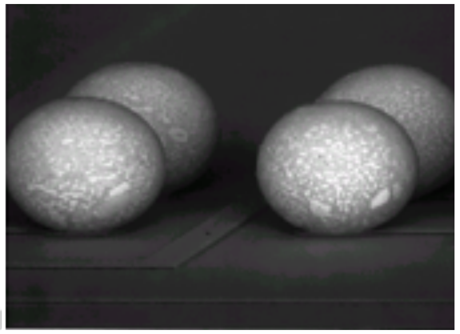

Structure of the Pixel Read-Out Cell

- Very small signals (fC) -> need amplification
- Several thousands to millions of channels

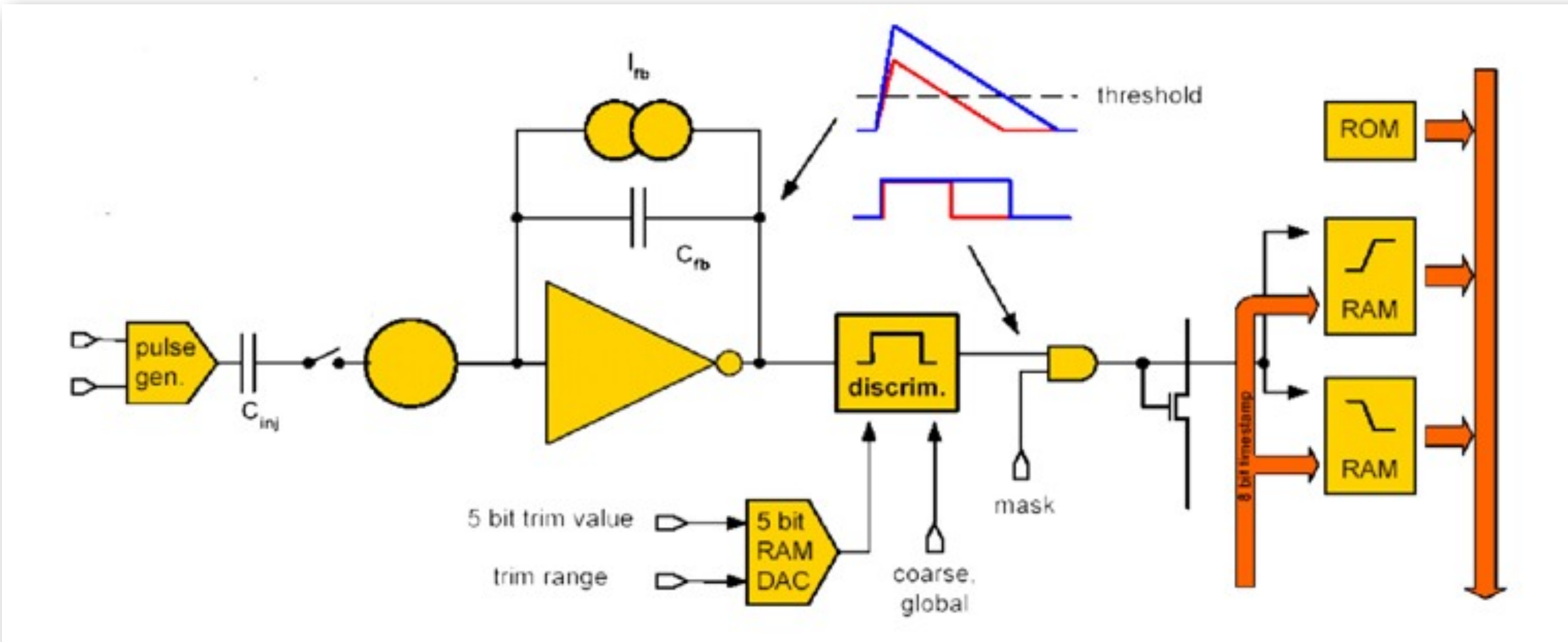

The Pixel Detector FE cell contains:

- a constant (adjustable) feedback current pre-amp
- a discriminator
- a 5 bit DAC to adjust threshold
- a circuitry to measure time over threshold (ToT)
- an analog and a digital injection point

Pixel Detector ToT Calibration

- The pixel read-out cell can measure (in 25 ns units) the time the discriminator input remains over threshold. This is correlated with the deposited charge.
- The pixel cell pre-amp feedback current can be adjusted to equalize the ToT response.

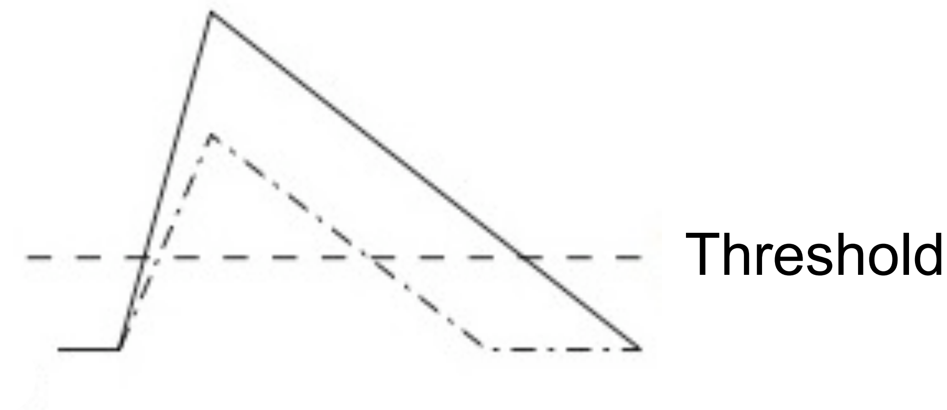

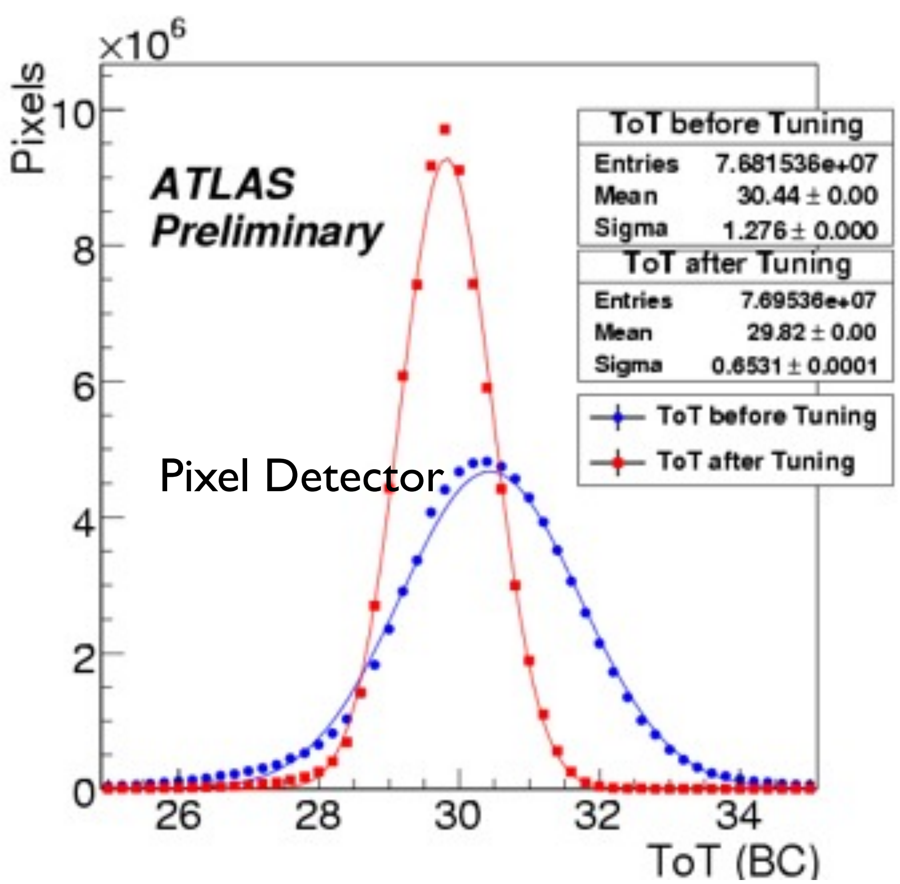

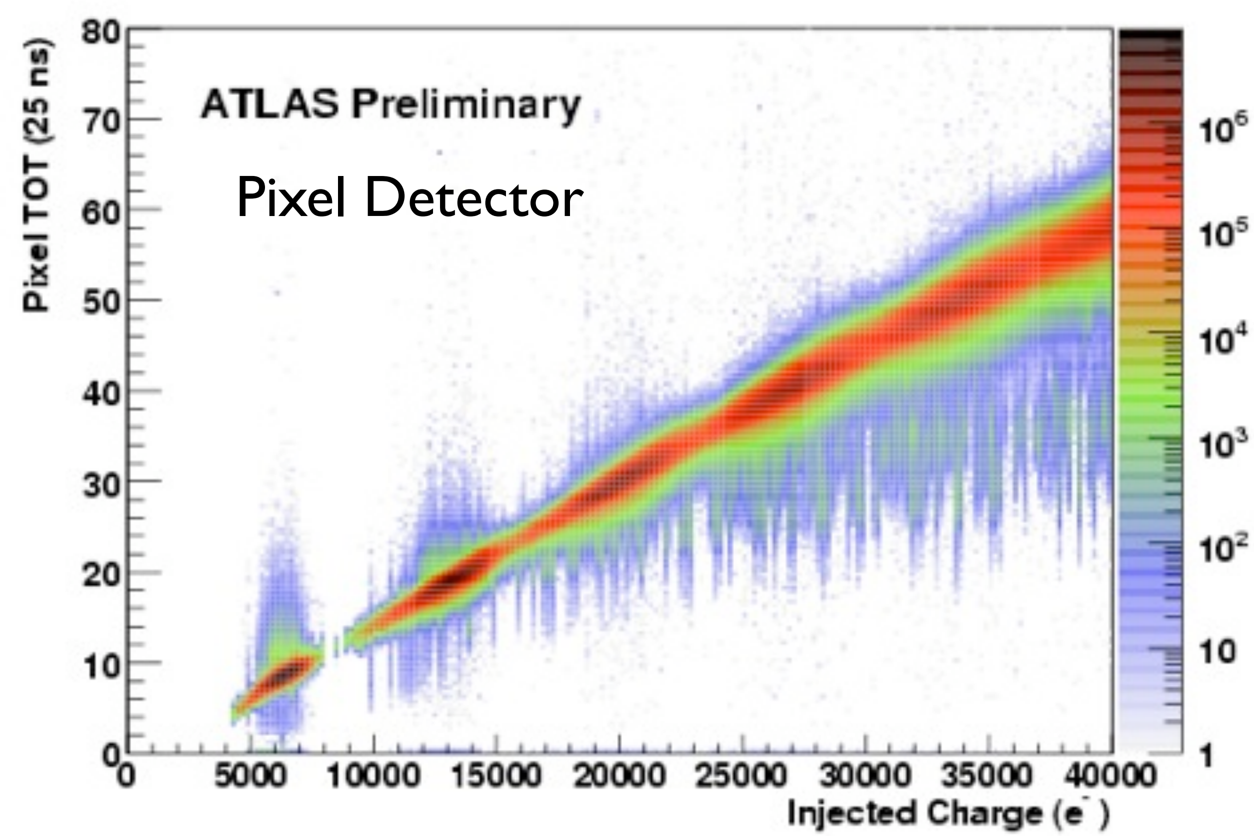

Pixel Detector dE/dx Measurement

- The ToT resolution achieved with the internal calibration (15%) is sufficient to distinguish p from K in minimum bias events below 1 GeV/c.

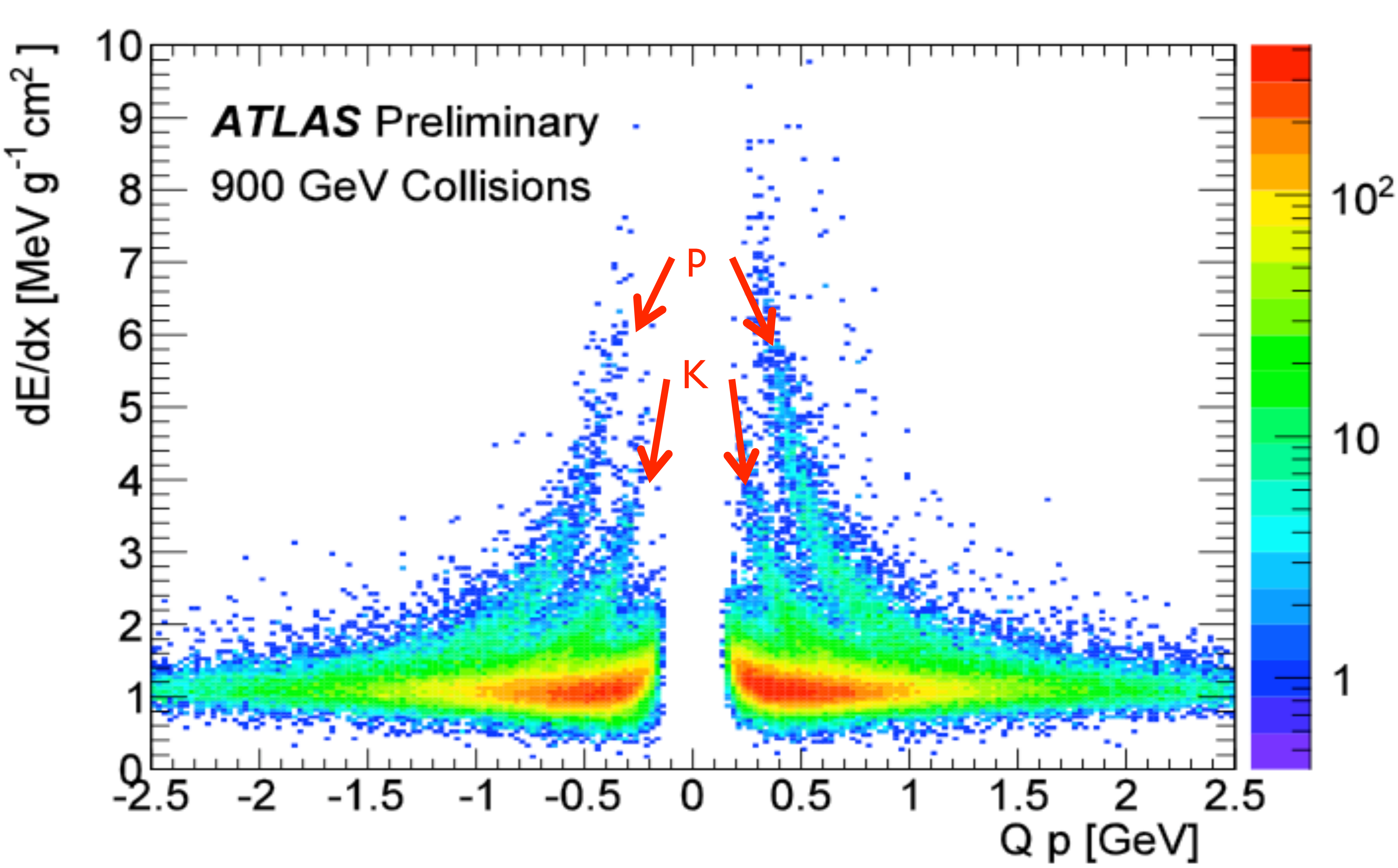

ATLAS-Pixels

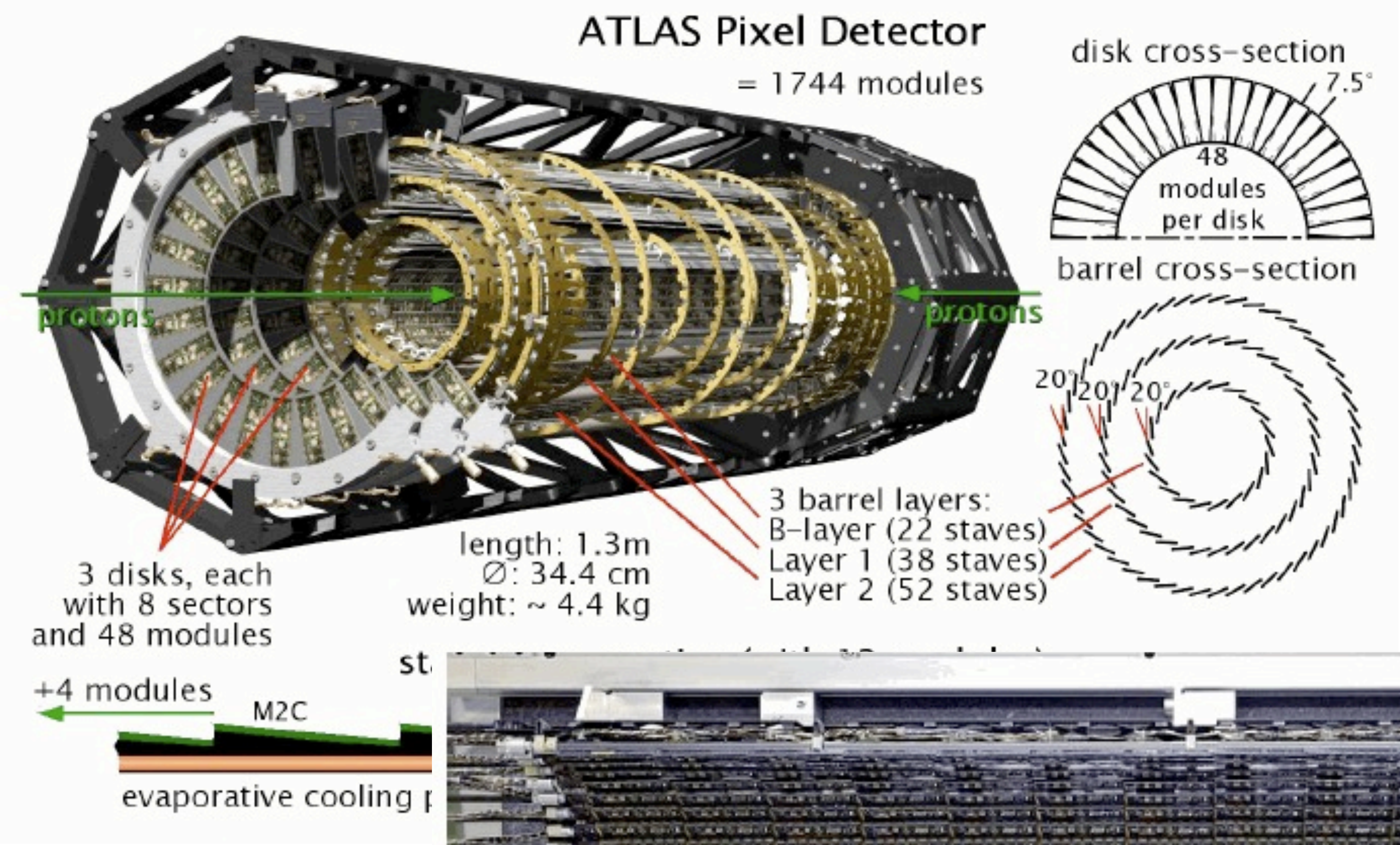

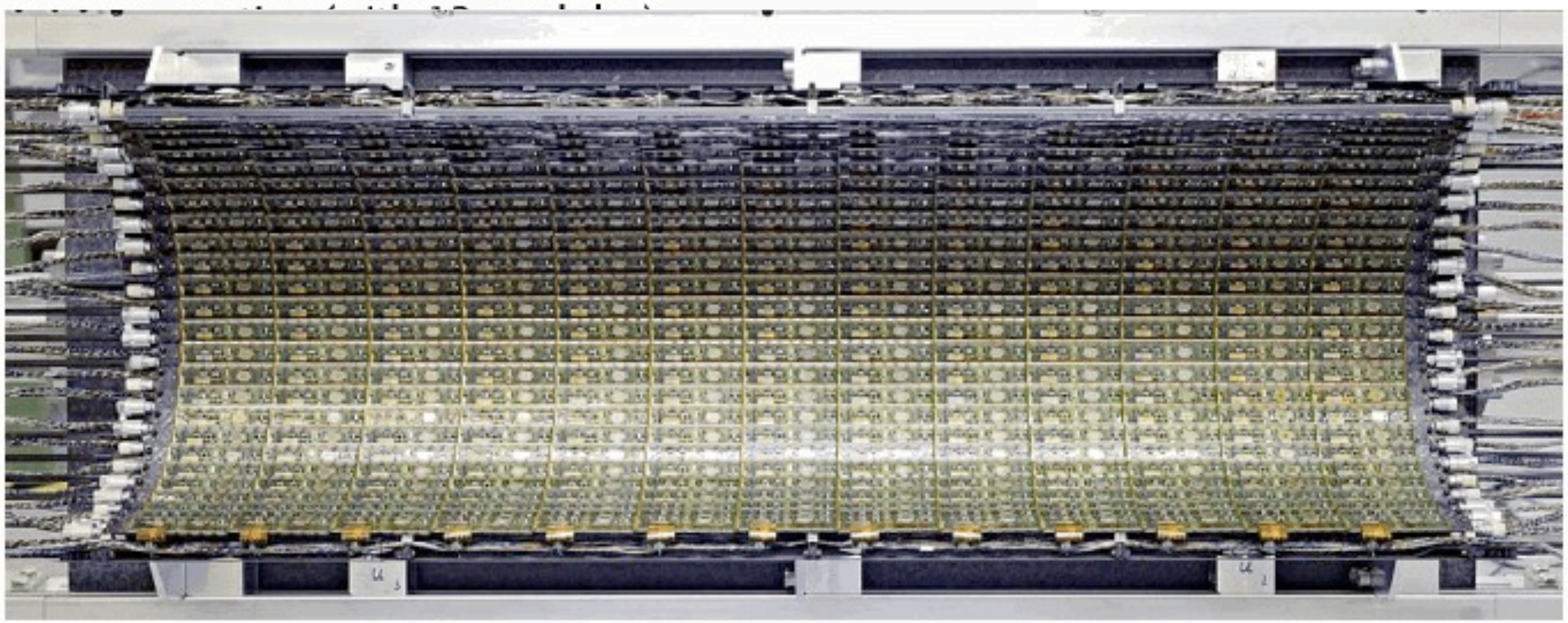

Services!!

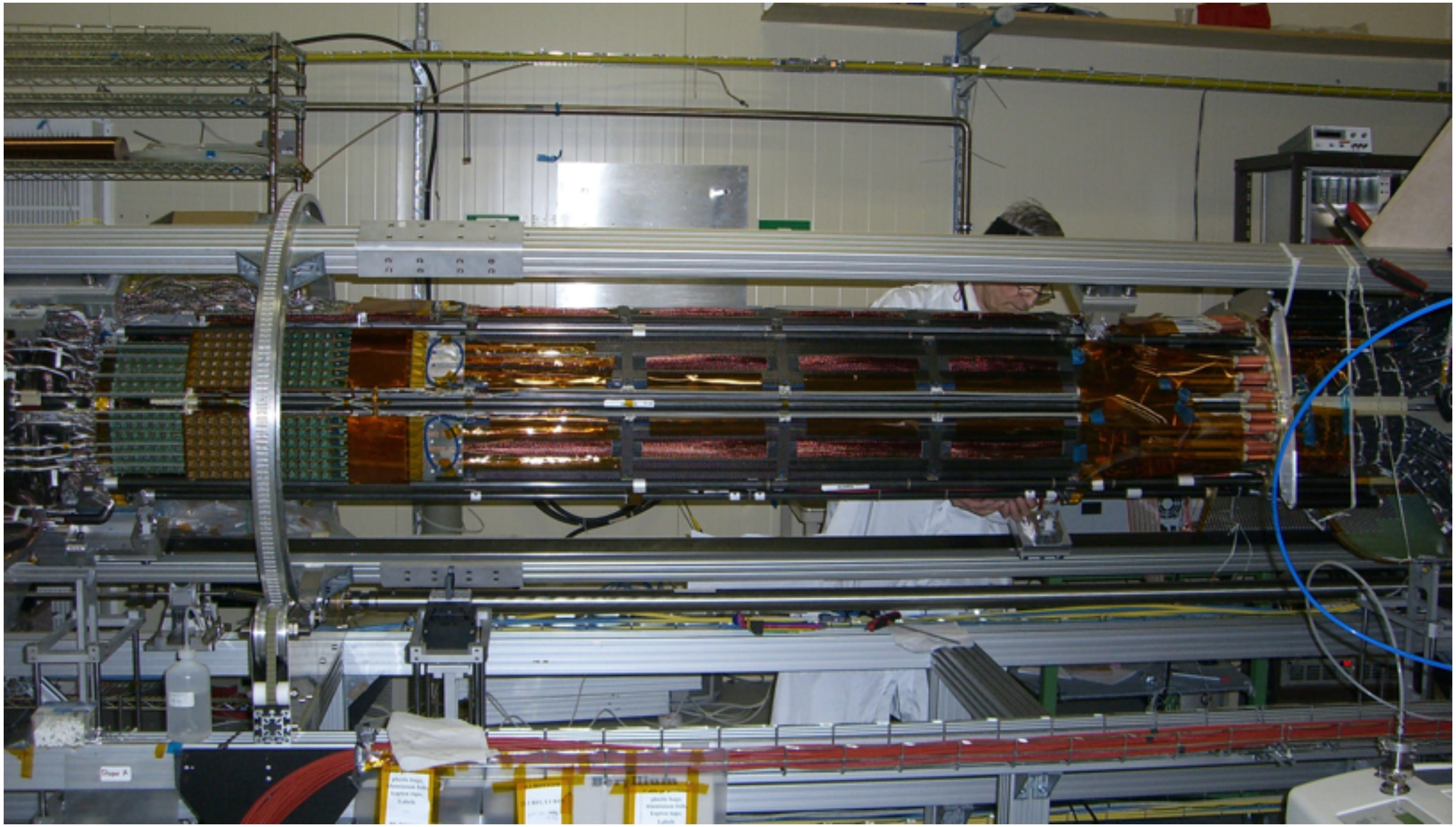

Services!!

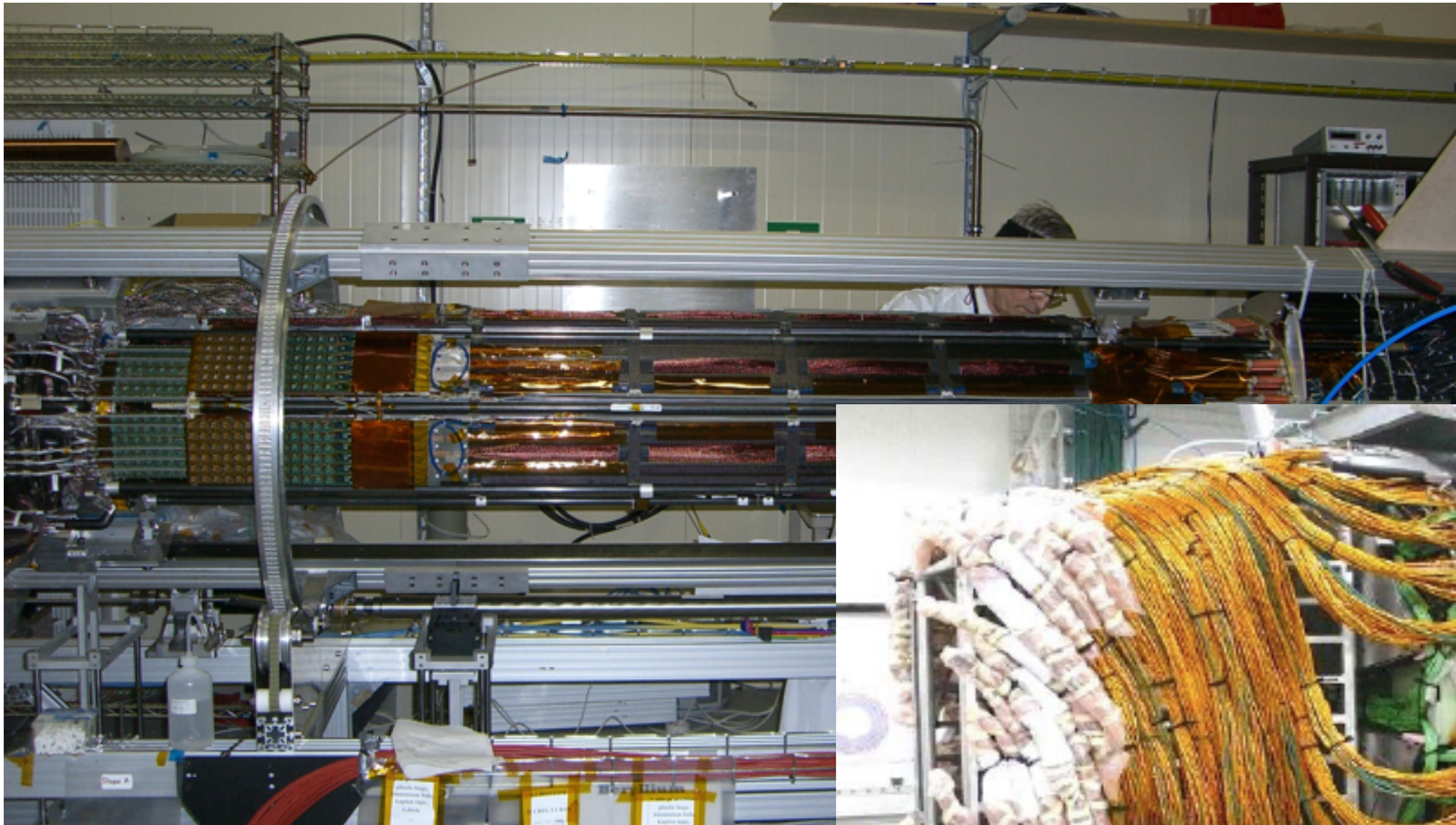

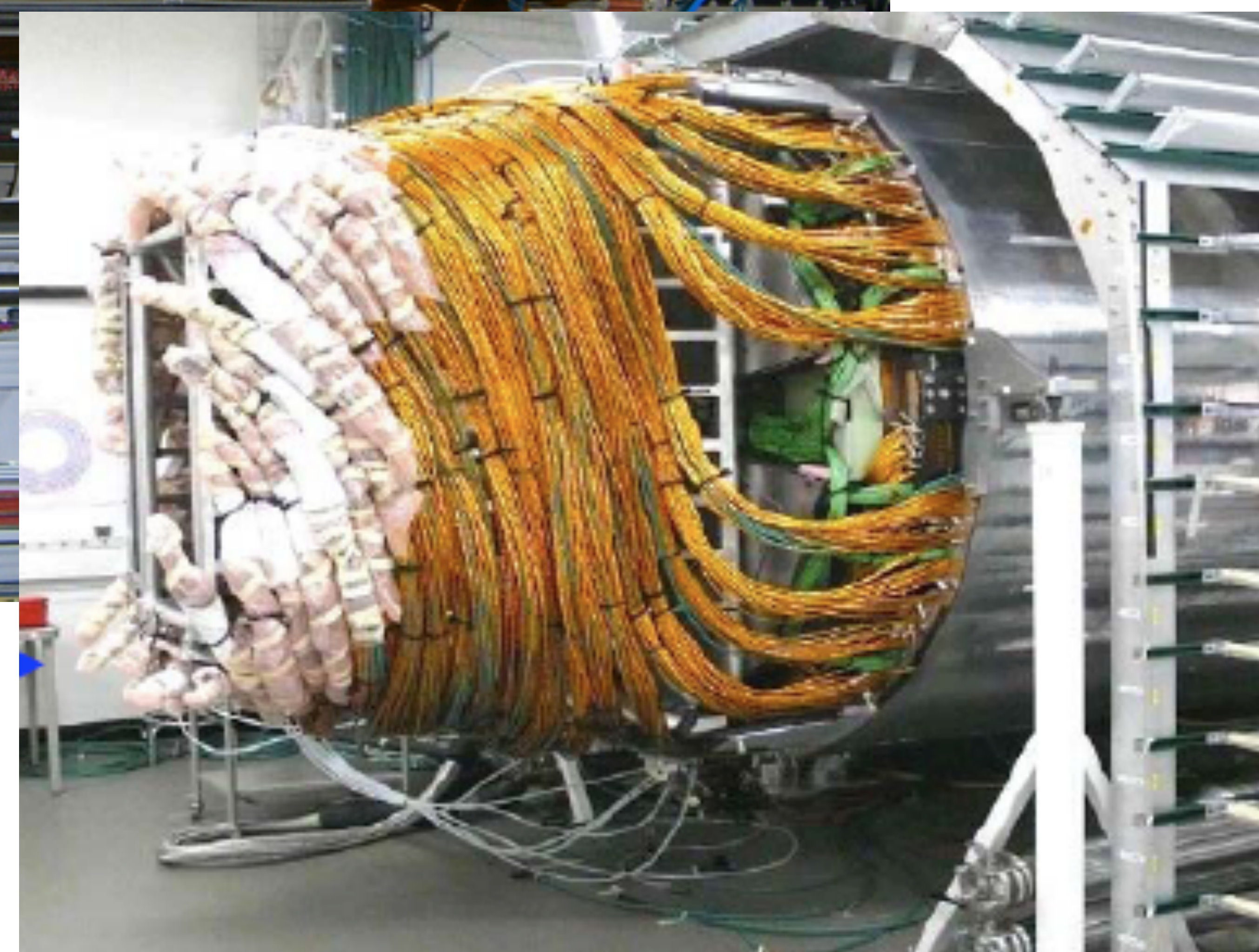

Commissioning and Some Measurements

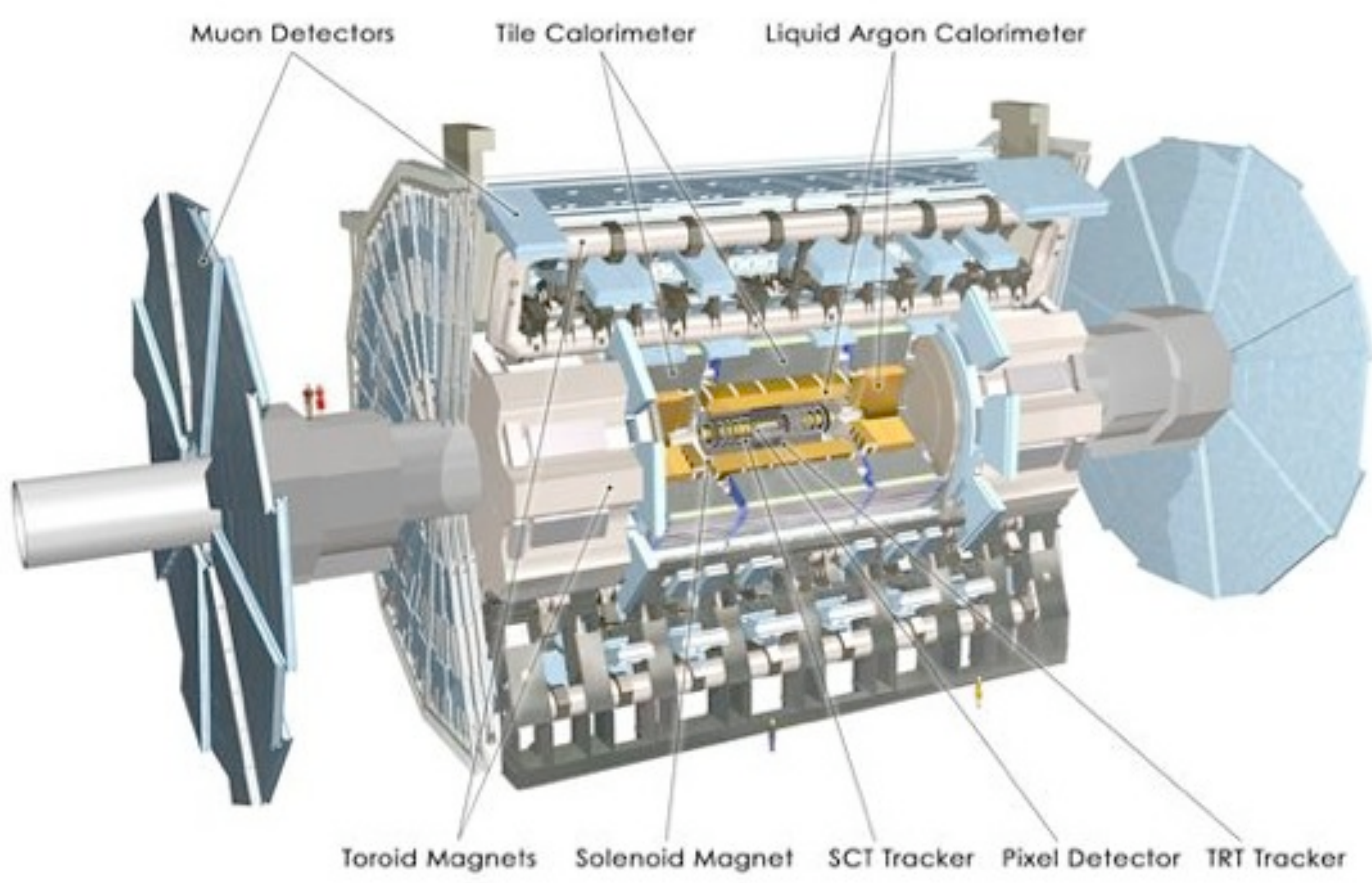
Muon Detectors
Tile Calorimeter
Liquid Argon Calorimeter
Toroid Magnets
Solenoid Magnet
SCT Tracker
Pixel Detector
TRT Tracker

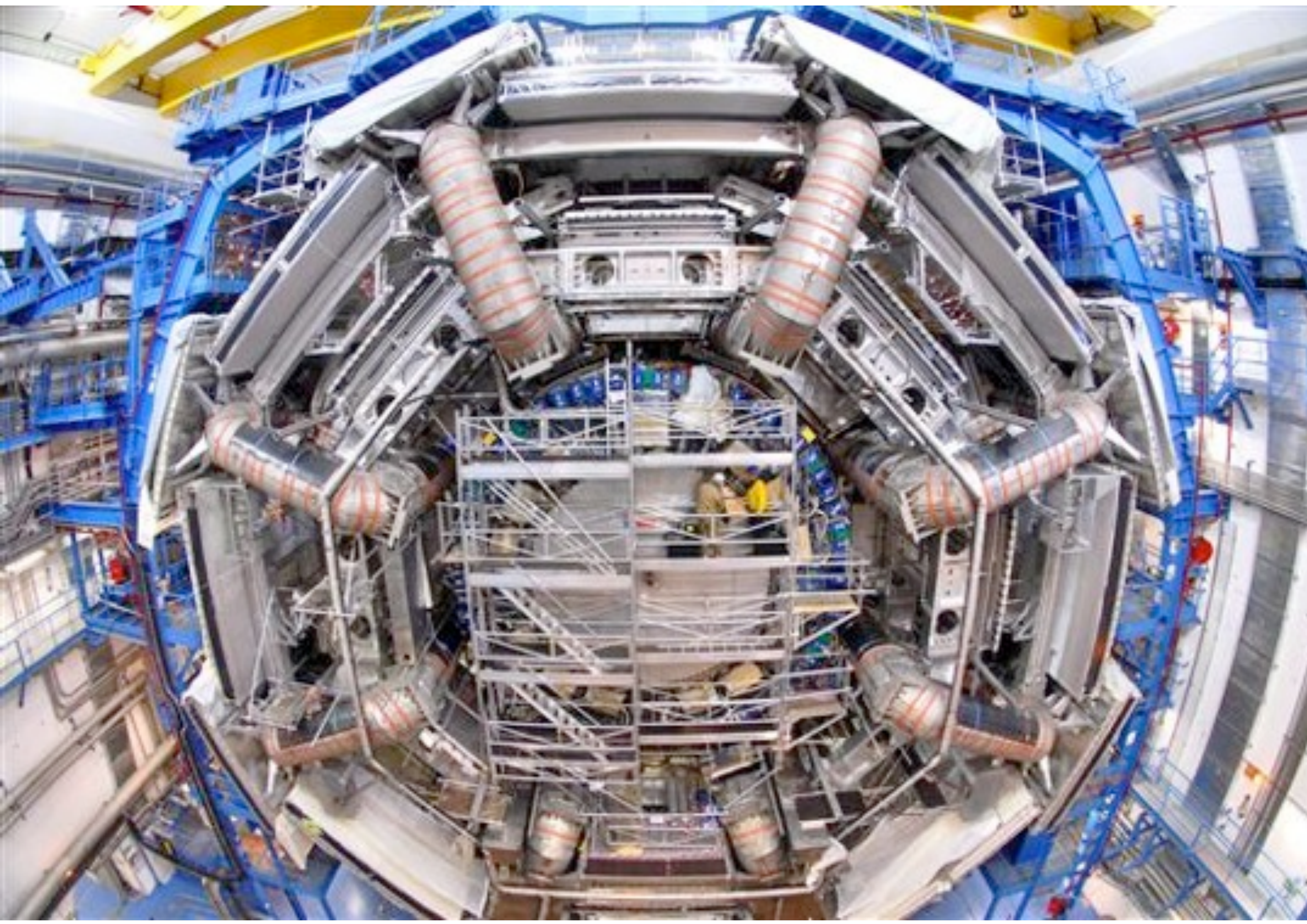

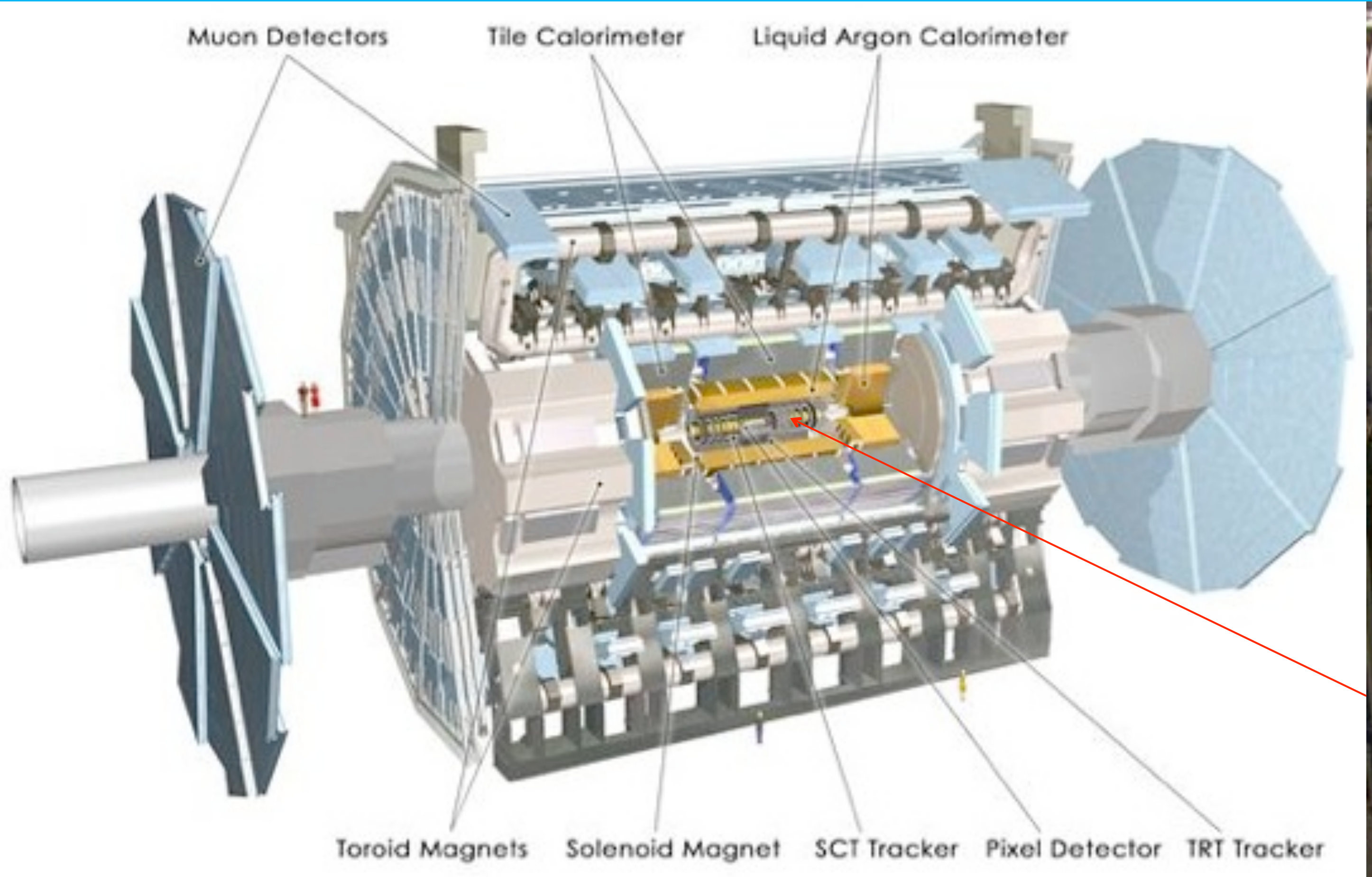
Muon Detectors
Tile Calorimeter
Liquid Argon Calorimeter
Toroid Magnets
Solenoid Magnet
SCT Tracker
Pixel Detector
TRT Tracker

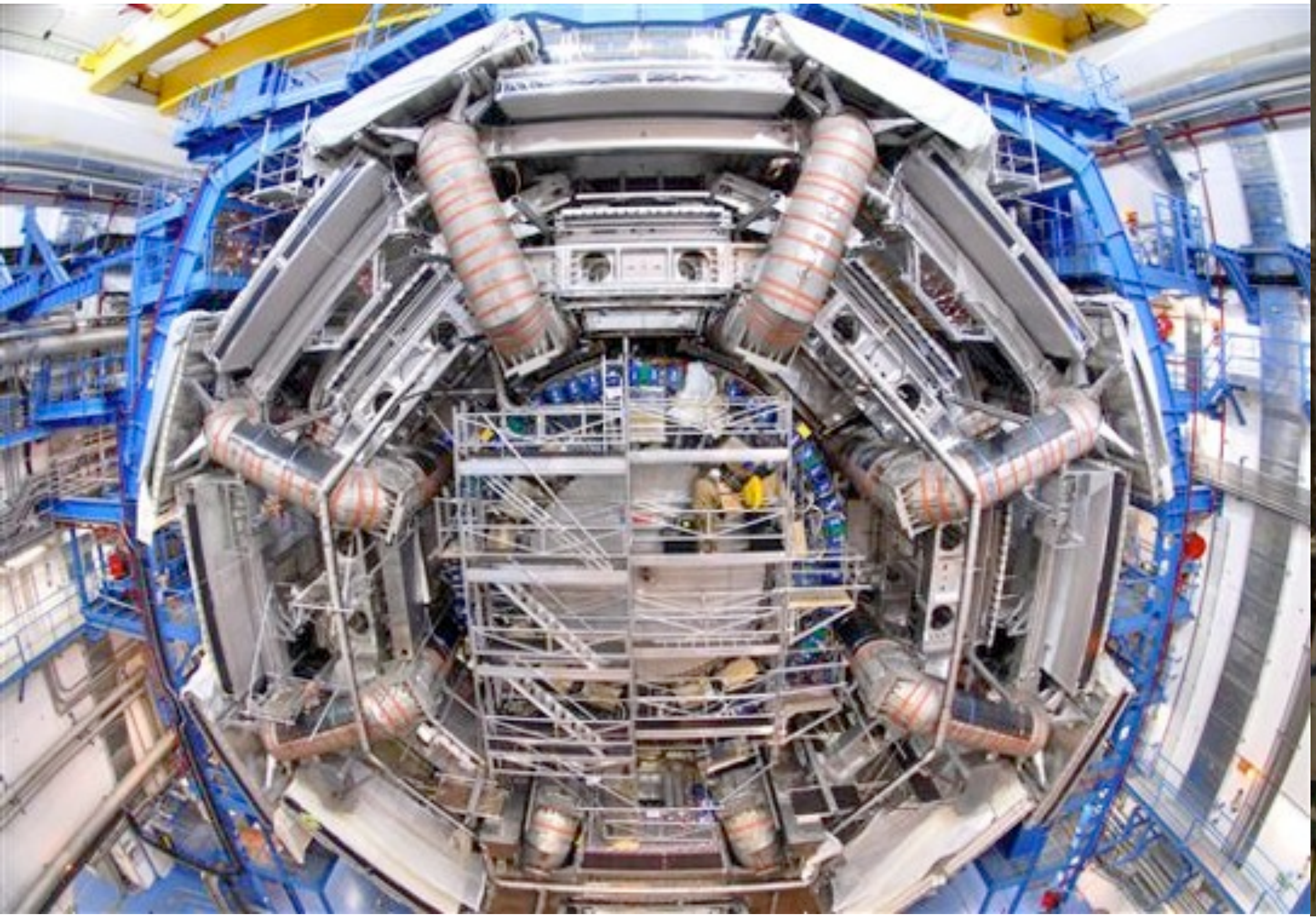

ID Commissioning

The installation in the ATLAS cavern was completed by July 07, but operation with the full detector cooled down was possible only starting from April 08.

The preparation for the LHC collision era consisted of three main activities:

- Commissioning of the services; in particular the C_3F_8 evaporative cooling plant, damaged in an accident in May 08, required significant upgrades.
- Now tooling system operates in a very stable way (-2^o to 4.5^{0}C for the SCT, -20^{o}C for the Pixel Detector).
- Detector calibration using the internal charge injection mechanism.
- Data taking with cosmics before LHC start up

SCT barrel installation, June 06

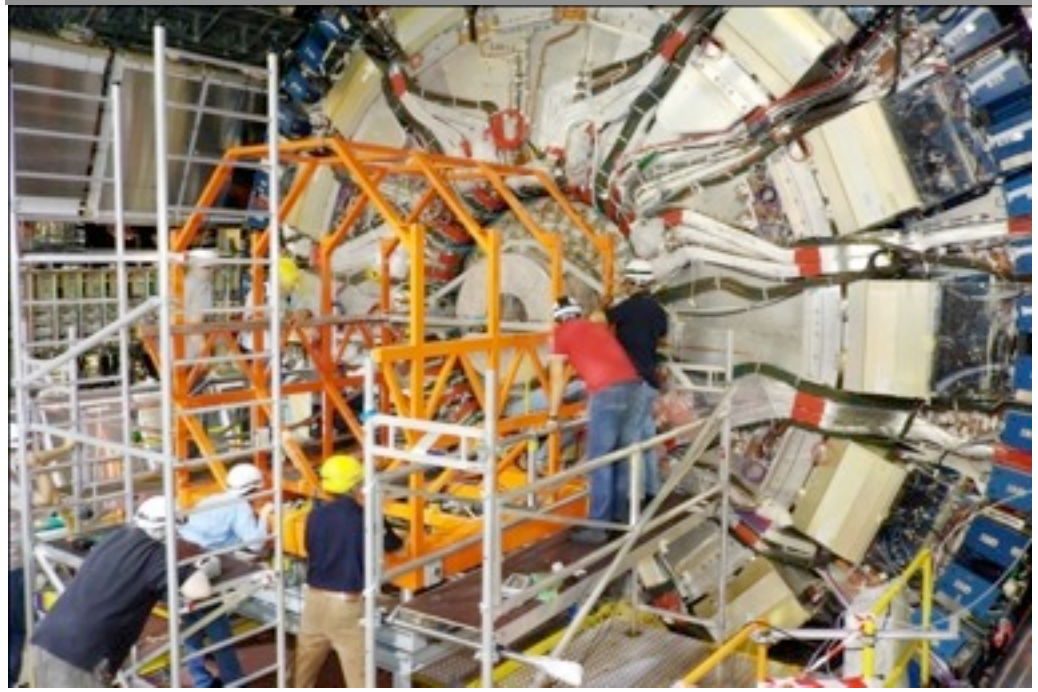

Pixel installation, July 07

Calibration Procedures

- The read-out electronics and the DAQ software were designed with calibration procedures.
- Using the internal front-end electronics self-test and charge injection capabilities enables:
  - Tune the custom rad-hard opto-link parameters to guarantee error free data transmission.
  - Adjust the discriminator threshold of each channel to minimize threshold dispersion.
  - Measure the noise of each channel.
  - Tune the time-over-threshold (Pixel Detector).

Pixel Detector opto-link tuning

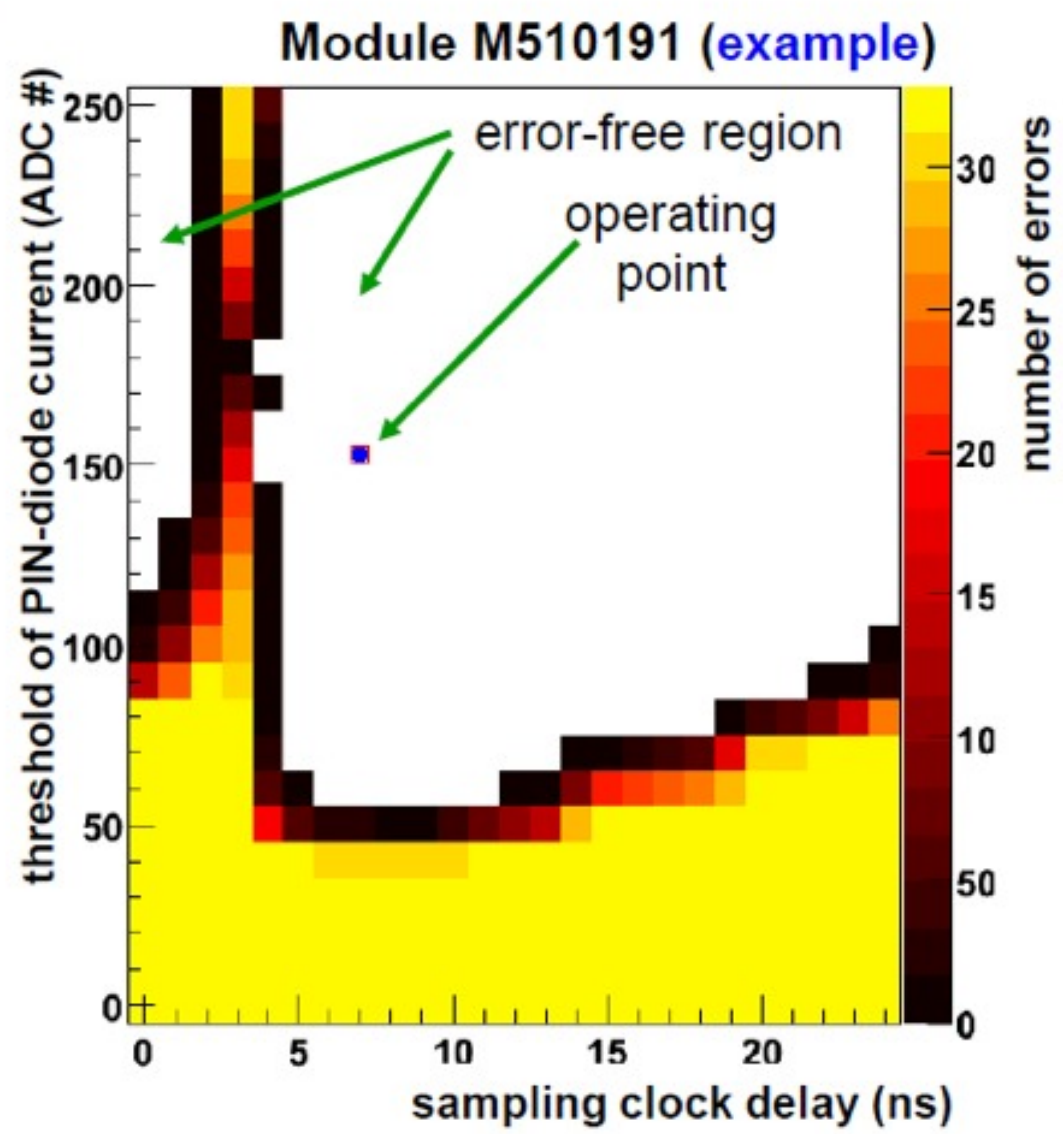

Threshold Uniformity

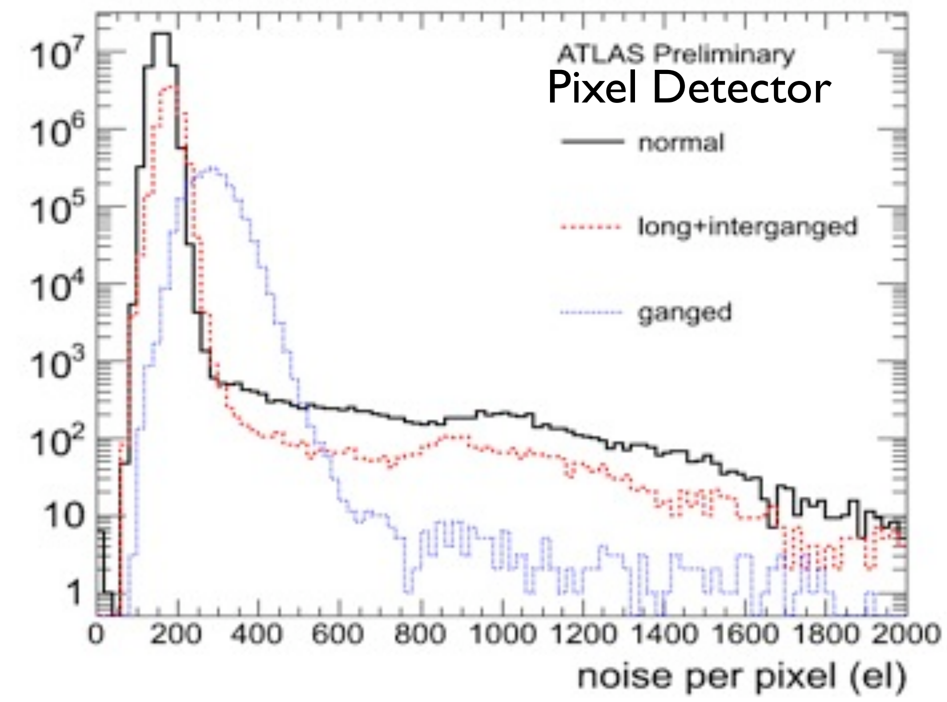

Threshold Uniformity

Measuring the discriminator activation curve as a function of the injected charge it's possible to determine threshold and noise.

- Pixel Detector is operated at 3000-4000 e threshold, and the typical noise of regular size pixels is below 200 e.
- This large S/N ratio ensures excellent system stability, despite the huge number of channels and the high density.

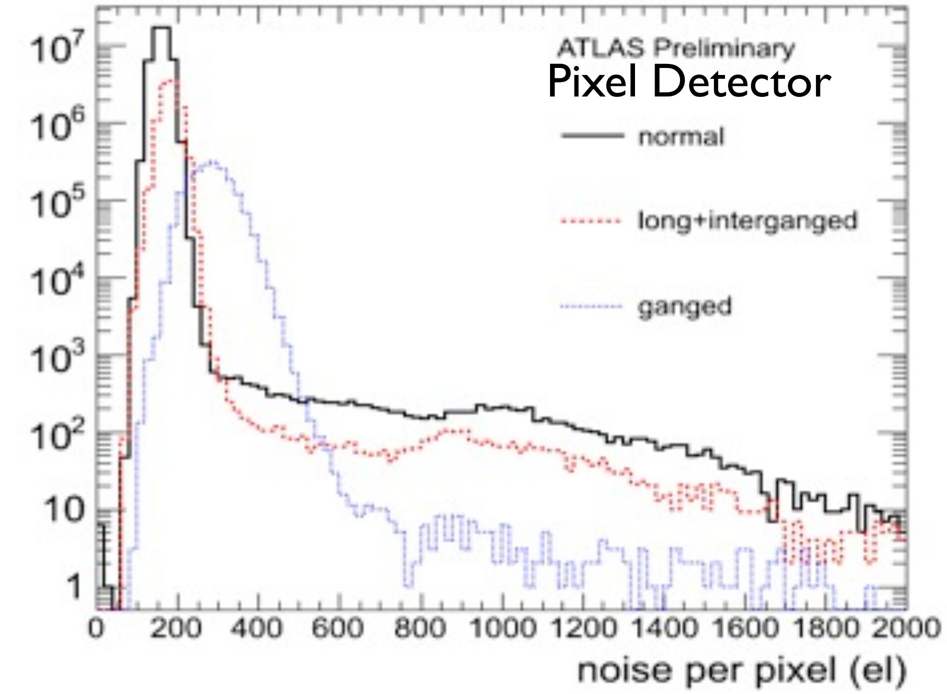

- Similar results for the SCT; the noise is larger (expected), of the order of 1500 e, but well below the typical threshold set at 1 fC.

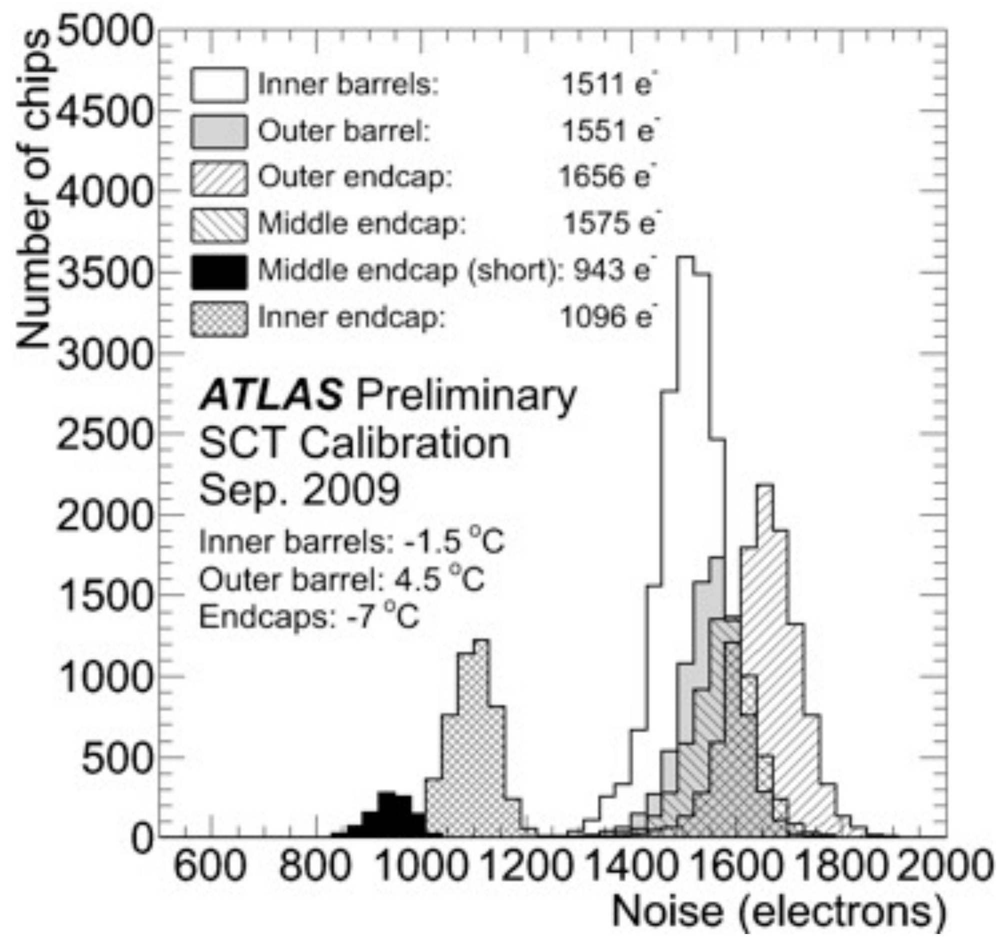

Conclusions

- Designed to precisely reconstruct charged particles
- 7-points silicon (pixels + strips) tracker ($|\eta|<2.5$) plus straw tube quasi-continuous tracker with electron identification capability (TRT) ($|\eta|<2$).
- All in a very good shape ….

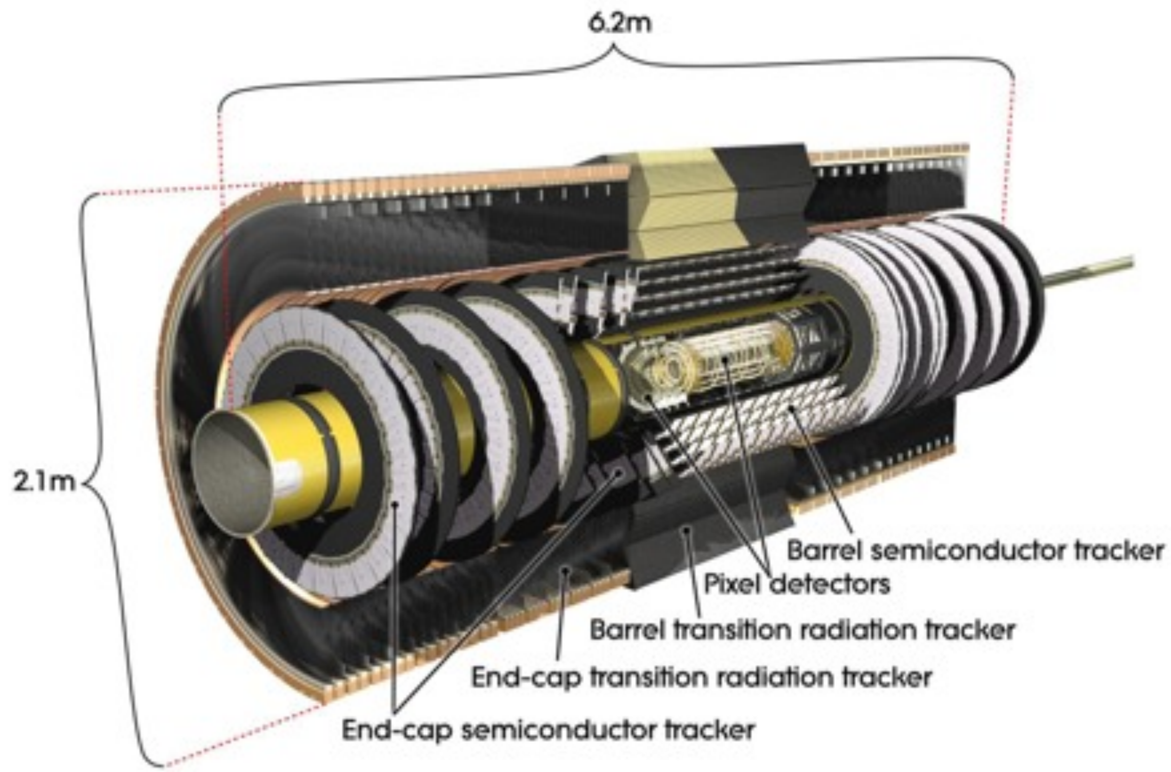

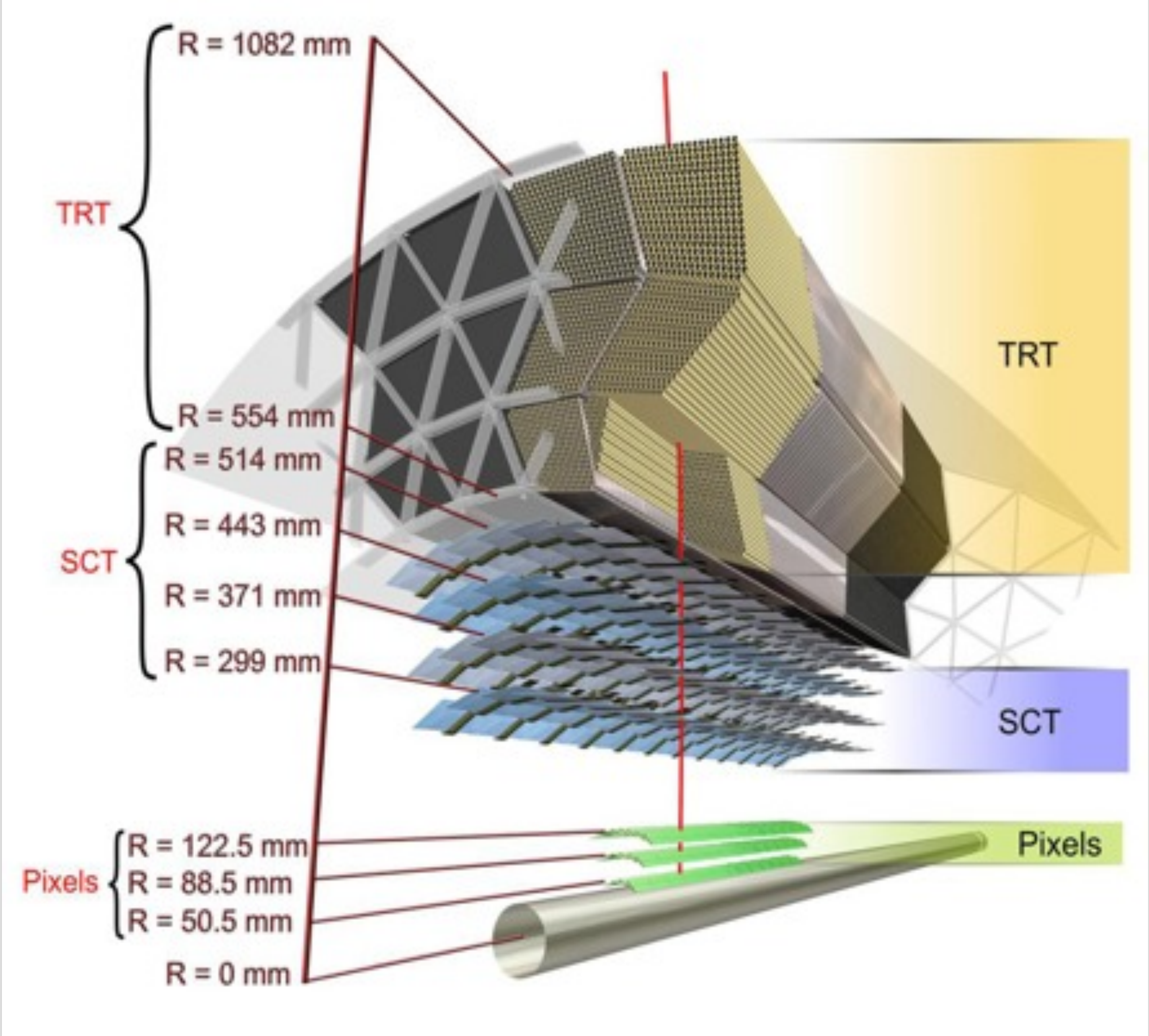

- Momentum resolution:

$$\sigma(p_t)/p_t = 0.05\% \, p_t(GeV/c) \oplus 1\%$$

- IP resolution:

$$\sigma(d_0) = 10\mu m \oplus 140\mu m / p_t(GeV/c)$$

Alignment

- The alignment of the ID is performed in subsequent steps, varying the number of degrees of freedom.
  - The first level only compensates for sub-detector global misalignments.
  - The second is used to align sub-detector components and the third aligns the individual mechanical units.
- Using the cosmics, it was possible to complete the second alignment step and part of the third one in the barrel region.
- Practically, this level is already close to the ideal alignment, as demonstrated by the comparison of the residuals determined with cosmics events and with a perfectly aligned MC (24 vs 16 μm for the Pixel Detector Barrel, 30 vs 16 μm for the SCT Barrel).

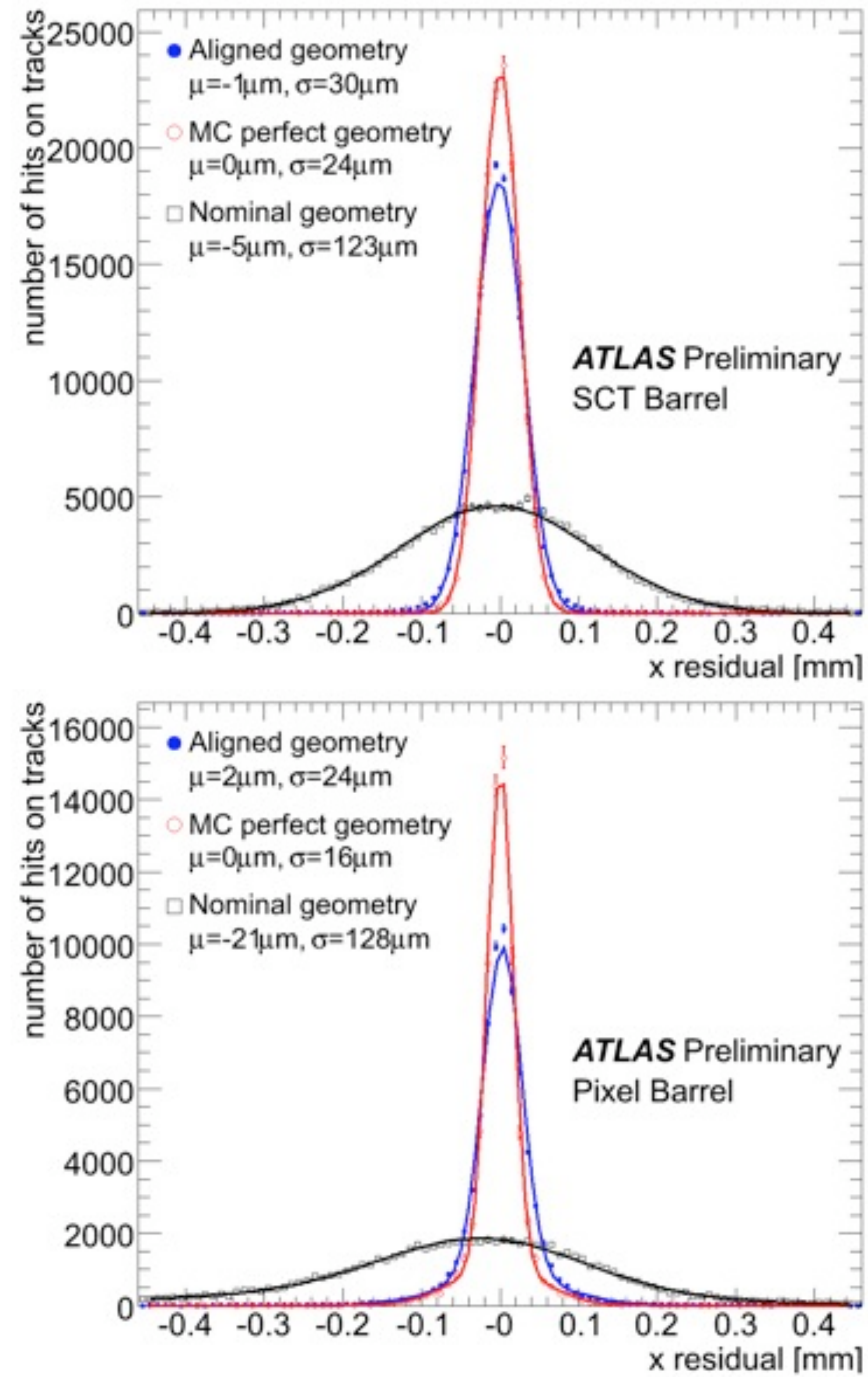

Literature

Text books:

C.Grupen: *Particle Detectors,* Cambridge UP 22008, 680p
D.Green: *The physics of particle Detectors,* Cambridge UP 2000
K.Kleinknecht: *Detectors for particle radiation,* Cambridge UP, 21998
W.R. Leo: *Techniques for Nuclear and Particle Physics Experiments,* Springer 1994
G.F.Knoll: *Radiation Detection and Measurement,* Wiley, 32000
Helmuth Spieler, *Semiconductor Detector Systems*, Oxford University Press 2005
L. Rossi, P. Fischer, T. Rohde, N. Wermes, *Pixel Detectors – From Fundamentals to Applications*, Springer Verlag 2006
Frank Hartmann, *Evolution of Silicon Sensor Technology in Particle Physics*, Springer Verlag 2009

W.Blum, L.Rolandi: *Particle Detection with Drift chambers,* Springer, 1994
G.Lutz: *Semiconductor radiation detectors,* Springer, 1999
R. Wigmans: *Calorimetry*, Oxford Science Publications, 2000

web:
Particle Data Group: *Review of Particle Properties: pdg.lbl.gov*

Tracking: Determination of the Momentum in Magnetic Field

- A tracking detector is typically placed within a B-field to enable momentum measurements
- Charged particles are deflected in a magnetic field:
  - takes only effect on the componente perpendicular to the field

Radius of the circular path is proportional to the transversal momentum:

$$\boxed{\frac{p_T}{\mathrm{GeV}/c} = 0.3 \, \frac{B}{\mathrm{T}} \, \frac{r}{\mathrm{m}}}$$

- parallel to the field is no deflection:

➾ particle is moving on a helix, the radius is determined by the field and p_T

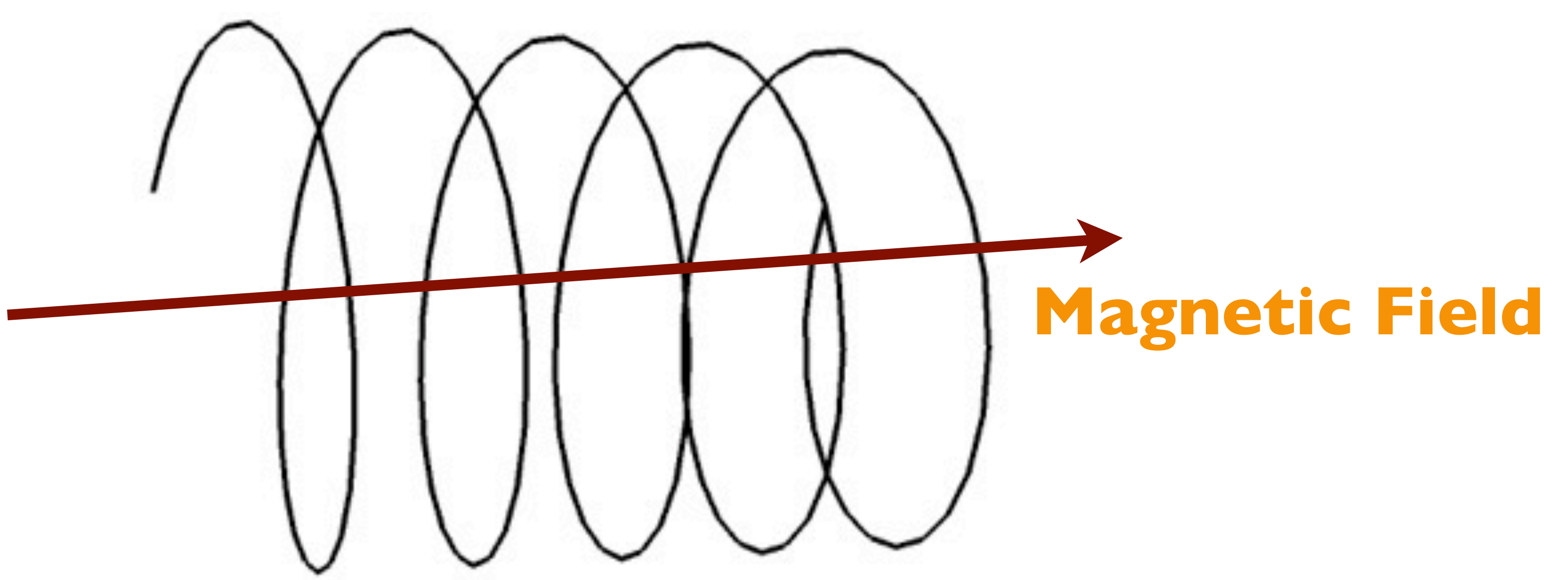

Determination of the Momentum in Magnetic Field II

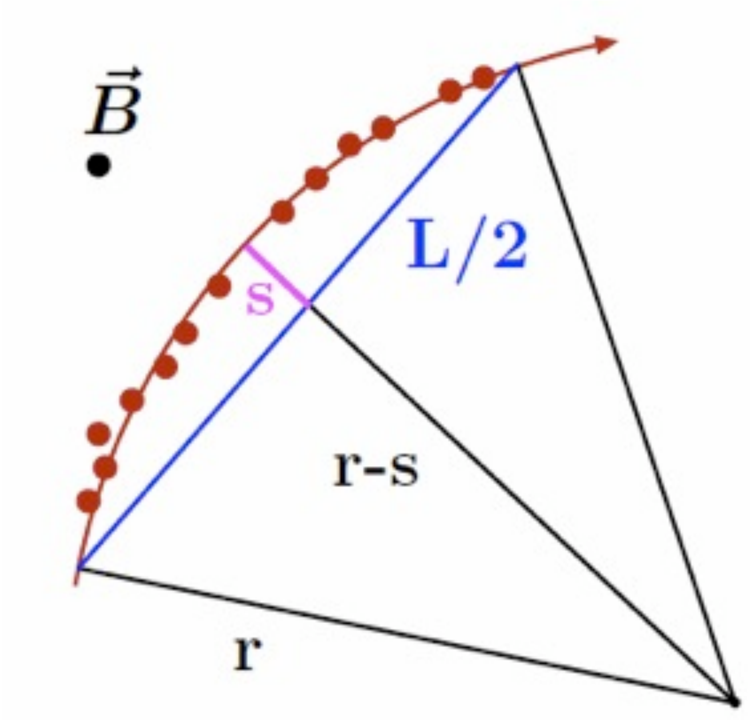

- In real applications usually only slightly bent track segments are measured
  - Figure of merit: Sagitta

Segment of a circle: $s = r - \sqrt{r^2 - \frac{L^2}{4}}$

$$\Rightarrow \ r = \frac{s}{2} + \frac{L^2}{8s} \approx \frac{L^2}{8s} \ (s \ll L)$$

With the radius-momentum-B-field relation: $r = \frac{p_T}{0.3\,B} \ \Rightarrow \ s = \frac{0.3\,B\,L^2}{8\,p_T}$

In general, for many measurement points:

$$\frac{\sigma(p_T)}{p_T} = \frac{\sigma(x)}{0.3\,B\,L^2}\sqrt{720/(N+4)}\,p_T$$

Determination of the Momentum in Magnetic Field II

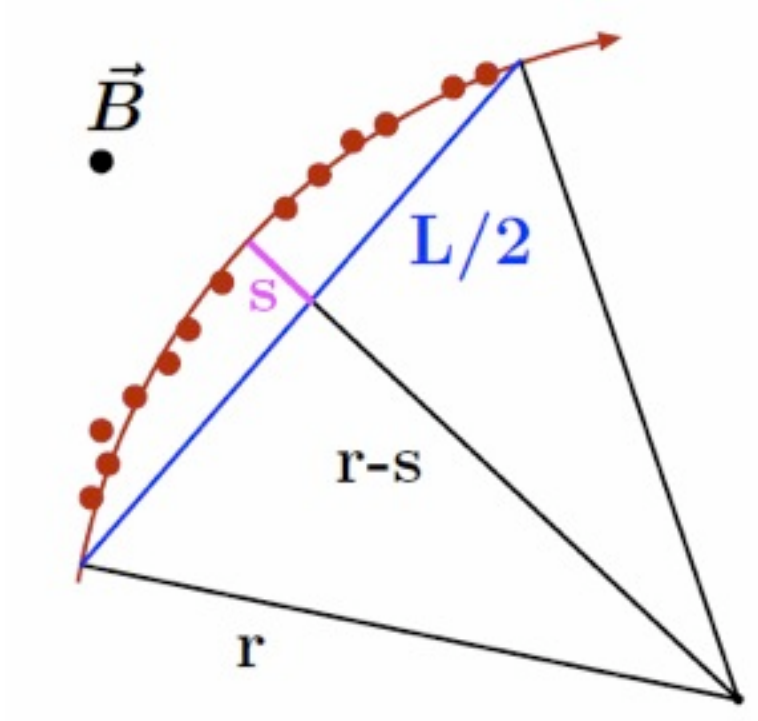

- In real applications usually only slightly bent track segments are measured
  - Figure of merit: Sagitta

Segment of a circle: $$s = r - \sqrt{r^2 - \frac{L^2}{4}}$$

$$\Rightarrow \quad r = \frac{s}{2} + \frac{L^2}{8s} \approx \frac{L^2}{8s} \quad (s \ll L)$$

With the radius-momentum-B-field relation: $r = \frac{p_T}{0.3\,B} \quad \Rightarrow \quad s = \frac{0.3\,B\,L^2}{8\,p_T}$

In general, for many measurement points:

$$\frac{\sigma(p_T)}{p_T} = \frac{\sigma(x)}{0.3\,B\,L^2}\sqrt{720/(N+4)}\,p_T$$

➠ Je larger the magnetic field B, the length L and the number of measurement points, and the better the spacial resolution, the better is the momentum resolution
ex.: N =7, L = 0.5, B = 2T, σ(x) = 20 μm, p_t = 5 GeV/c:
$\Delta p_t / p_t$ = 0.5 %, r = 8.3 m, s = 3.75 mm

Impuls resolution: Spacial resolution and multiple scattering

- Two component are influencing the momentum resolution $\sigma(p_T)/p_T$ of a tracking system:

  - Inaccuracy of the tracking detector: $\sigma(p_T) \propto p_T$
  - Influence of the particle due to MS:

$\theta \propto \frac{1}{p}$ and therefore also the spacial imprecision: $\sigma(x)_{MS} \propto \frac{1}{p}$

Impuls resolution: Spacial resolution and multiple scattering

- Two component are influencing the momentum resolution $\sigma(p_T)/p_T$ of a tracking system:
  - Inaccuracy of the tracking detector: $\sigma(p_T) \propto p_T$
  - Influence of the particle due to MS:

$\theta \propto \frac{1}{p}$ and therefore also the spacial imprecision: $\sigma(x)_{MS} \propto \frac{1}{p}$

Known: $$\frac{\sigma(p_T)}{p_T} \propto \sigma(x)_{MS} \times p_T$$

and therefore $$\left.\frac{\sigma(p_T)}{p_T}\right|_{MS} = const$$

Impuls resolution: Spacial resolution and multiple scattering

- Two component are influencing the momentum resolution $\sigma(p_T)/p_T$ of a tracking system:

  - Inaccuracy of the tracking detector: $\sigma(p_T) \propto p_T$
  - Influence of the particle due to MS:

$\theta \propto \frac{1}{p}$ and therefore also the spacial imprecision: $\sigma(x)_{MS} \propto \frac{1}{p}$

Known: $$\frac{\sigma(p_T)}{p_T} \propto \sigma(x)_{MS} \times p_T$$

and therefore $$\left.\frac{\sigma(p_T)}{p_T}\right|_{MS} = const$$

> The measurement of low momentum particles is limited by multiple scattering!
> At higher momenta the spacial resolution of the detector is dominating!

Industry Scaling Roadmap

- New generation every ~2 years with $\alpha = \sqrt{2}$
- from 1970 (8 µm) to 2009 (35 nm) (industrial application)
- End of the road ? Power dissipation sets limits
- HEP nowadays at 90nm and 130nm
- Problem: by the time a technology is ready for HEP -> “old” in industry standards

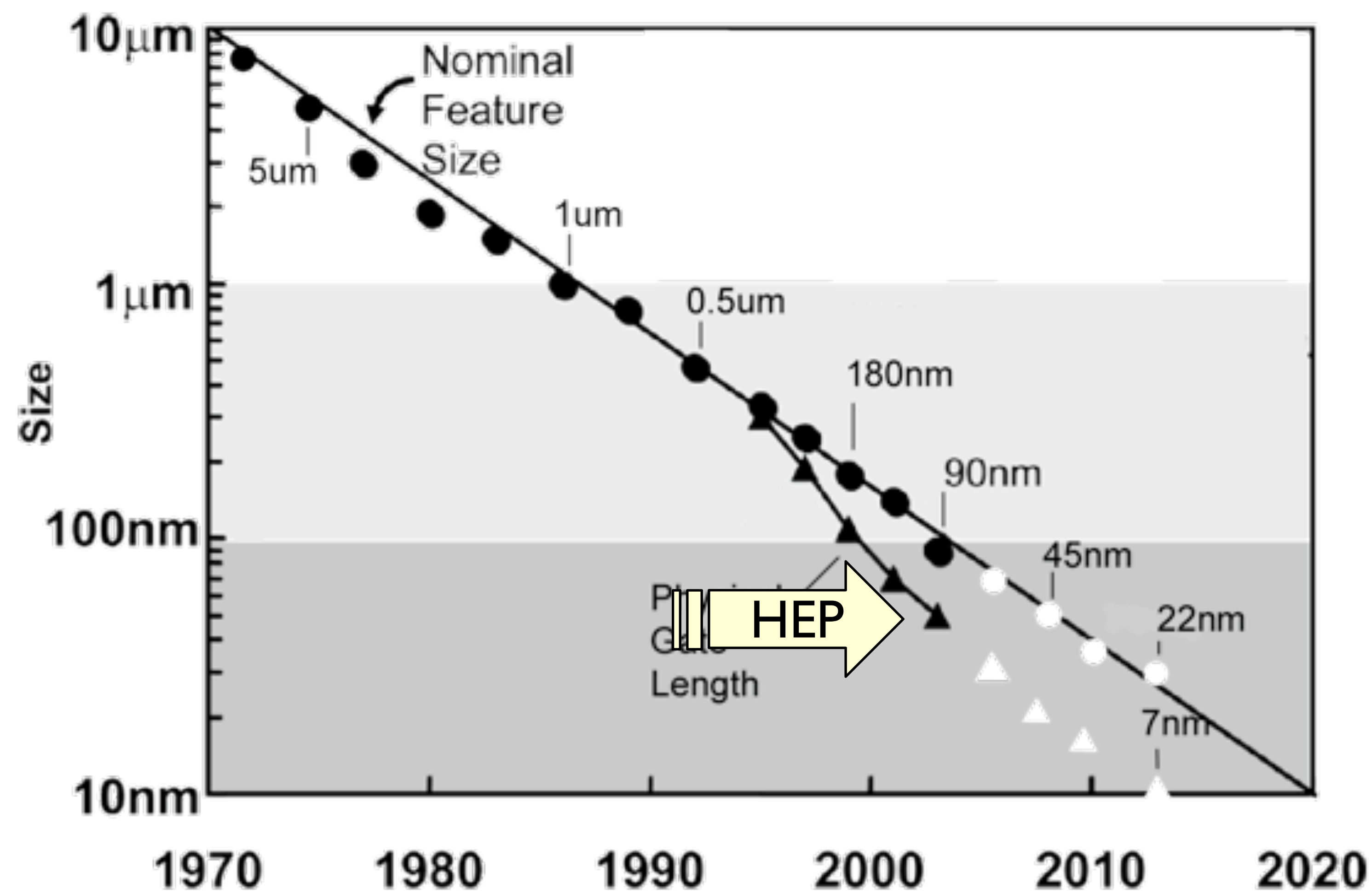

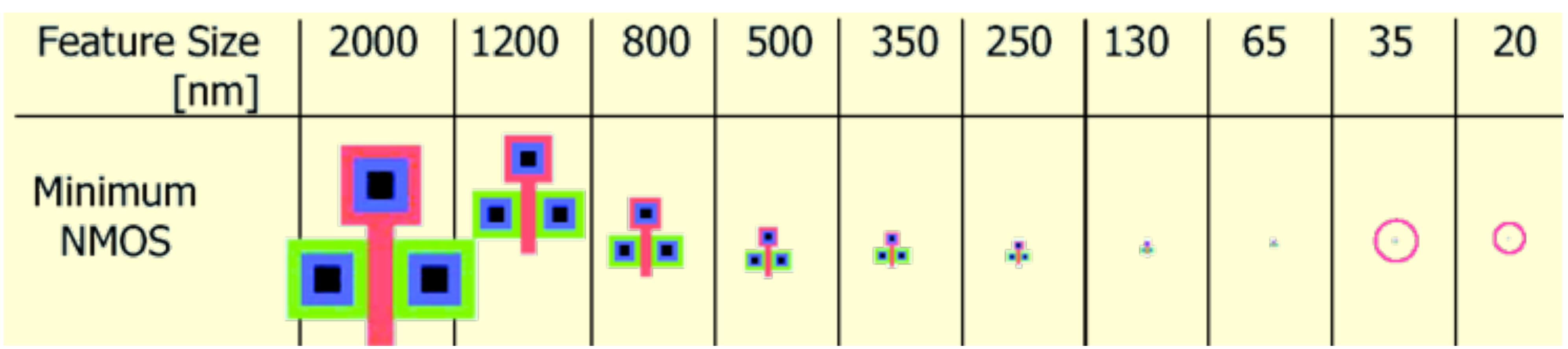

Radiation effects on CMOS: ionizing

- Decrease of feature size: higher radiation tolerance:
  - Positive charge trapped in gate and field oxides
  - Trapped charge dissipates by tunnelling in thin-oxide transistors

- Radiation tolerant layout techniques designed by CERN RD49 in 0.25µm to avoid parasitic transistor leakage

Standard device layout

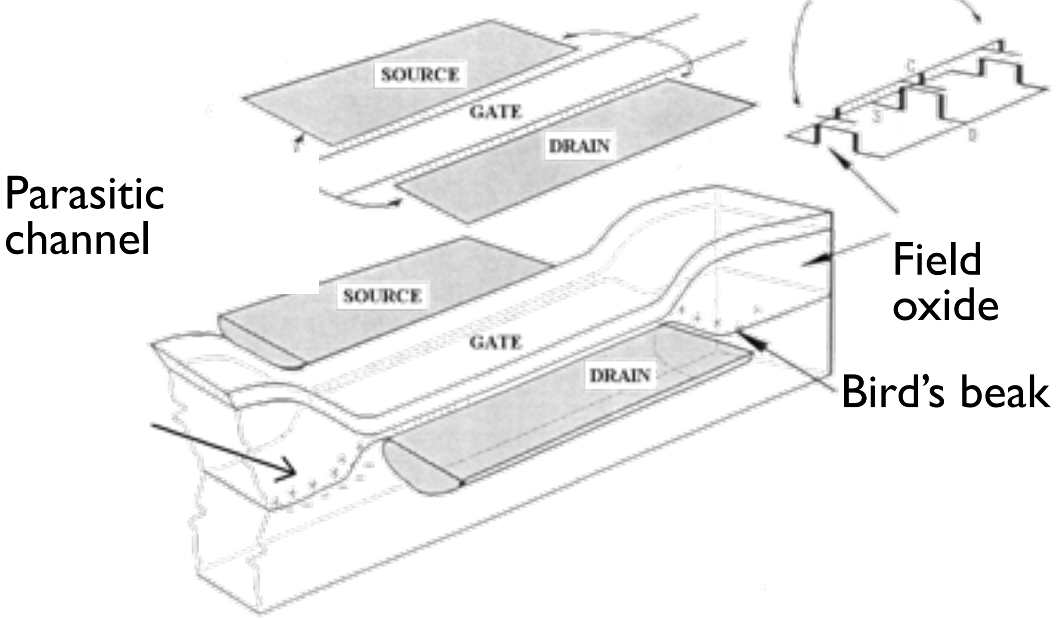

Enclosed layout

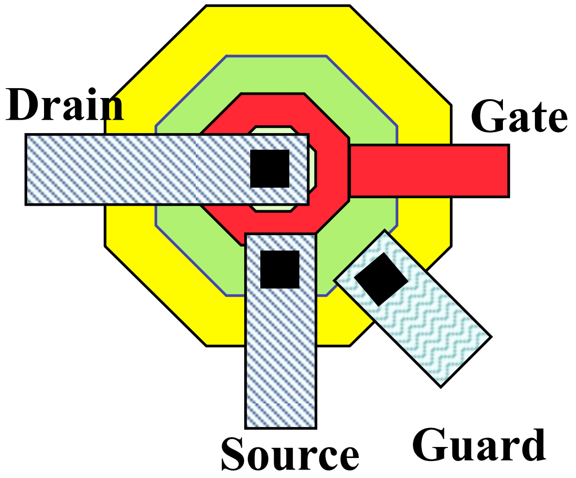

- gate encloses all n+ regions avoiding any thick transistor relevant oxide structures

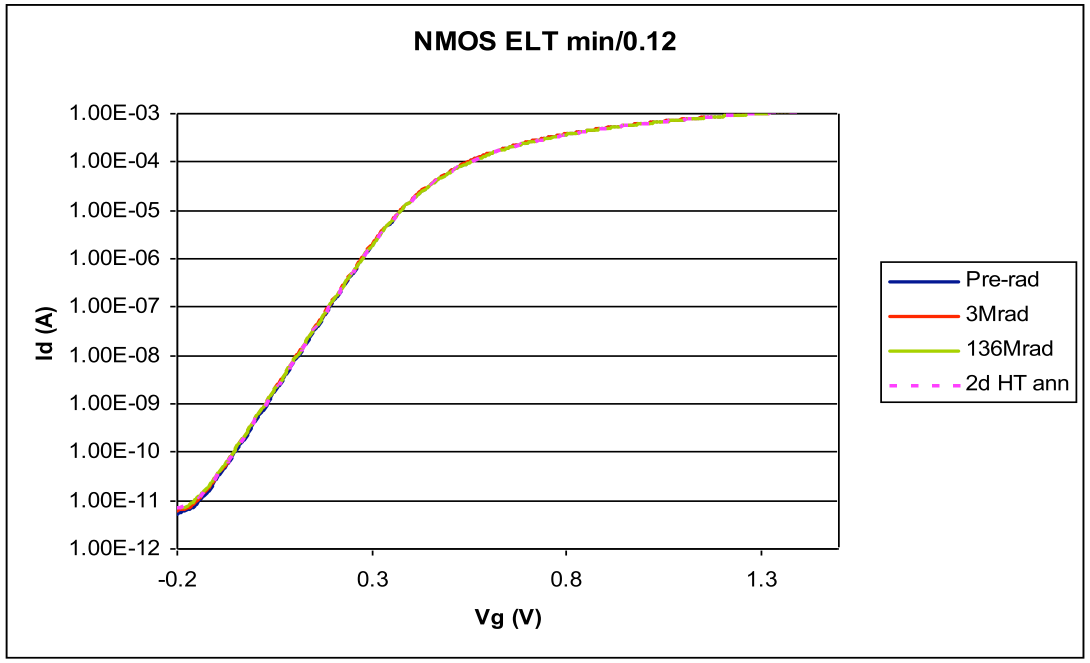

TID on IBM 130nm NMOS [F. Faccio CERN]

Data Taking with Cosmics

- Cosmics have been taken in two long, dedicated periods, in 2008 (in preparation for the first LHC startup, and after September 19 accident) and the second in 2009.

- Even if not replacing collisions, cosmic muons were useful to:
  - align the Inner Detector
  - test the tracking algorithms and compute hit efficiency
  - adjust detector timing
  - test the trigger and data acquisition system

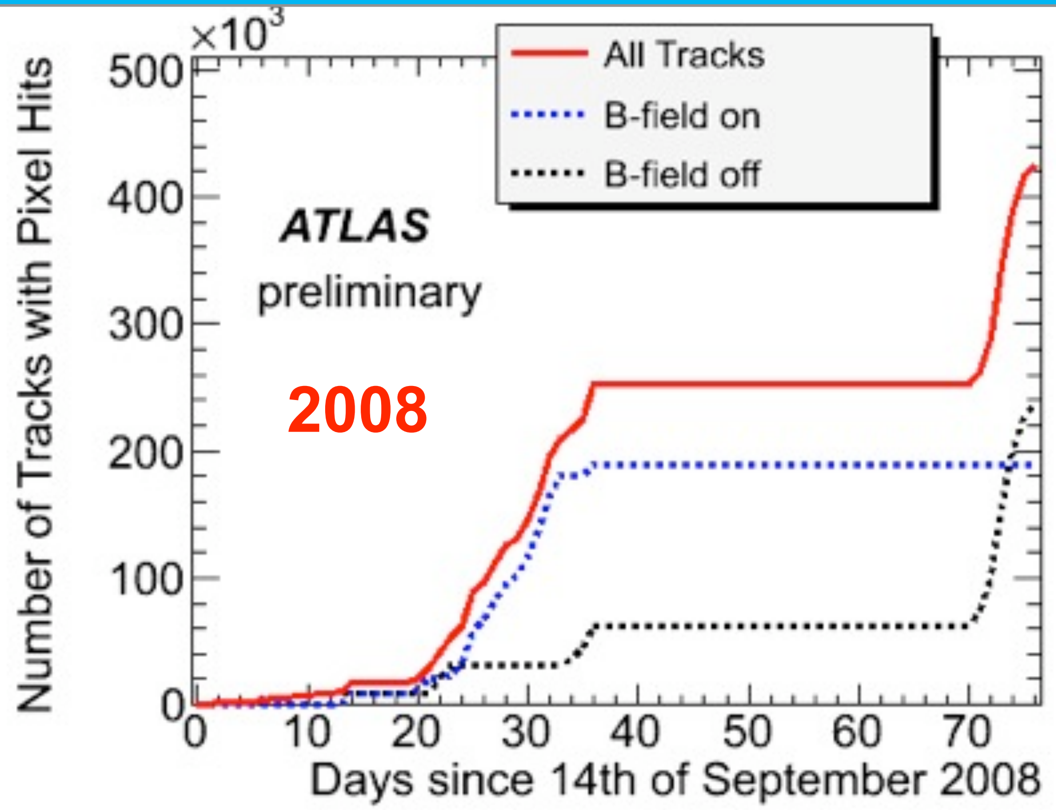

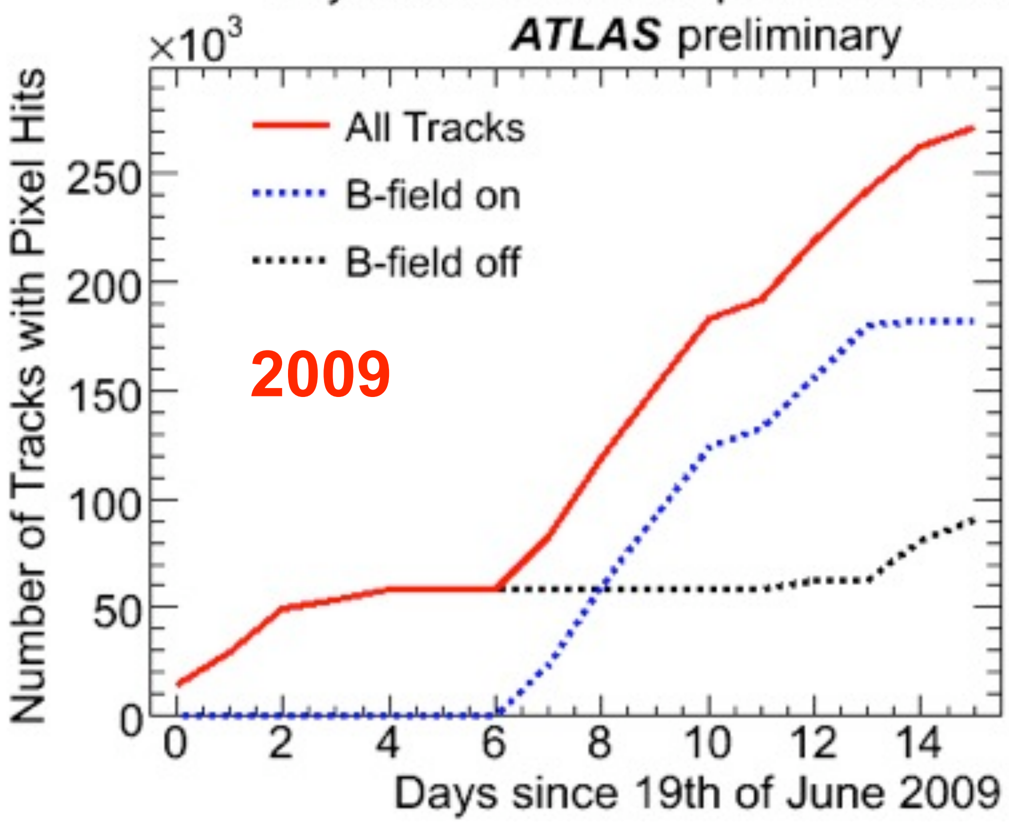

Data Taking with Cosmics

- Cosmics have been taken in two long, dedicated periods, in 2008 (in preparation for the first LHC startup, and after September 19 accident) and the second in 2009.

- Even if not replacing collisions, cosmic muons were useful to:
  - align the Inner Detector
  - test the tracking algorithms and compute hit efficiency
  - adjust detector timing
  - test the trigger and data acquisition system

Lorentz Angle Measurement

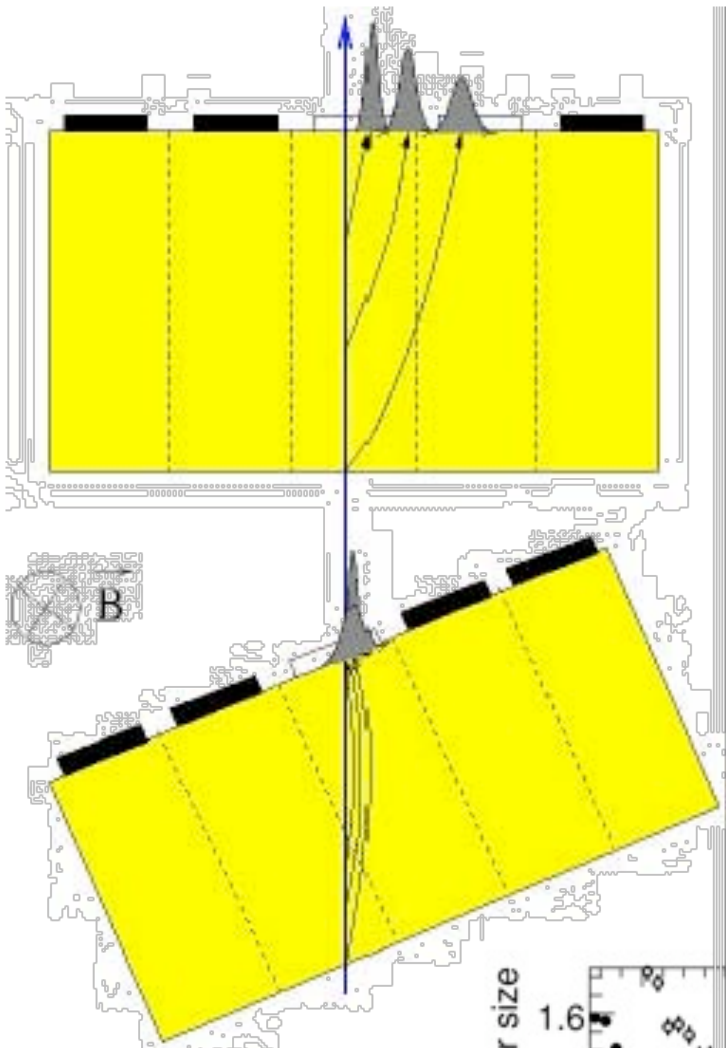

- The Lorentz angle can be calculated as the track incidence angle corresponding to the minimum of the average cluster size.
- The minimum is at normal incidence when the solenoidal field is off. With field on, the measured values are:

SCT: θ_L = 68.6 ± 0.5 ± 1.6 mrad

Pixel Detector: θ_L = 213.9 ± 0.5 mrad

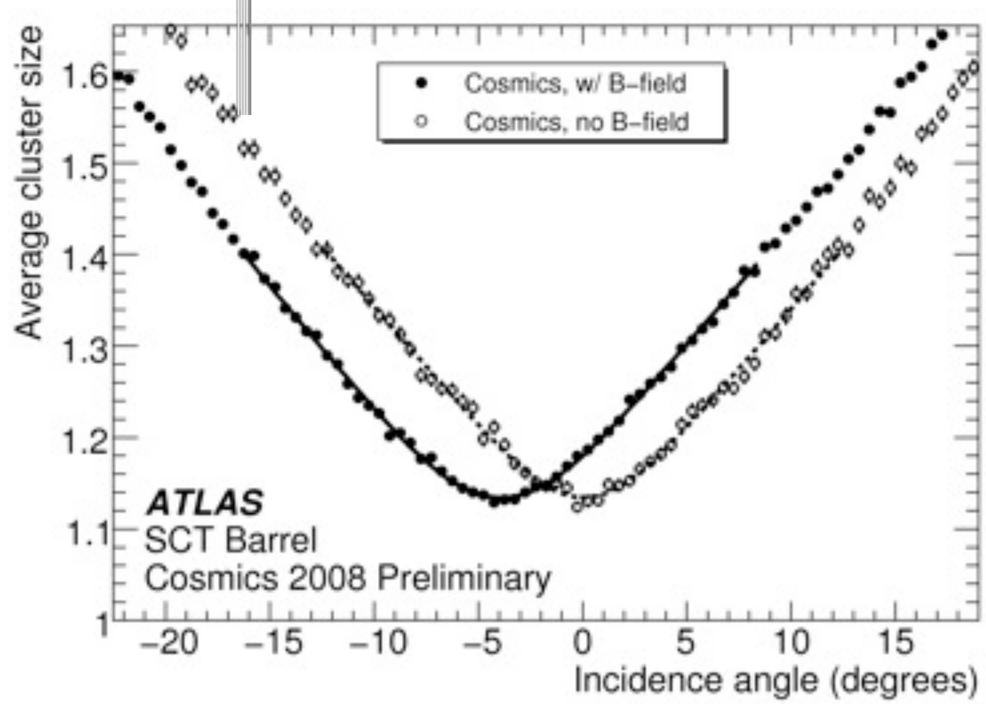

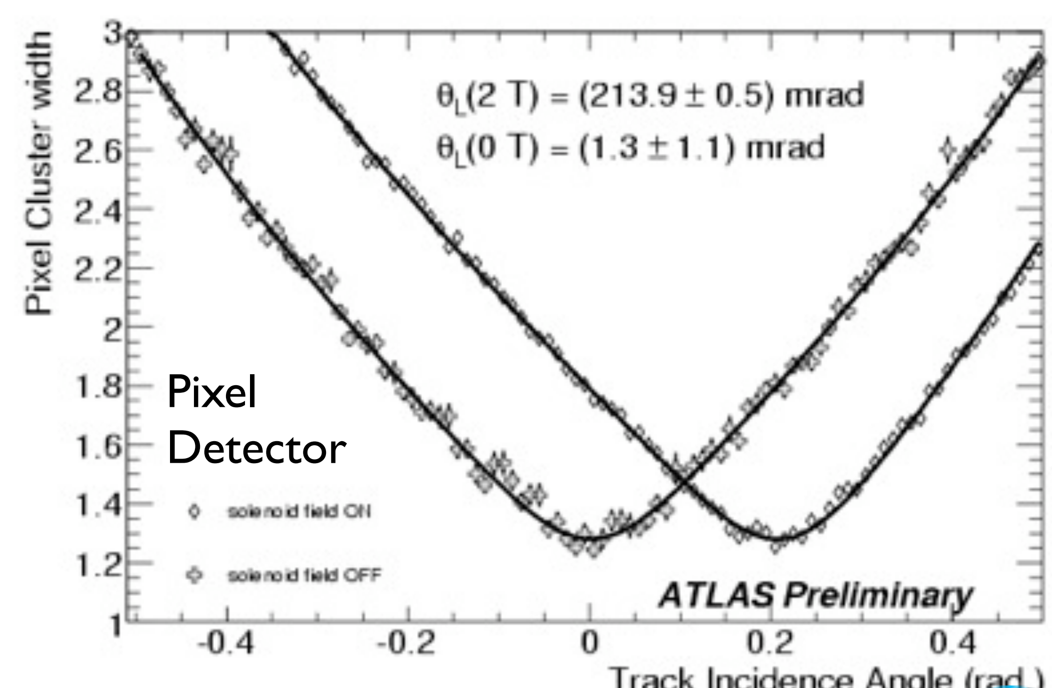

Detector timing

Both SCT and Pixel Detector have multi-bunch crossing read-out capability (3 consecutive BC for the SCT, from 1 to 16 for the Pixel Detector). This capability increases detector efficiency in the initial phase, when the inter-module timing is not perfectly adjusted, and can be a useful tool to check the relative timing of different trigger components. The goal is to align the modules to 1 ns, as soon as the necessary track statistics will be available.

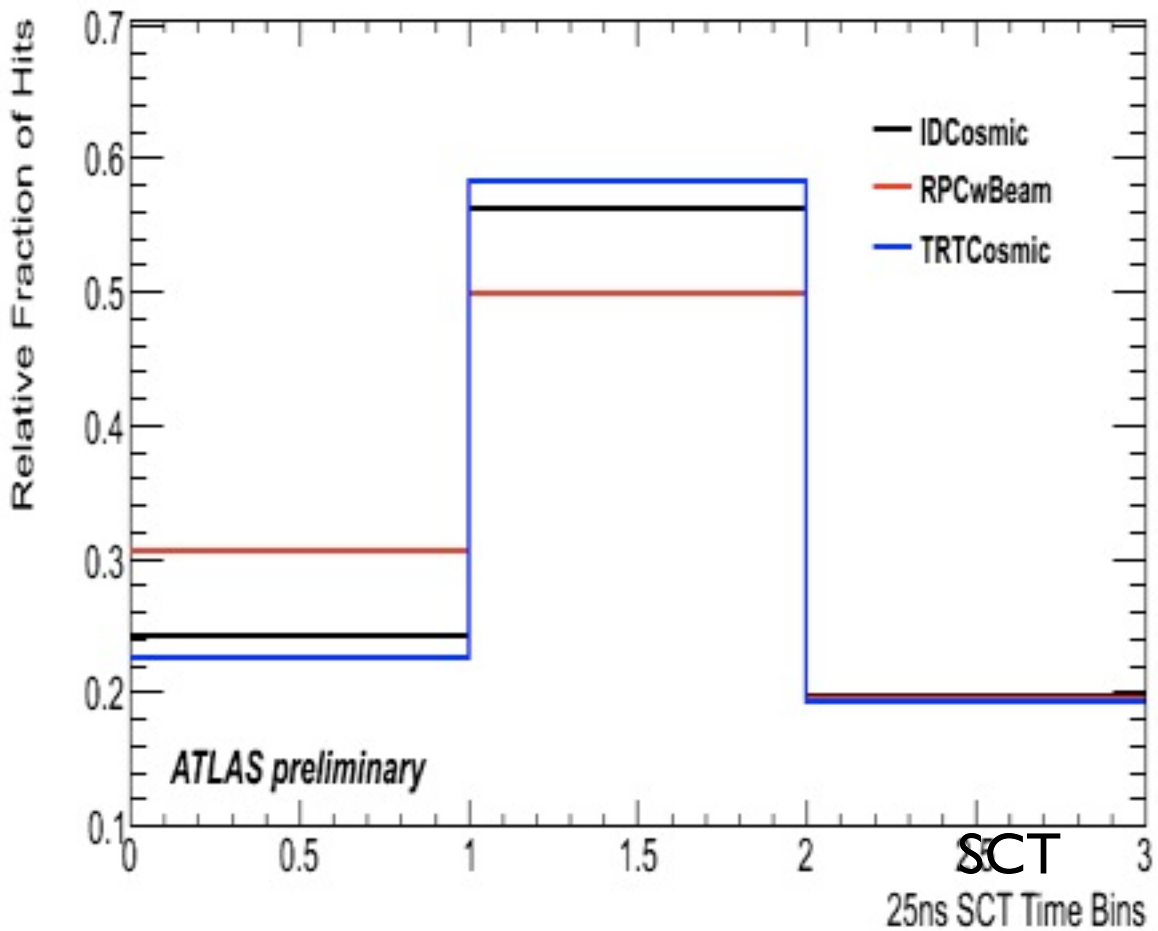

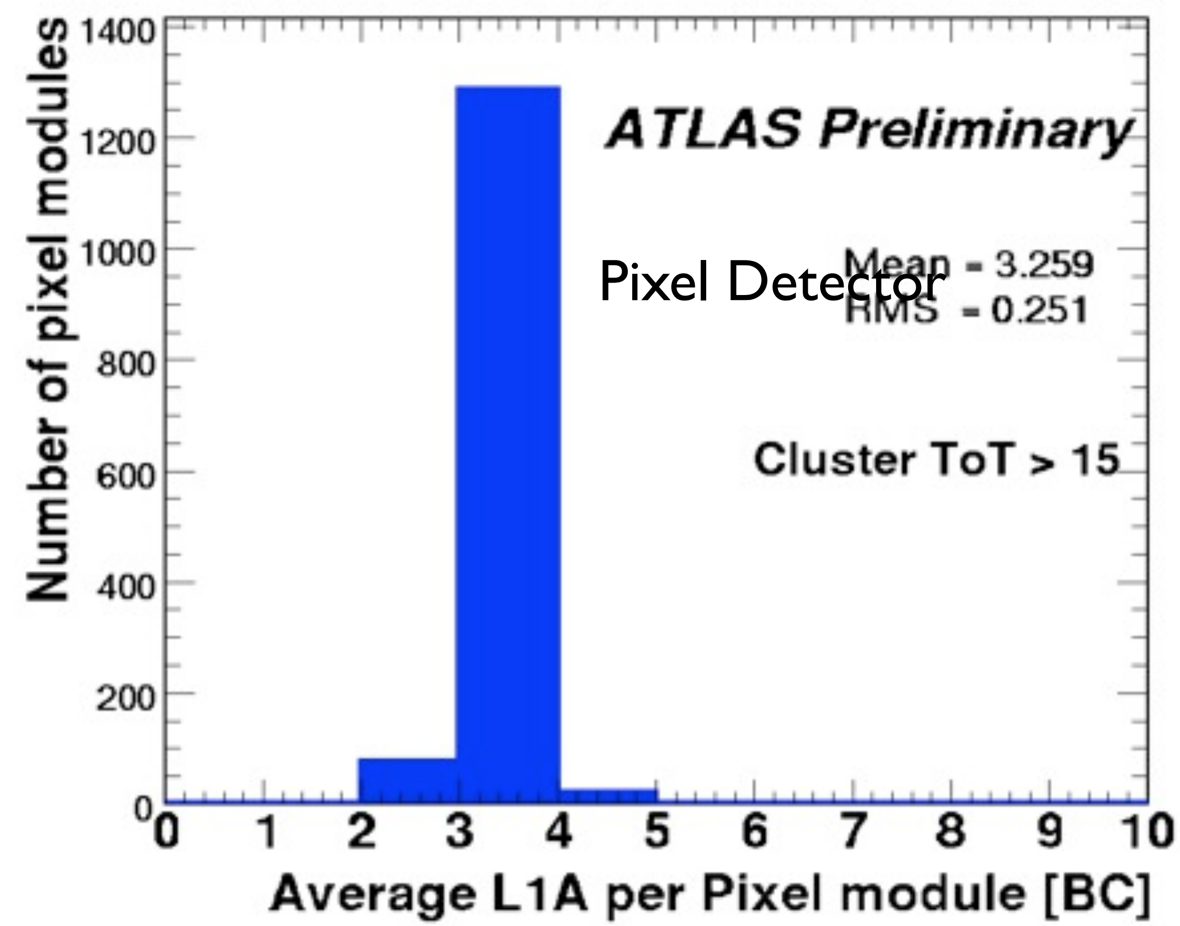

First collisions (at last…)

After very quick injection and RF capturing commissioning, LHC started to produce pp collisions at 900 GeV on November 23 (!!!!!).

In the following days, ATLAS collected 917 k collision candidates at 900 GeV and 34 k at 2.36 GeV (new world record).

Thanks to the intense commissioning program, the silicon trackers arrived well prepared to this rendez-vous: 99.3% of strips active for the SCT, 97.9% of pixels active). However, for obvious security concerns, the two detectors were fully on only when stable beams condition was declared (538 k events).

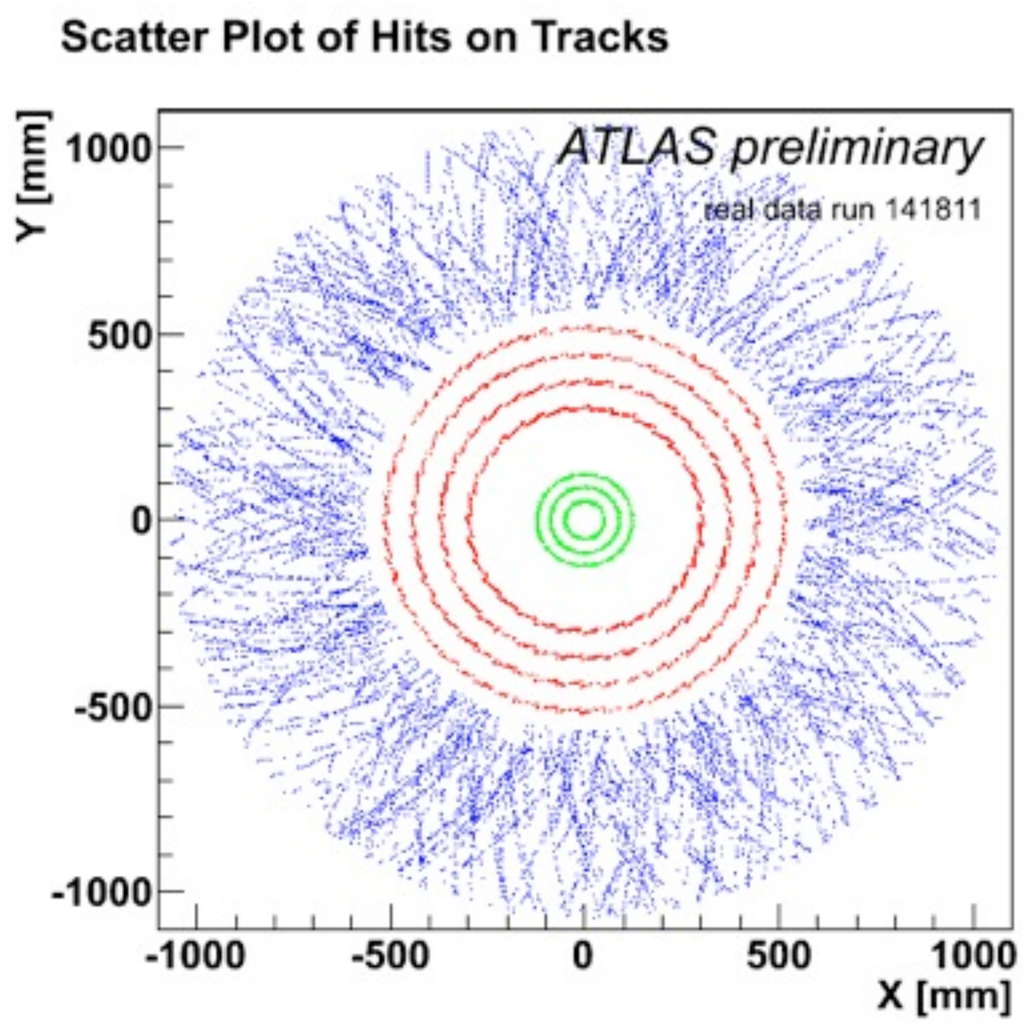

First collisions (at last…)

After very quick injection and RF capturing commissioning, LHC started to produce pp collisions at 900 GeV on November 23 (!!!!!).

In the following days, ATLAS collected 917 k collision candidates at 900 GeV and 34 k at 2.36 GeV (new world record).

Thanks to the intense commissioning program, the silicon trackers arrived well prepared to this rendez-vous: 99.3% of strips active for the SCT, 97.9% of pixels active). However, for obvious security concerns, the two detectors were fully on only when stable beams condition was declared (538 k events).

Mass peaks with the ID

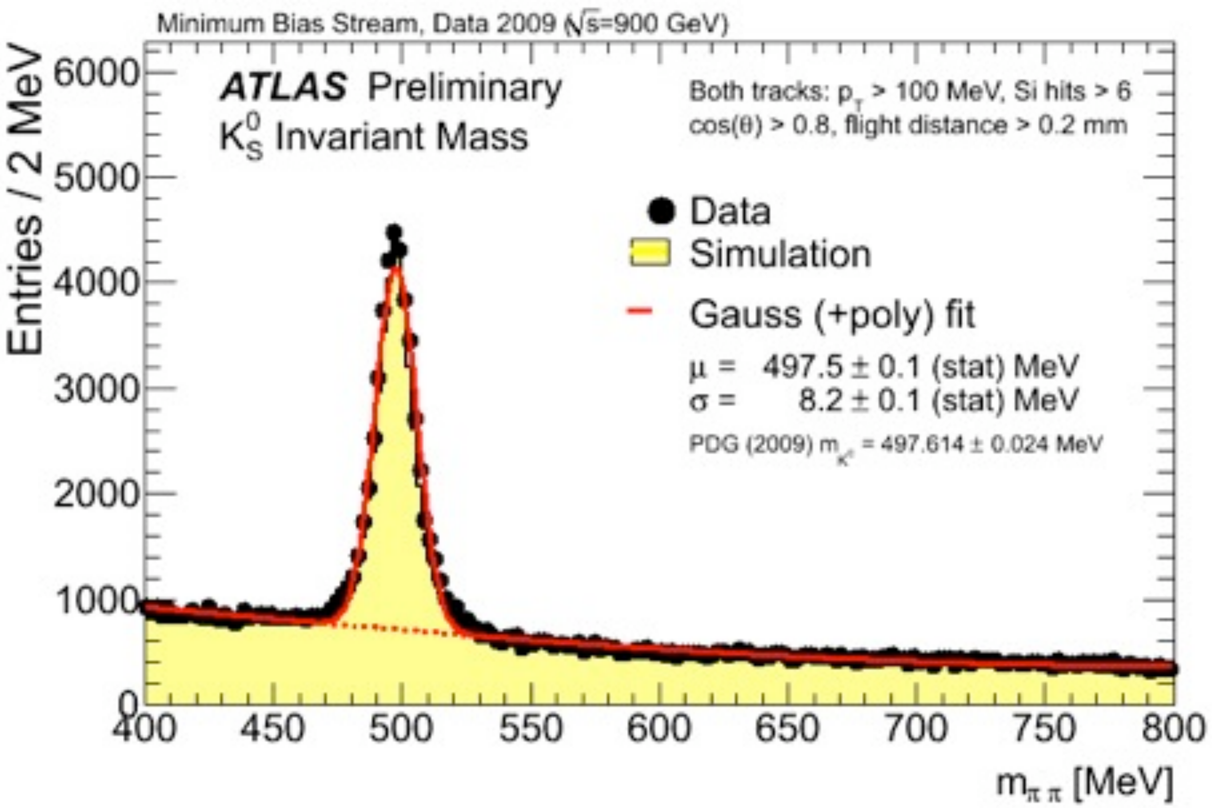

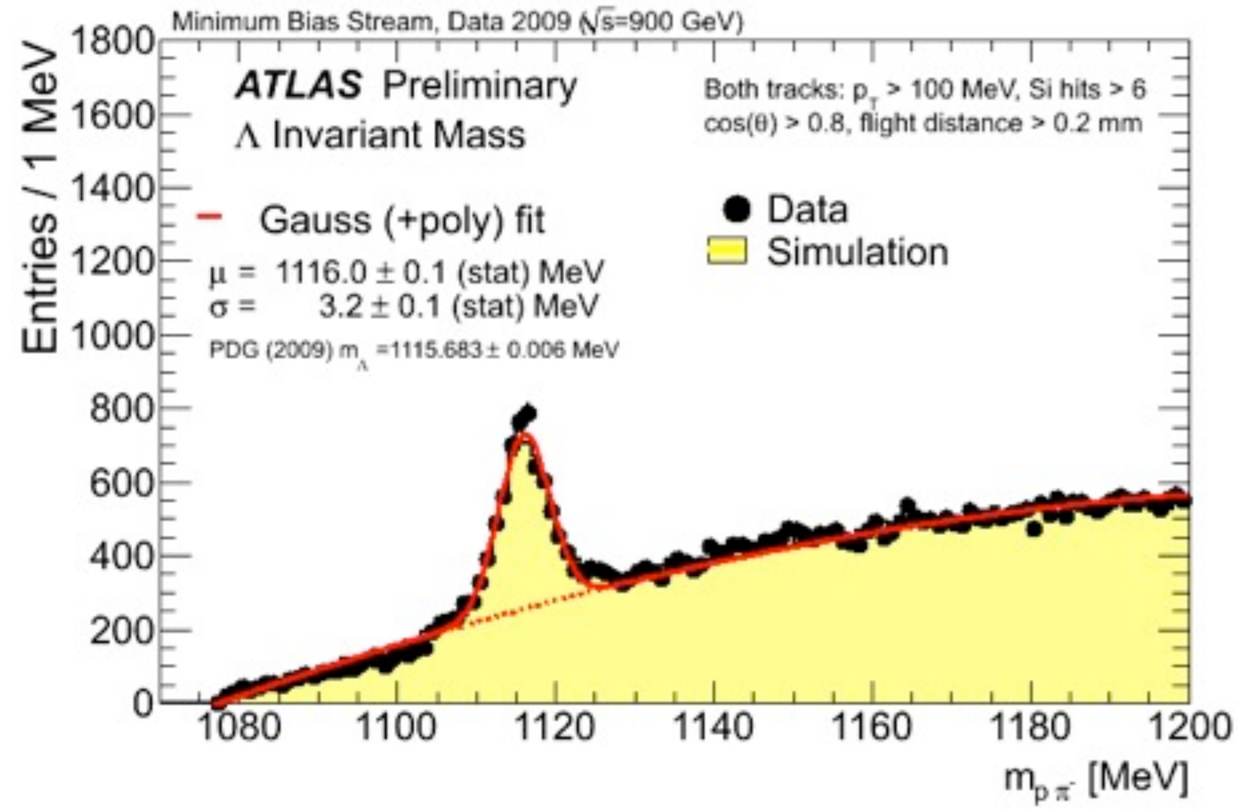

- The ID alignment obtained during the commissioning is good enough to identify K_s and Λ mass peaks in the sample of minimum bias events.
- The mass values agree with the PDG values, the resolutions with the MC expectations (dominated by multiple scattering).

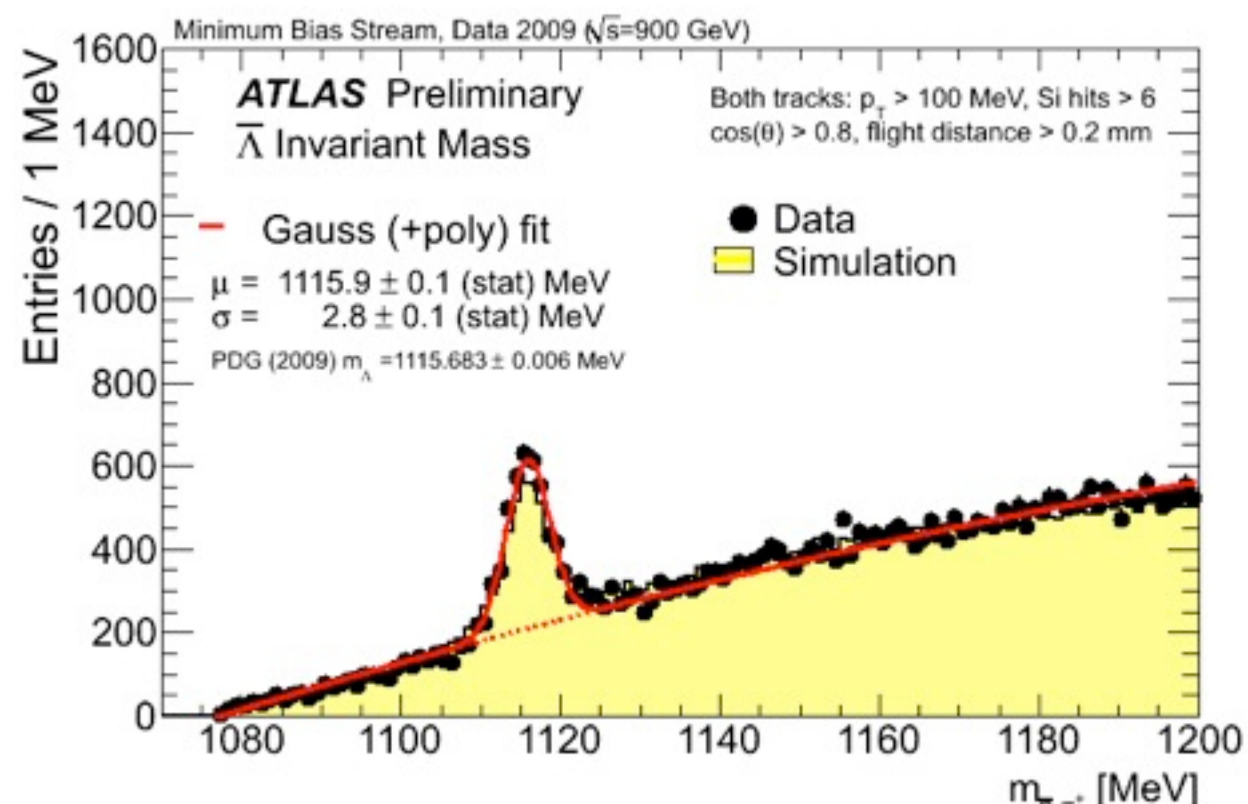

On-line Tracking

Another indicator of the decent shape of the silicon tracker comes from the Level 2 trigger algorithms, that are largely based on the silicon components of the ID. These algorithms are simplified compared to the ones used in the off-line, but provide track reconstruction within the 10 ms Level 2 latency.

As an example, the center of the beam spot region determined from the d_0 vs φ distribution of the tracks reconstructed on-line is in good agreement with the off-line. results.